Turkish Straits System and Black Sea Observations and Modeling

Emin Özsoy

Institute of Marine Sciences, (IMS-METU), Mersin

and now (since September 1, 2015):

Eurasia Institute of Earth Sciences, (EIES-ITU), İstanbul

ICTP-METU School

Ocean Climate Modelling: Physical and Biogeochemical Dynamics of Semi- enclosed Seas

Middle East Technical University (METU) Ankara, Turkey

September 28 - October 1, 2015

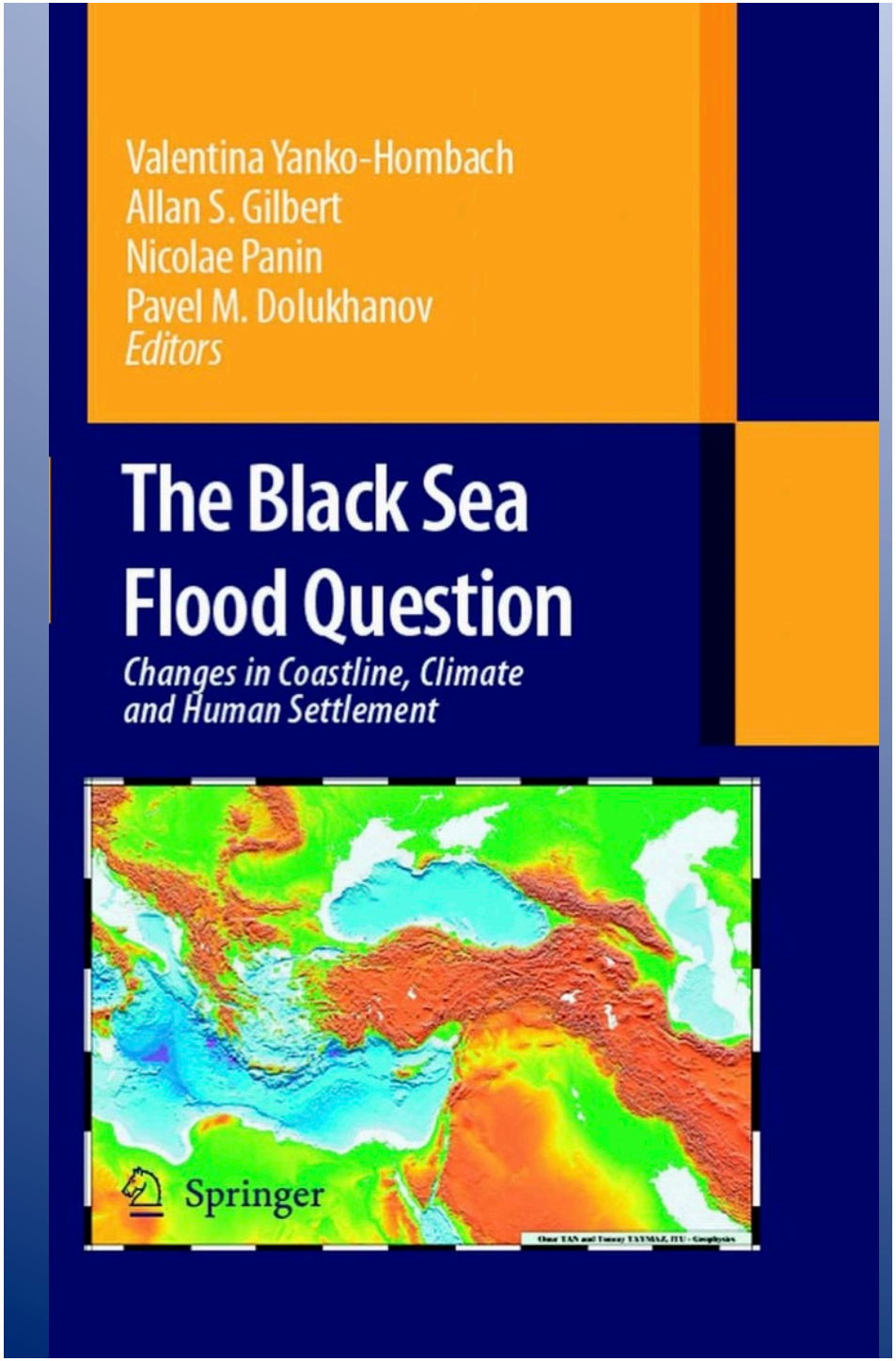

3.2 The Evidence of Early Prehistory (Paleolithic to Mesolithic Periods)

Wherever intensive surface surveys have been conducted along the Black Sea coast, abundant Paleolithic and Mesolithic evidence has been discovered. Lithic scatters from these cultural horizons are found on the first coastal terraces, and they extend inland within the valley systems. None of these sites has been excavated, so it is not possible to say whether any represent *in situ* campsites or whether they are all secondarily deposited. It is undeniable that the frequency of discovery indicates a high concentration of activity.

Figure 2. Archaeological sites mentioned in the text.

The area around the Bosphorus has been studied most intensively (Gatsov and Özdoğan 1994; Runnels and Özdoğan 2003). Lithic scatters or debris concentrations have been recovered most often within the fossilized coastal dunes, but they are not found here exclusively. Locations containing lithic assemblages typologically datable to the Early and Middle Paleolithic periods are known throughout the coastal area. The geological setting of these sites has not yet been worked out, however, and therefore, they do not yet provide a reliable basis for discussion here. On the other hand, some early Upper Paleolithic sites with Early Aurignacian assemblages have been discovered, the most prolific of which is situated within the coastal dunes of Ağaçlı, about 30 km west of the Bosphorus. There is no clear evidence of sites inhabited during

Historical beginnings of the science of the seas:

starts with navigation and map making
Kristof Kolomb - Cristoforo Colombo - Chios 1474 - America 1492
Isolario – geographers and captains of thr middle ages
Piri Reis 1465 - 1554 - Mediterranean - Indian Ocean
First reference to tides in relation to moon - 'Bahriye' – 1526
Galileo (1564-1642) - tide related to sun – 1632
Isaac Newton (1642-1727) - first scientific theory of tides - 1686
Luigi Ferdinando Marsili (1658-1730) – first 'oceanographic' Investigation In the Bosphorus!

Bosphorus:
Luigi Ferdinando Marsili (1658-1730)
Bosphorus - 'Osservazioni intorno al Bosforo Tracio' - 1681
Histoire physique de la mer - 1725
Danube – 1732
Spratt 1870, Wharton 1872, Makaroff, 1881, Magnaghi 1882, Gueydon 1886, Spindler 1894, Nielsen 1910, Merz 1917, Möller 1928
Kosswig (1903-1982) - first marine science effort in Turkey
Ulyott, Ilgaz, Pektaş 1943-1956
Defant 1961, Carruthers 1963, Özturgut 1964, Bogdanova 1961,

Karlowitz
Karlofça
1699

L. F. Marsili (1658 – 1730)
İstanbul visits (1679-1680, 1691)
Serving Habsburg Empire (1682 – 1690)
Siege of Vienna (1683) and Buda (1686)
Karlowitz border demarcation (1699)
Osservazioni interne al Bosforo Tracio (1681)
Histoire physique de la mer (1725)
Danubius Pannonico-mysicus (1726)
Accepted to Royal Society, London (1699)
Académie des Sciences, Paris (1715)
Bologna Institute of Sciences and Arts (1715)
Stato militare dell'Imperio Ottomanno (1732)

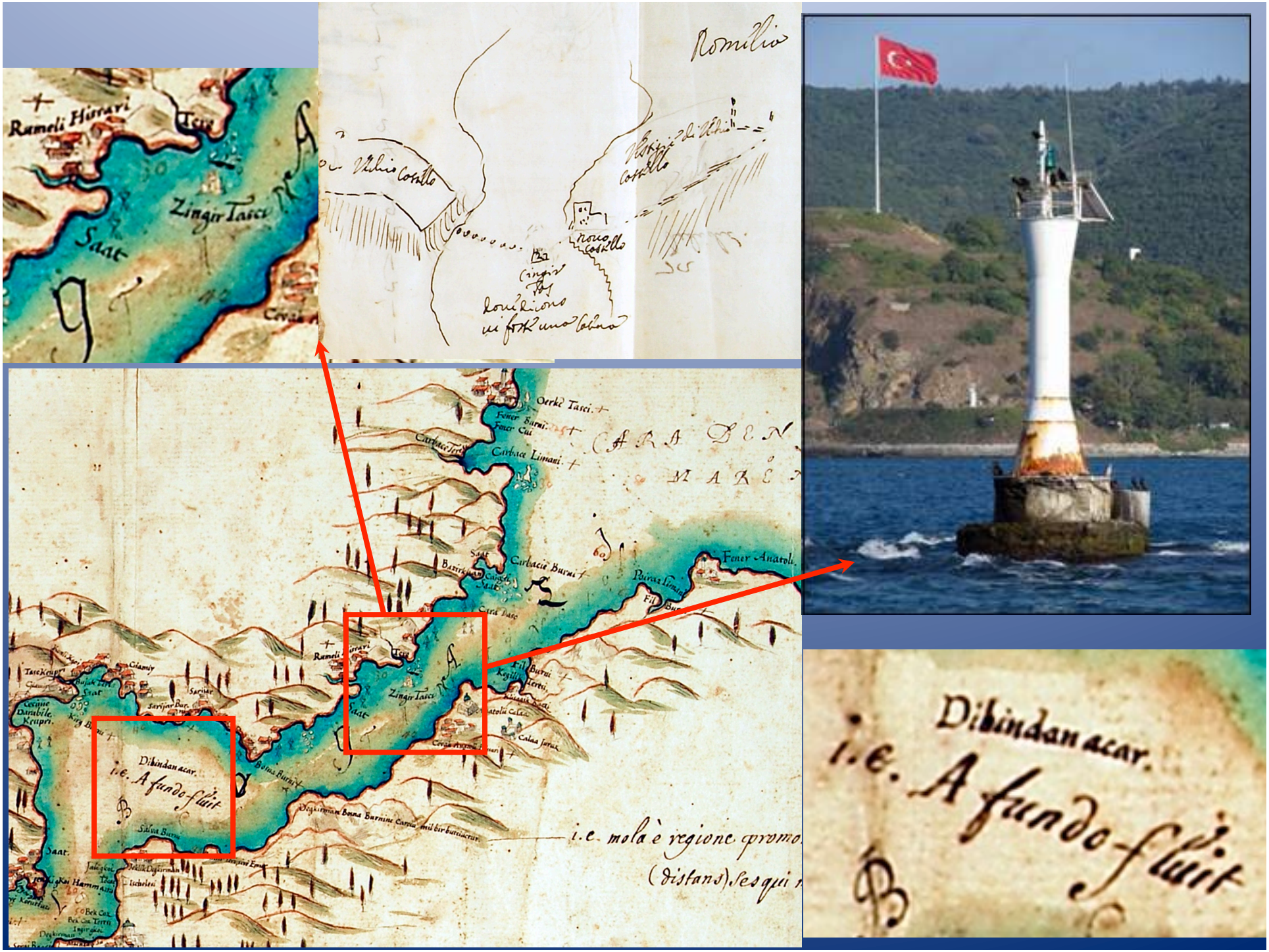
Romilia
Rameli Hisari
Zingir Tasci
Saat
Dibindan acar.
i.e. A fundo-flust
Dibindan acar.
i.e. A fundo-flust

L. F. Marsili
1658 – 1730

İstanbul
1680

Measurements of the current reversal with depth in the Bosphorus

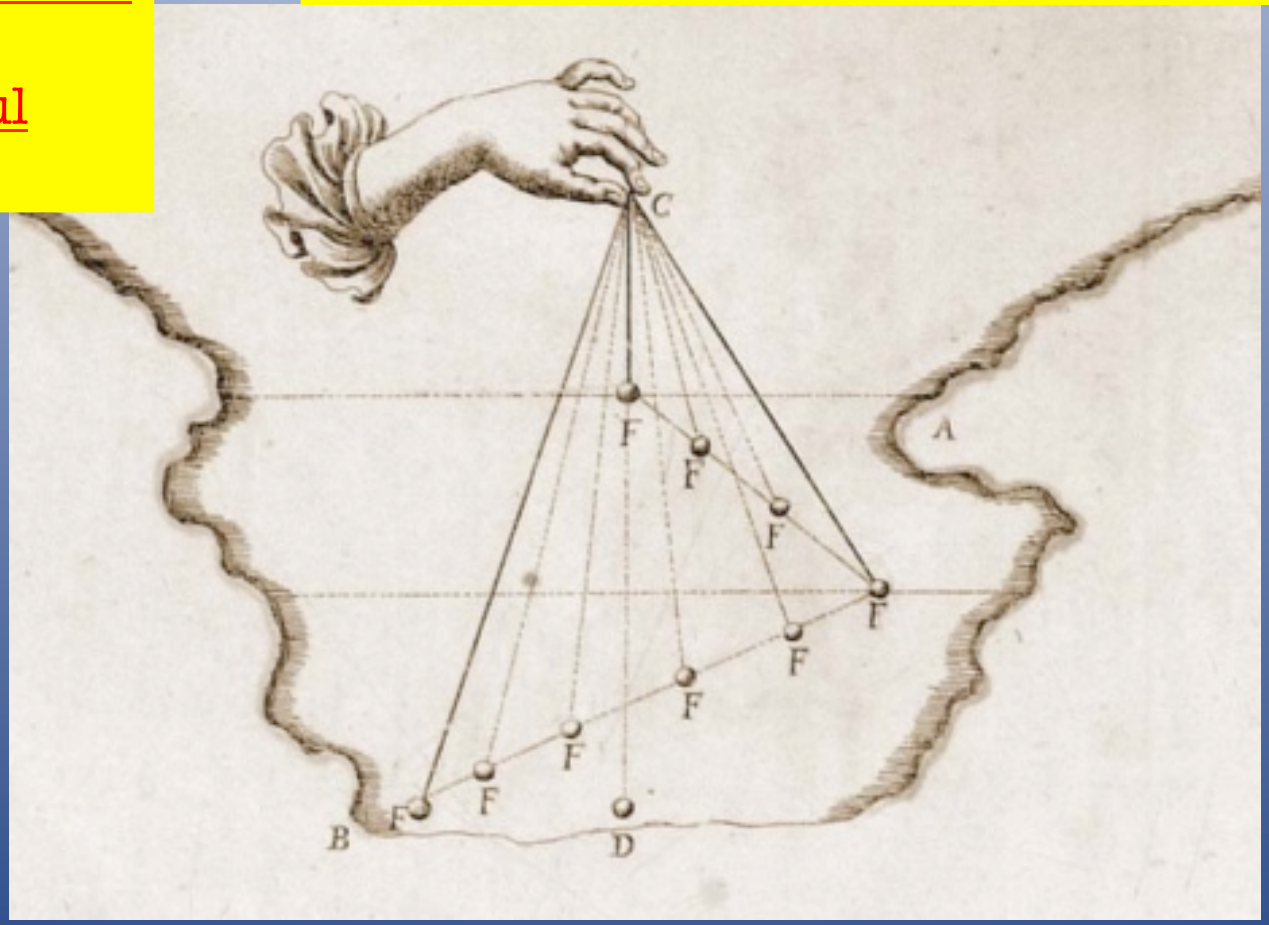

6th century AD, people already knew
–> Manfred Korfmann – archeologist of Troy

The laboratory experiment done with Porzio in Rome (1681)

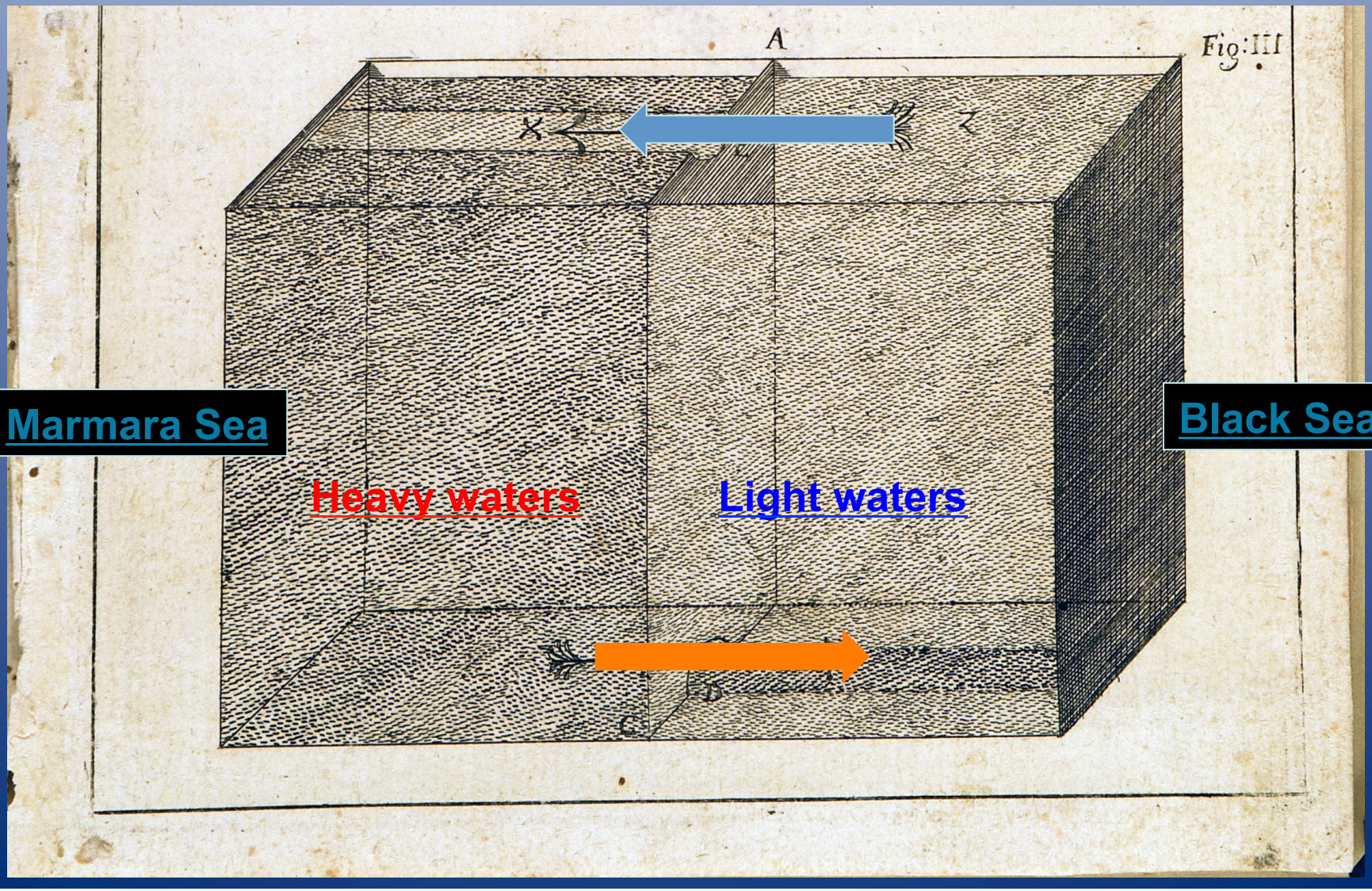

L. F. Marsili 1658 – 1730

Marsili, L. F. (1681).
Osservazioni Intorno al Bosforo Tracio overo Canale di Constantinopoli

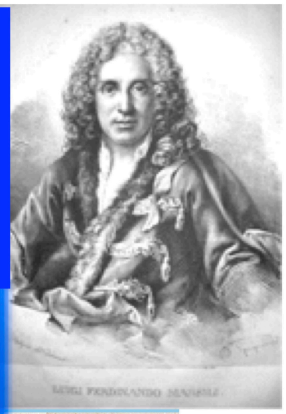

Keras – Haliç – Golden Horn

Petri Gyllii (1561). *De Bosporo Thracio*

Dionysios Byzantios 2nd century AD

Source of richness for two empires of İstanbul

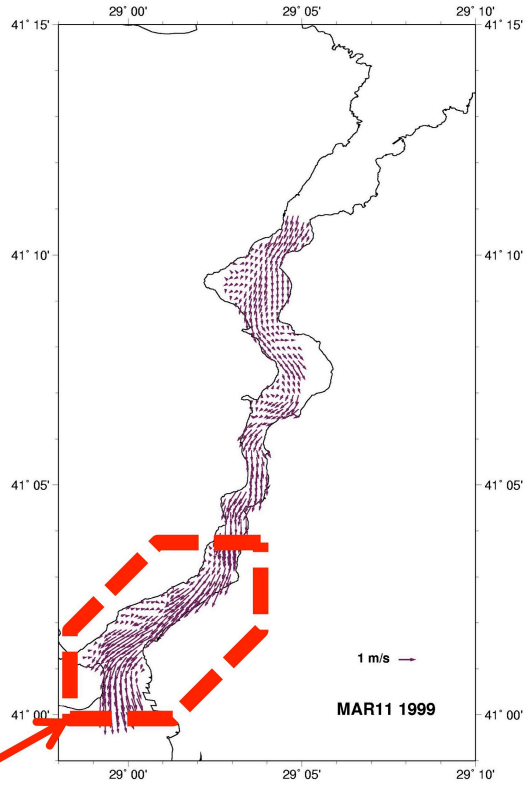

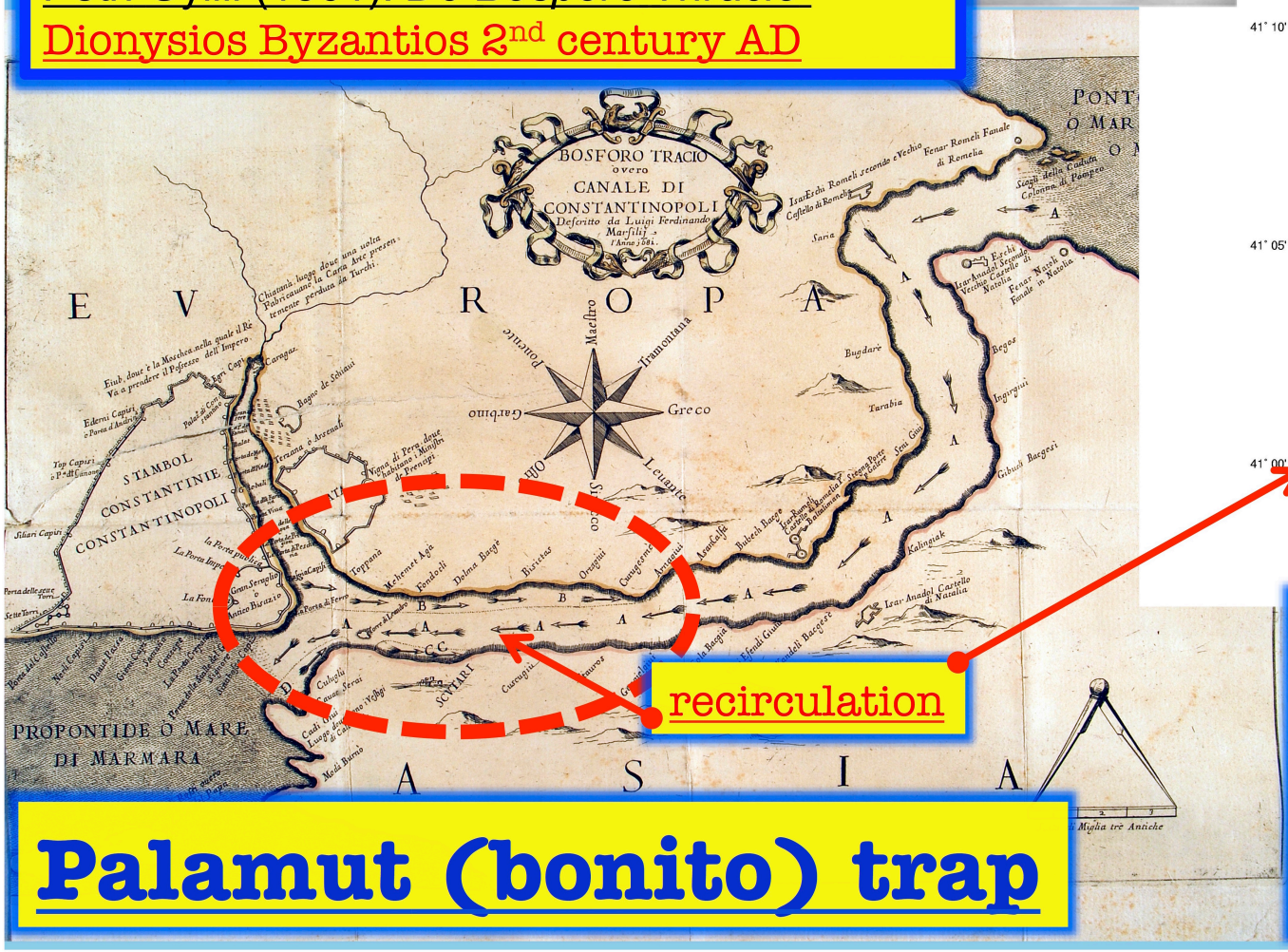

recirculation

Bosphorus surface currents
ADCP measurements
ODTÜ-DBE, 1999

Palamut (bonito) trap

Fishermen flocking at the recirculation zone of Beşiktaş – Haliç
Ara Güler (2012)

Keras – Haliç
Trap for Palamut
Petri Gyllii (1561)

Palamut (Bonito) fishery

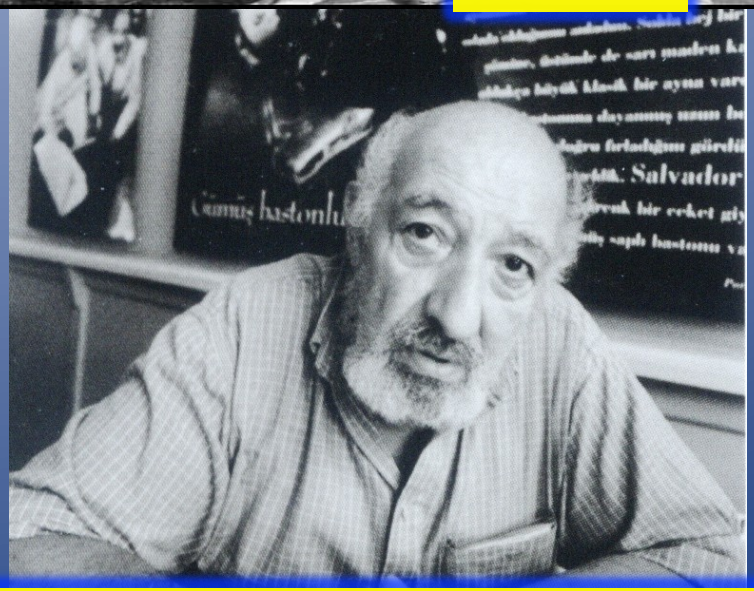

Ara Güler (2012)
Kumkapı Ermeni Balıkçıları
Armenian Fishermen of Kumkapı
1952

Population of megalopolis İstanbul

Possible population explosion of 'new İstanbul' !

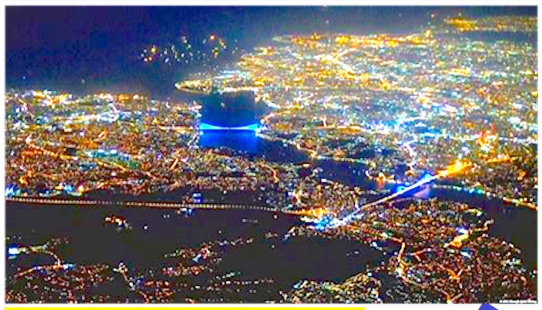

Star wars !

now

1960

year

population ($x10^6$)

0 5 10 15 20

1700 1725 1750 1775 1800 1825 1850 1875 1900 1925 1950 1975 2000 2025 2050

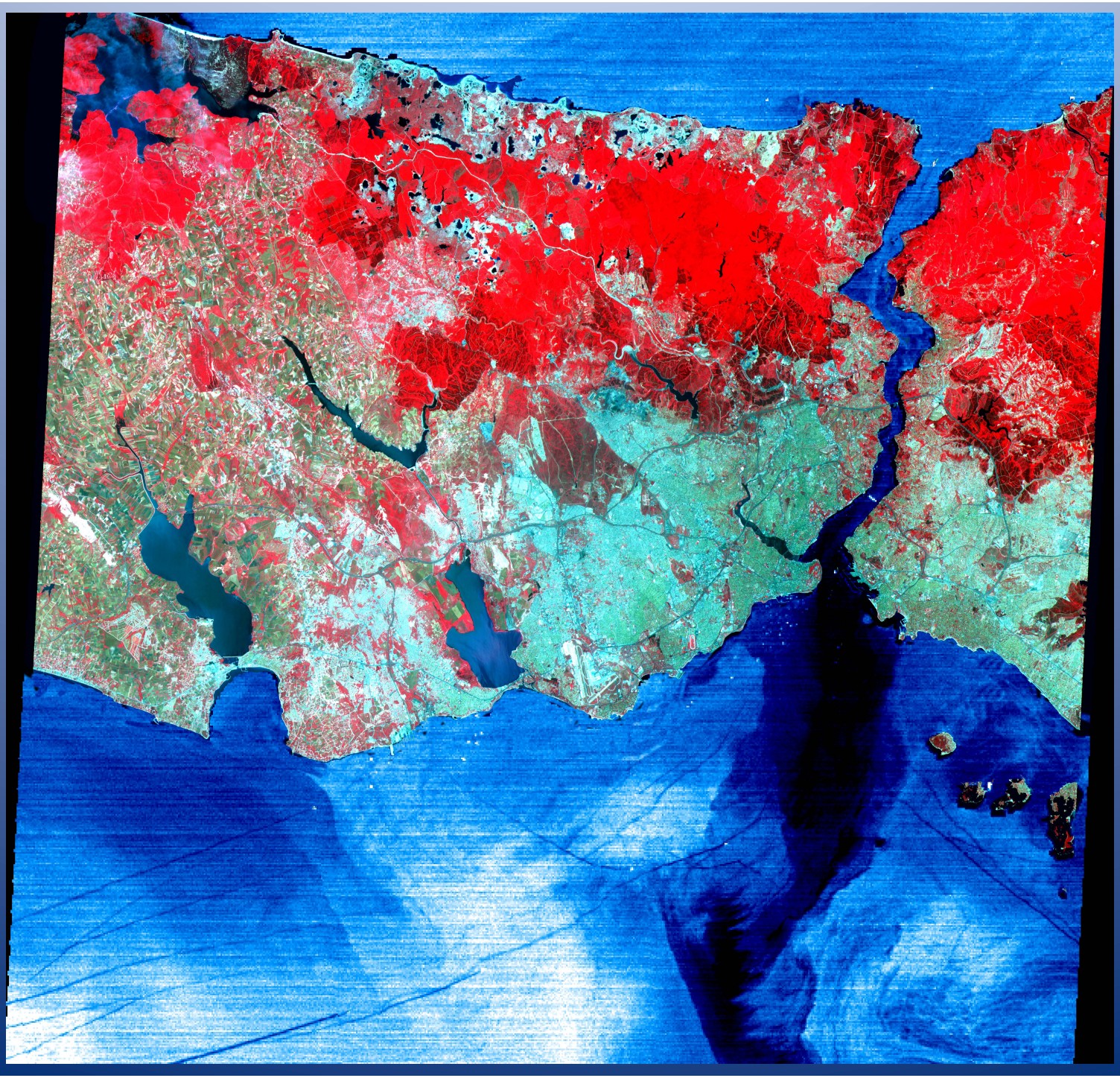

Chlorophyll distribution obtained from a satellite ocean color picture (MODIS aqua image obtained from eosdis) on 12 May 2015, showing phytoplankton bloom in the Marmara Sea, and the jet bringing in nutrient-rich Black Sea water through the Bosphorus and spreading in the Sea of Marmara.

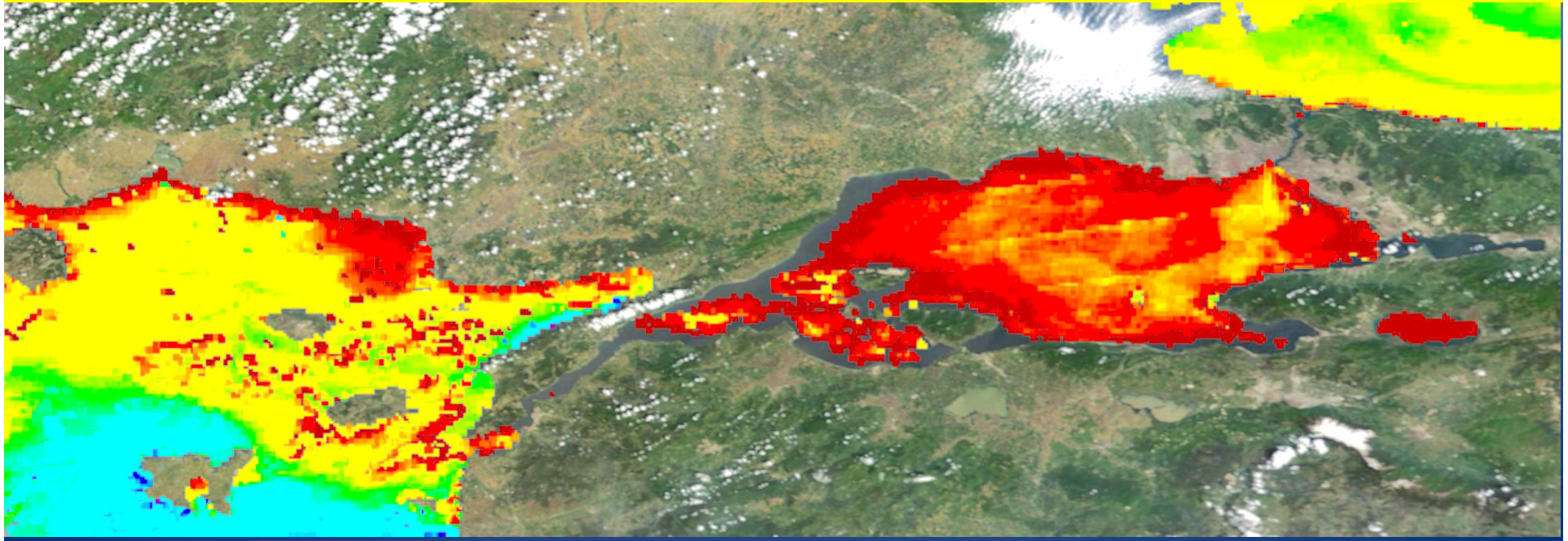

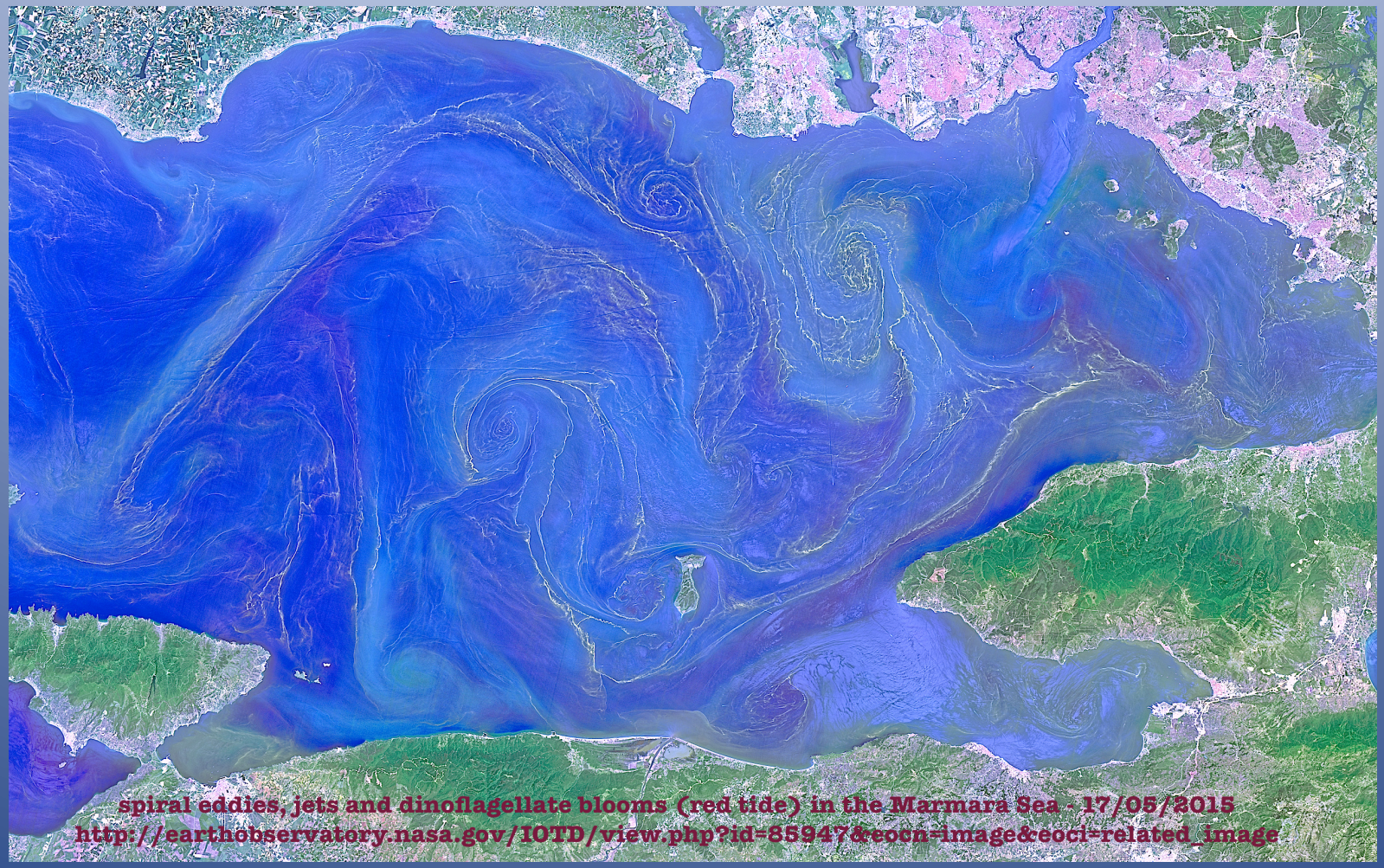

17 May 2015 satellite image of red tide (or harmful algal bloom, HAB)
(http://earthobservatory.nasa.gov/IOTD/view.php?id=85947&eocn=image&eoci=moreiotd)

http://www.milliyet.com.tr/marmara-iste-boyle-oluyor-gundem-2061522/

Turkish Straits captured by ISS astronaut Samantha Cristoforetti on June 9, 2015
https://twitter.com/astrosamantha/status/608197918395400192

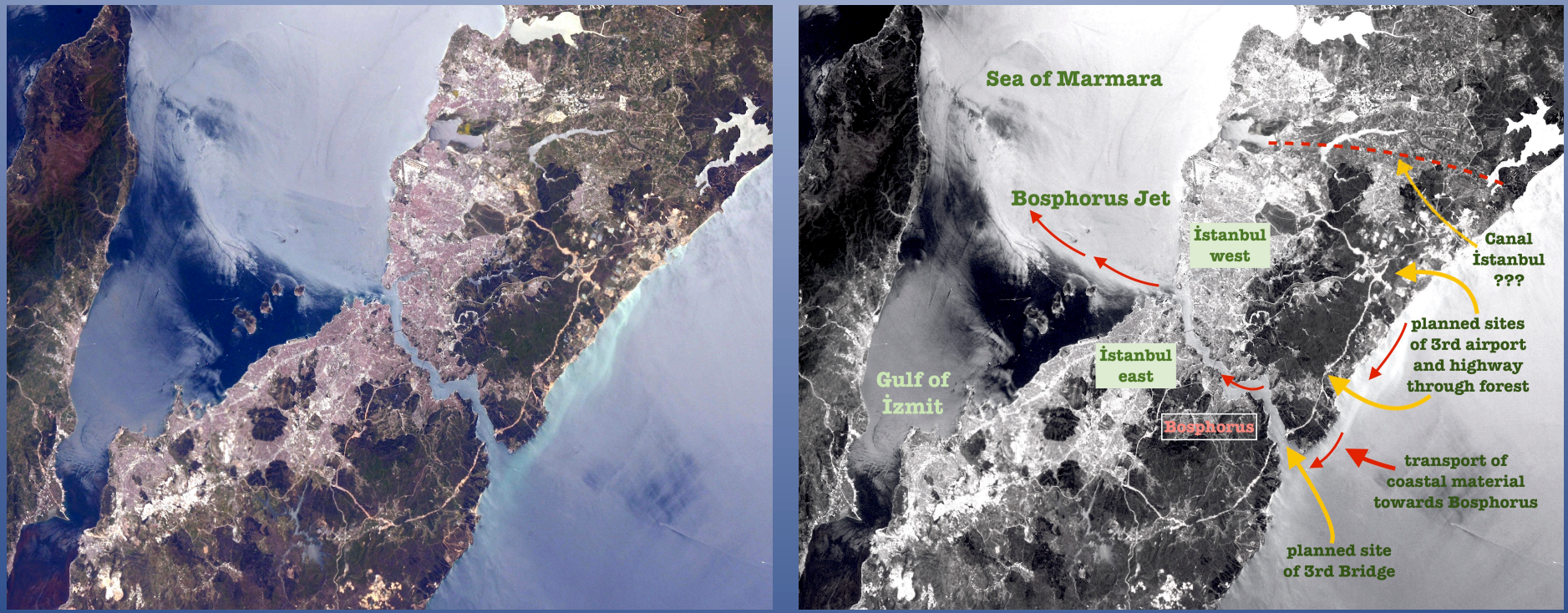

Clay Mathematics Institute 1 million $ prize !
for proof of uniqueness of solutions of the Navierf Stokes equations

CMI

ABOUT PROGRAMS MILLENNIUM PROBLEMS PEOPLE PUBLICATIONS EVENTS EUCLID

Navier–Stokes Equation

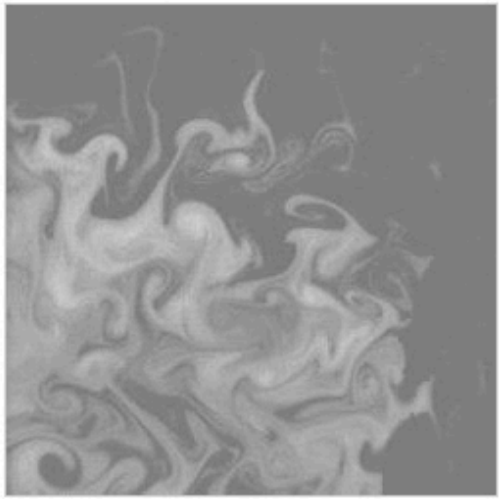

Waves follow our boat as we meander across the lake, and turbulent air currents follow our flight in a modern jet. Mathematicians and physicists believe that an explanation for and the prediction of both the breeze and the turbulence can be found through an understanding of solutions to the Navier-Stokes equations. Although these equations were written down in the 19th Century, our understanding of them remains minimal. The challenge is to make substantial progress toward a mathematical theory which will unlock the secrets hidden in the Navier-Stokes equations.

This problem is: Unsolved

Rules:

Rules for the Millennium Prizes

Related Documents:

Official Problem Description

Related Links:

Lecture by Luis Cafarelli

NONLINEAR PROCESSES, DISORDER, PREDICTABILITY:

Instability is a fundamental property of fluids that cannot be ignored or escaped !

- waves, eddies, fronts, turbulence are essential components
- nonlinear systems – sensitivity to initial conditions, divergence of solutions
  the 'butterfly effect' !
- significant loss of predictability in nonlinear coupled systems of high degrees of freedom
- forecasting success limited to no more than ~ 5 days in atmosphere / ocean
- 'open systems': global versus limited area model forecasts
  need external forcing or global closed budgets
- with appropriate parameterizations in climate models it is possible to make longer term, climatic predictions, but with less confidence
- partial solution with data assimilation
  use of observations to update model forecasts
  the Galilean 'scientific method': using observations along with models based on physics
  importance of experiments:
  http://mentalfloss.com/article/22913/hammer-and-feather-drop-moon
- ensemble forecasting (ensemble of models, forecasts with varying ic and bc)
- Bayesian statistics and Bayesian inference
  update the probability estimate for a hypothesis as additional evidence is acquired

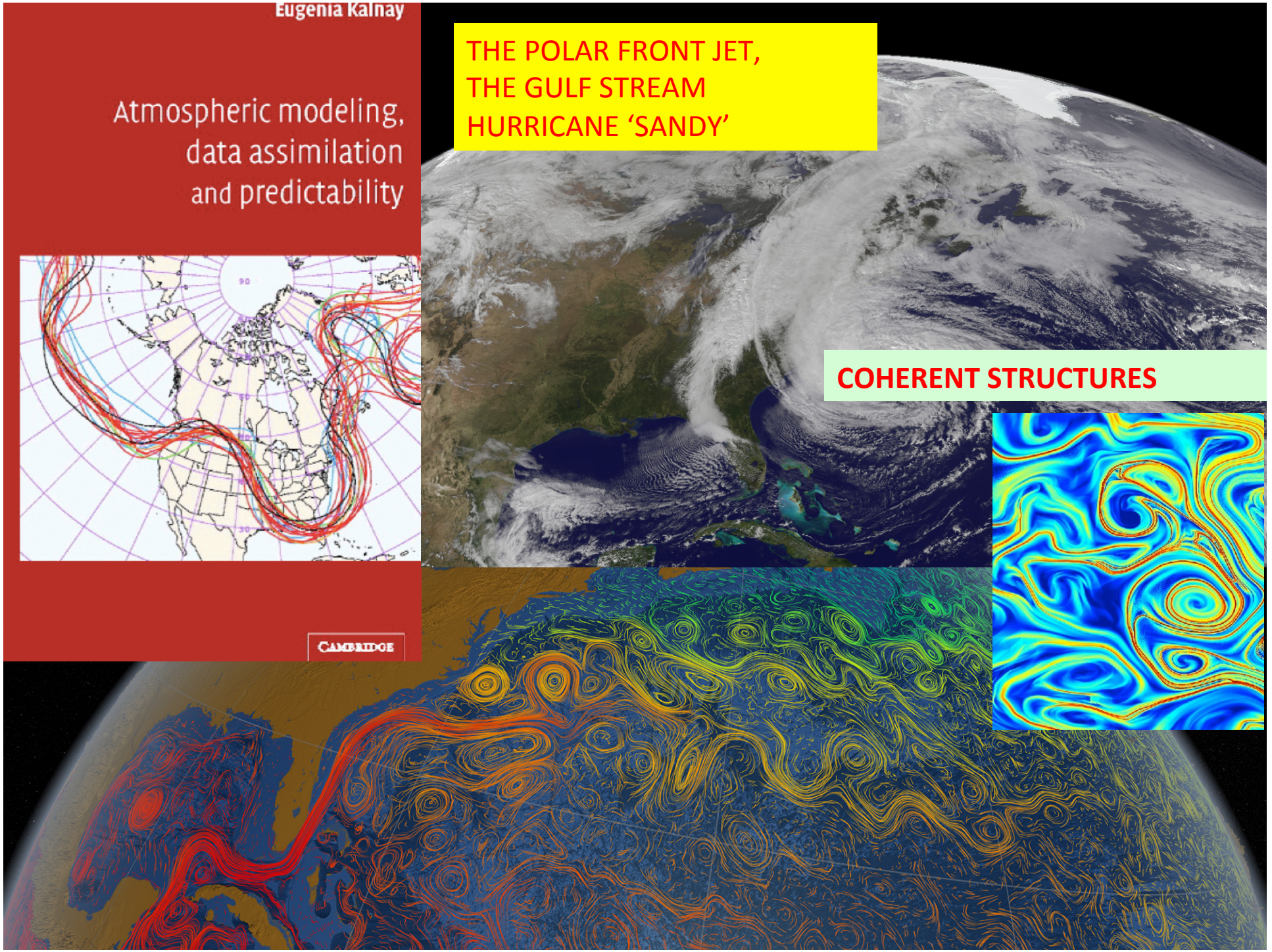
Eugenia Kalnay
Atmospheric modeling, data assimilation and predictability
CAMBRIDGE
THE POLAR FRONT JET,
THE GULF STREAM
HURRICANE 'SANDY'
COHERENT STRUCTURES

Composite Froude Number
Analogue of Mach Number in aerodynamics

$$G^2 = F_1^2 + F_2^2 = \frac{U_1^2}{g' h_1} + \frac{U_2^2}{g' h_2} = 1 \qquad \text{(Eq. 3.13)}$$

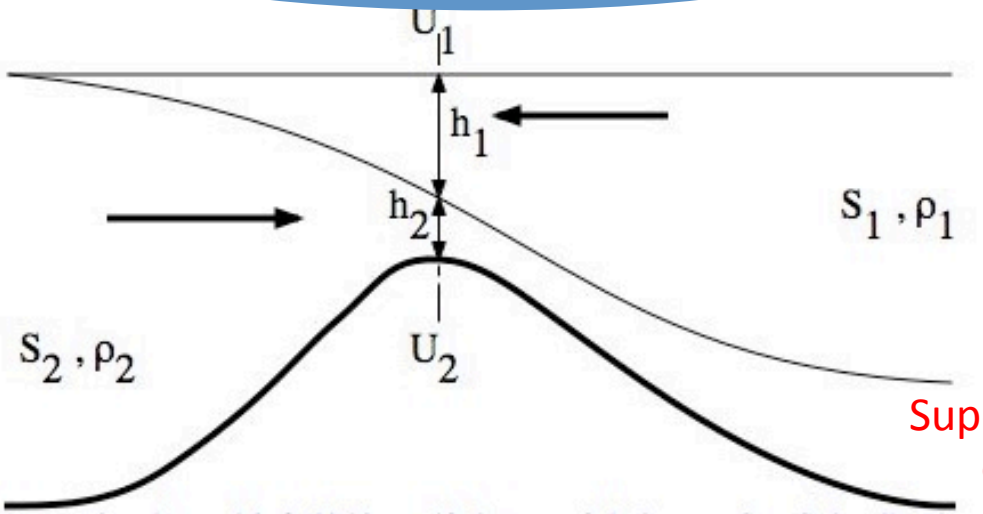

Subcritical
$G^2<1$

Supercritical
$G^2>1$

Figure 3.7. A general section model of a highly stratified estuary. Q_j is the water flow, S_j describes the salinity over the j-th border (Tomczak, 1998.)

where $g' = g\Delta\varrho / \varrho = g(S_2-S_1)/S_2\varrho$ is the reduced gravity and U_1 and U_2 are the velocities in each layer. The situation is shown in Figure 3.7 and is usually applicable to fjord-like estuaries.

The sill has a width B and depth H, the freshwater inflow to the estuary is Q_f. Setting $u_1h_1 = q_1 = Q_1/B$, $u_2h_2 = q_2 = Q_2/B$ and $q_f = Q_f/B$ and defining the relative layer thickness as

$$h_1 = (1-\eta)H;\ \ h_2 = \eta H \qquad \text{(Eq. 3.14)}$$

gives together with Eq. 3.13 the dynamic sill condition i terms of q.

$$\frac{q_1^2}{(1-\eta)^3} + \frac{q_2^2}{\eta^3} = g' H^3 \qquad \text{(Eq. 3.15)}$$

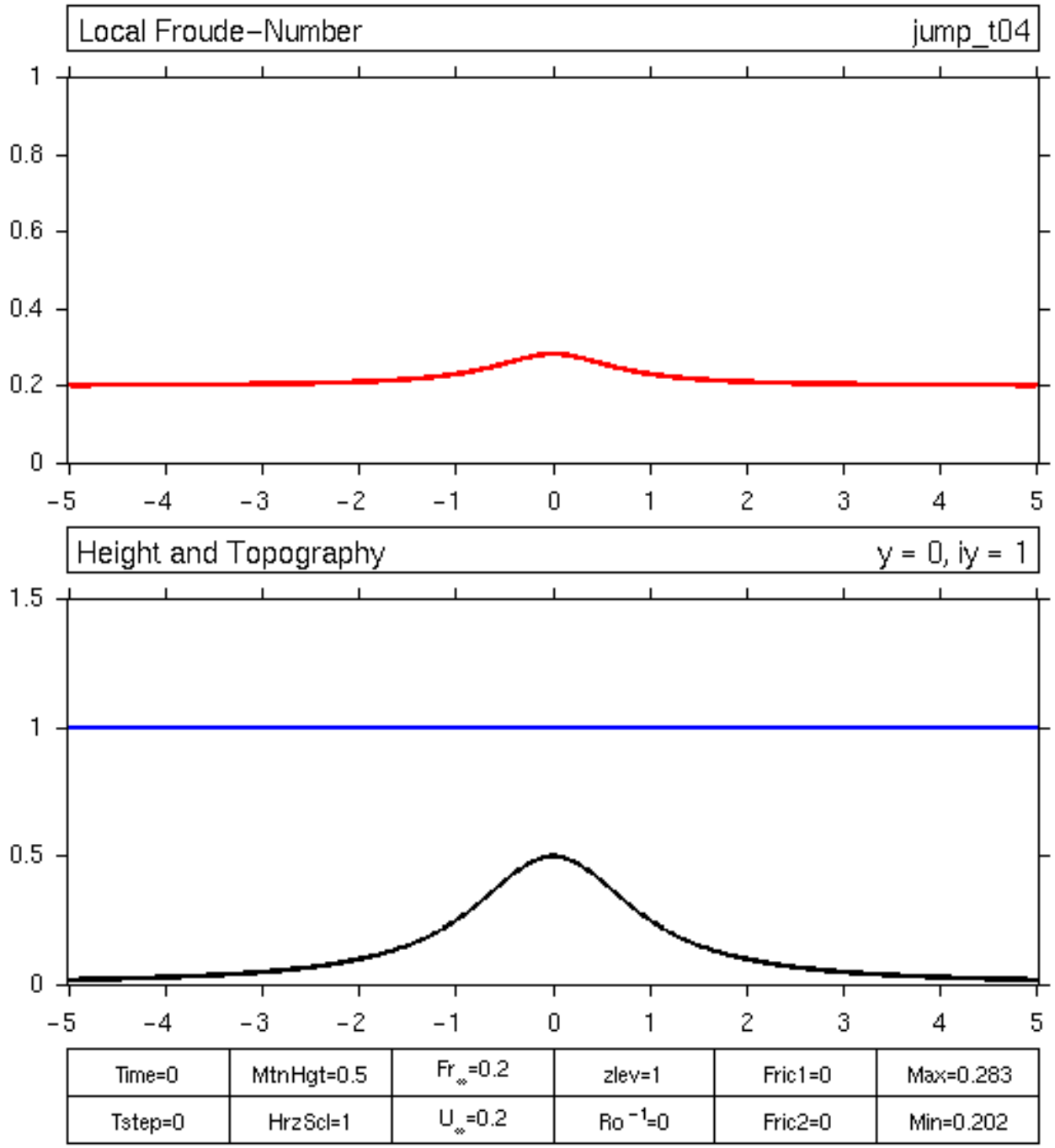
Local Froude–Number
jump_t04
1
0.8
0.6
0.4
0.2
0
−5
−4
−3
−2
−1
0
1
2
3
4
5
Height and Topography
y = 0, iy = 1
1.5
1
0.5
0
Time=0
MtnHgt=0.5
Fr∞=0.2
zlev=1
Fric1=0
Max=0.283
Tstep=0
HrzScl=1
U∞=0.2
Ro−1=0
Fric2=0
Min=0.202

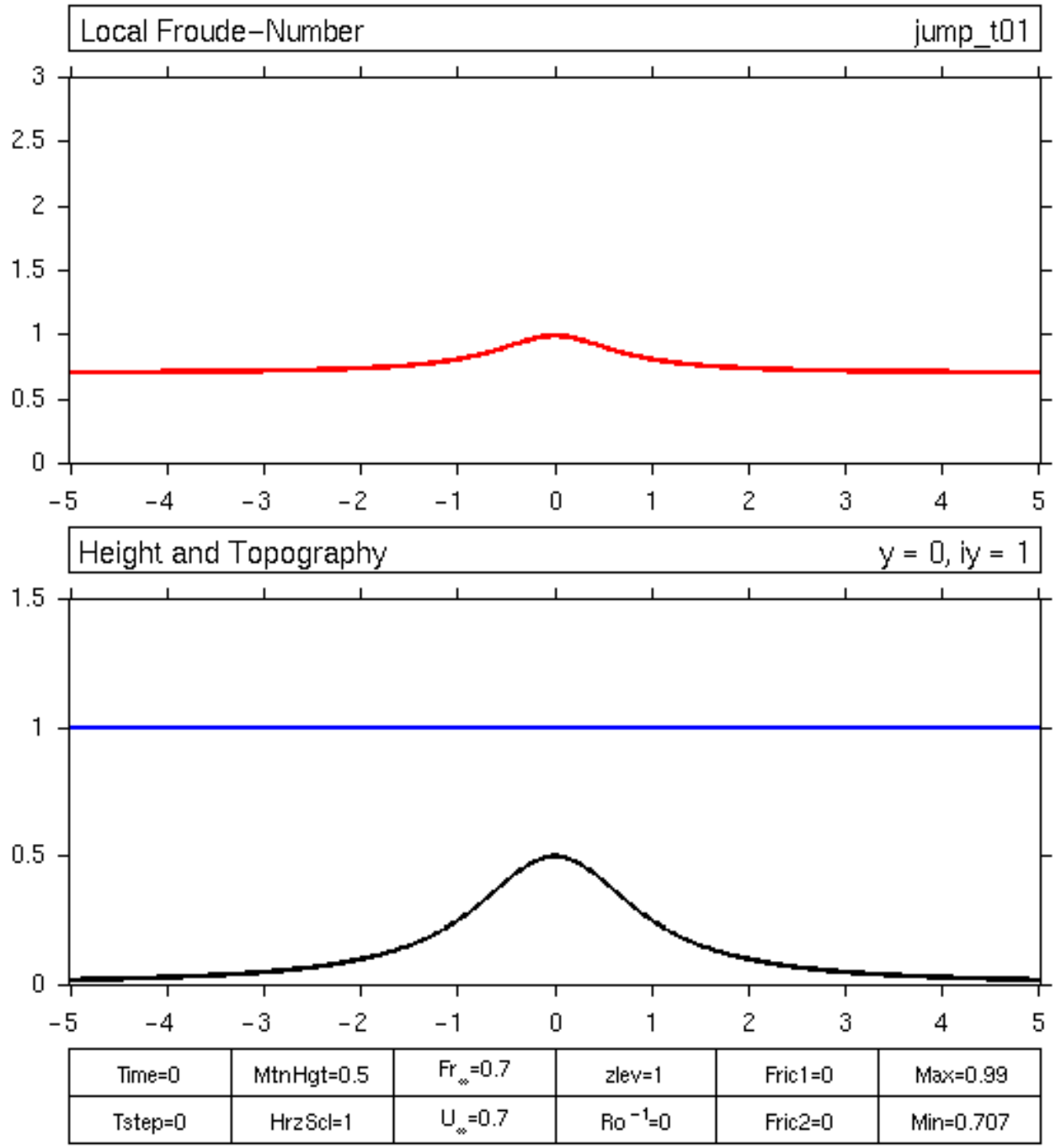
Local Froude−Number
jump_t01
3
2.5
2
1.5
1
0.5
0
−5
−4
−3
−2
−1
0
1
2
3
4
5
Height and Topography
y = 0, iy = 1
1.5
1
0.5
0
−5
−4
−3
−2
−1
0
1
2
3
4
5
Time=0
MtnHgt=0.5
Fr∞=0.7
zlev=1
Fric1=0
Max=0.99
Tstep=0
HrzScl=1
U∞=0.7
Ro−1=0
Fric2=0
Min=0.707

Hydraulic jump in boat’s wake

Circular hydraulic jump in kitchen sink

Armi and Mayr, 2011, J. Appl. Met. Clim.
The Descending Stratified Flow and Internal Hydraulic Jump
In the Lee of the Sierras

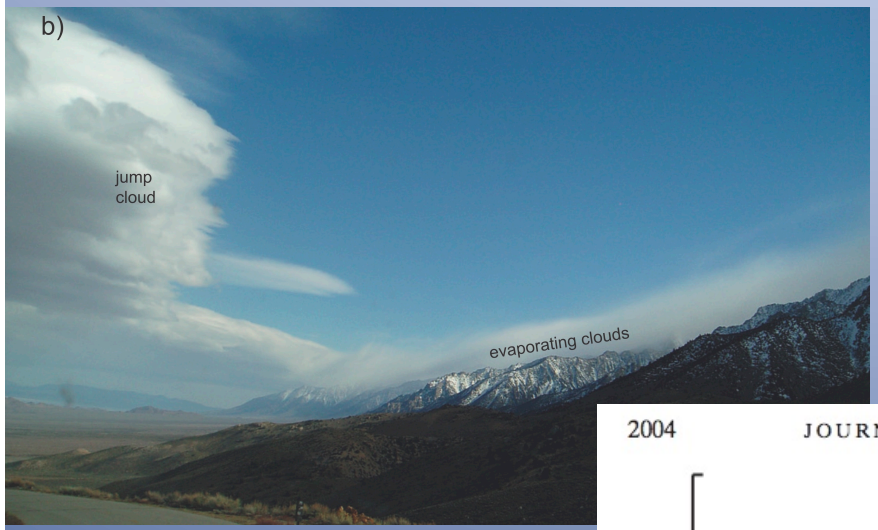

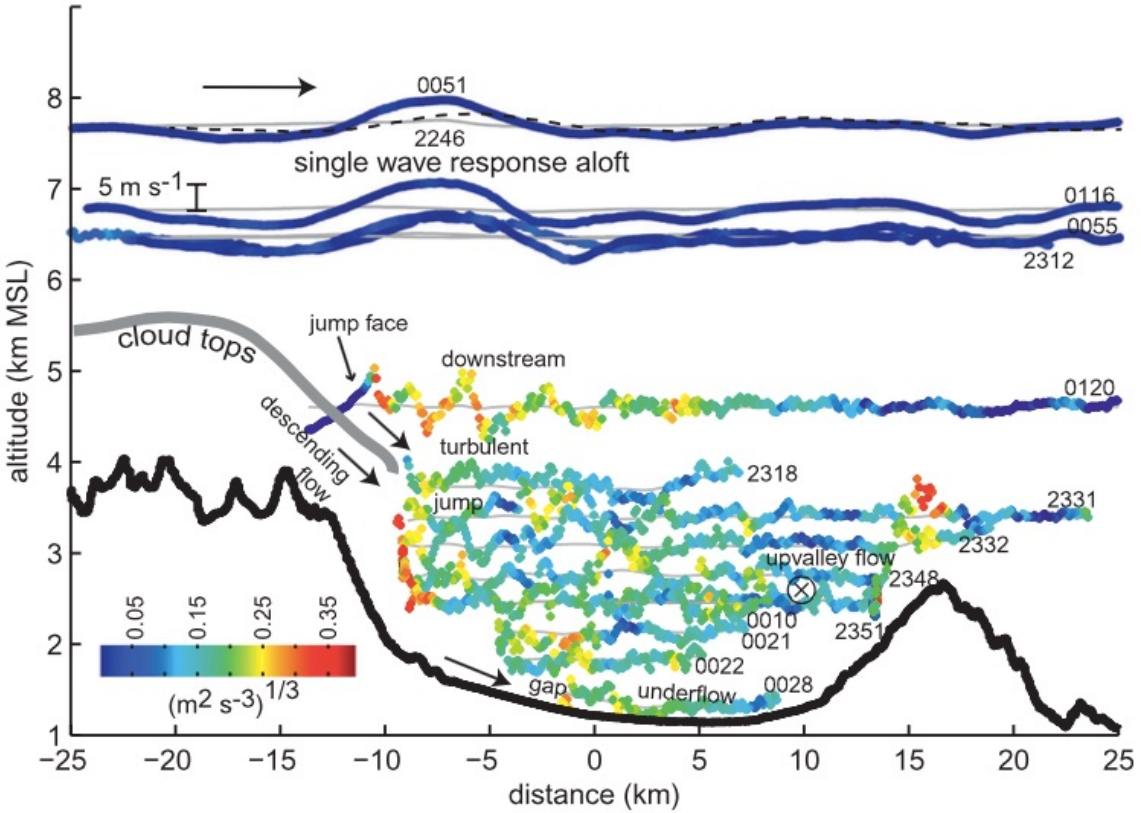

FIG. 10. Vertical cross section of King Air aircraft data approximately from west to east: vertical wind speed (m s^{-1}) is shown as lines oscillating around aircraft tracks and color coded with the u component of the turbulent dissipation rate [color bar; $(m^2\ s^{-3})^{1/3}$]. The early leg at 7.7 km is dashed for clarity.

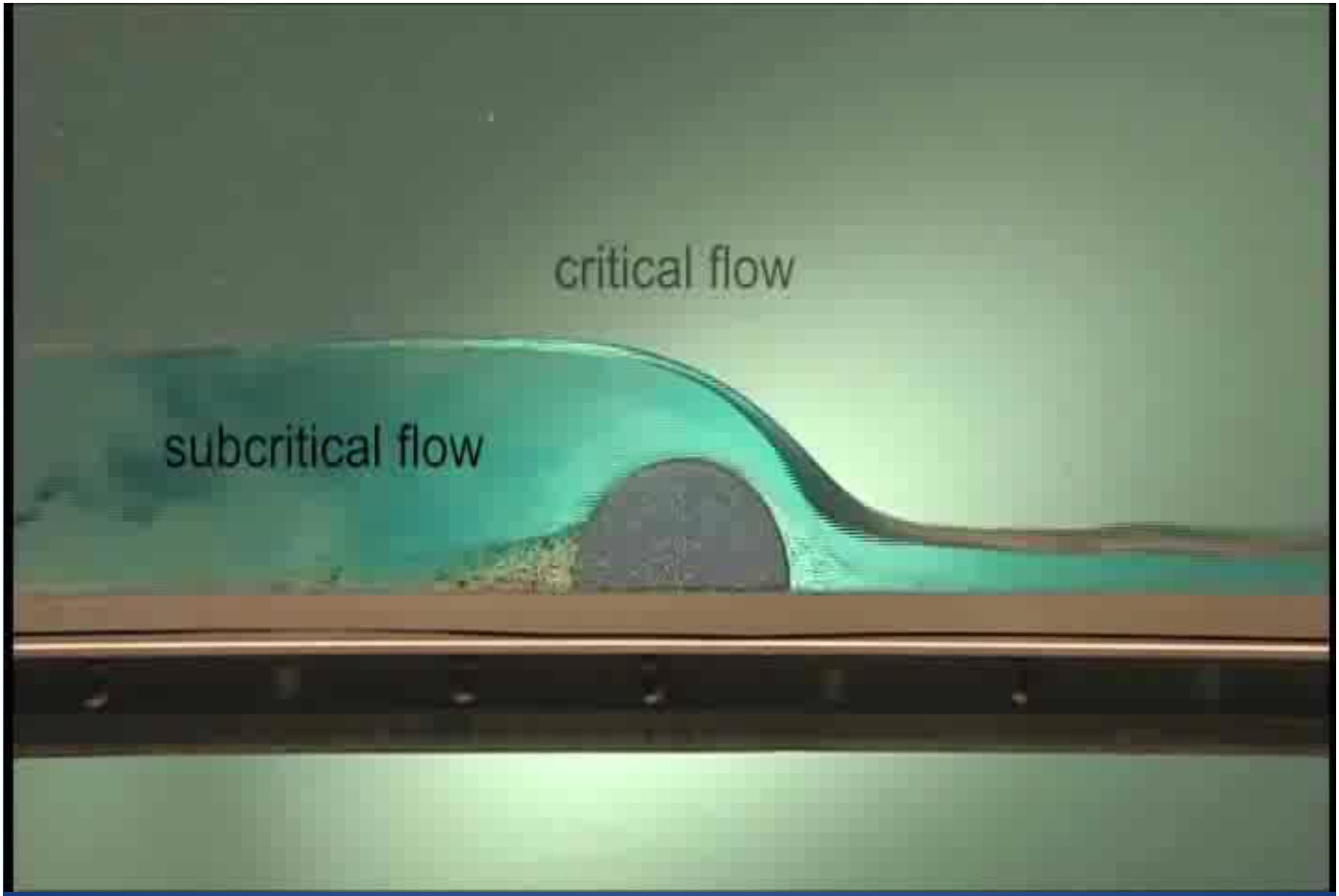
critical flow
subcritical flow

MAXIMAL EXCHANGE THEORY
for a two-layer flow

$$F_i^2 = \frac{u_i^2}{g' h_i}, \qquad g' = g\frac{\varrho_2 - \varrho_1}{\varrho_2} \qquad G^2 = F_1^2 + F_2^2 = 1.$$

Summary sketch of the Bosphorus flow, Özsoy et al., 1998

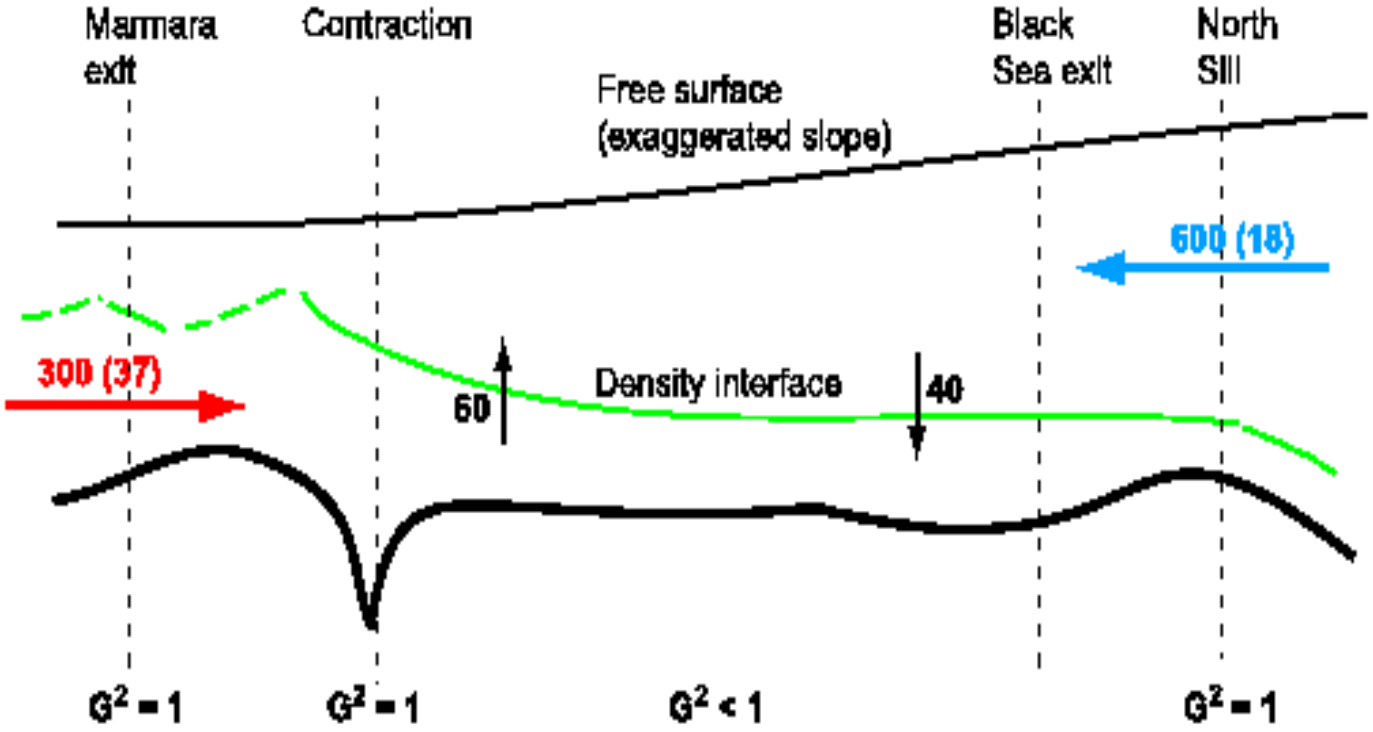

Maximal exchange solution:
If two topographic controls (a sill on the lower density side, and a contraction on the higher density side, there is a unique solution fully determined by the strait, for which the exchange is the greatest.
Armi and Farmer, 1986

Samsung

Bosphorus Inter-continental Swim Competition 26 July 2015

Boğaziçi Kıtalararası Yüzme Yarışı, 26 Temmuz 2015

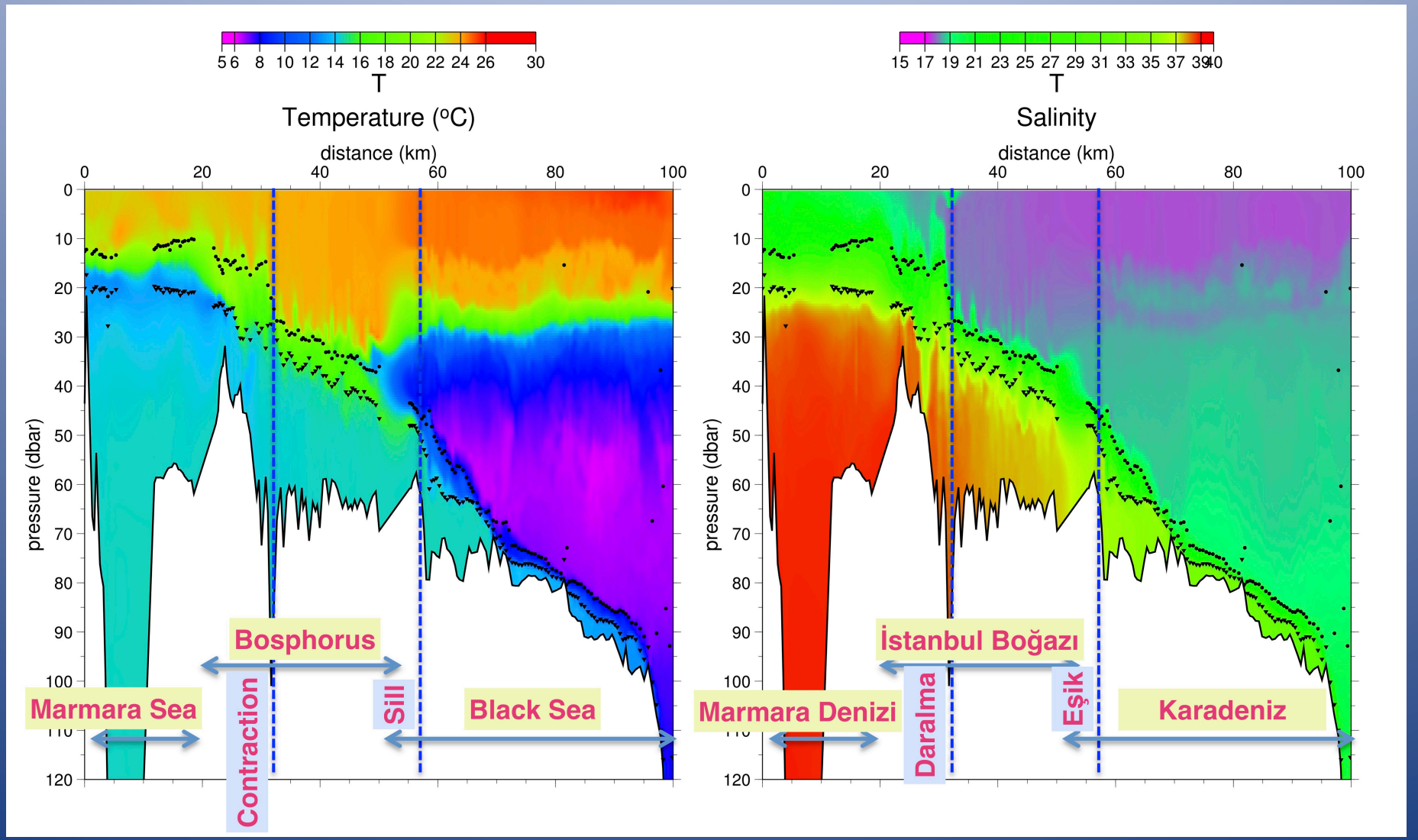

Measurements in the Bosphorus (1994)
Gregg et al., 1999; Gregg and özsoy, 1999, 2002

normal lower layer blocked

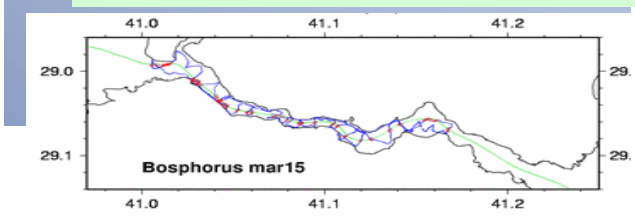

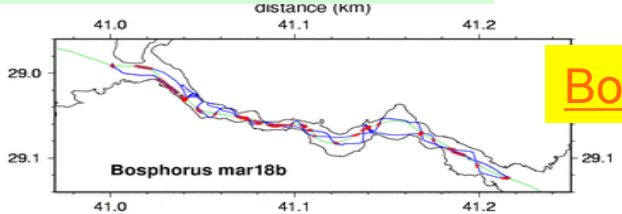

Bosphorus ADCP measurements

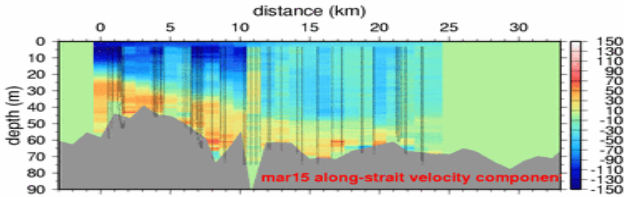

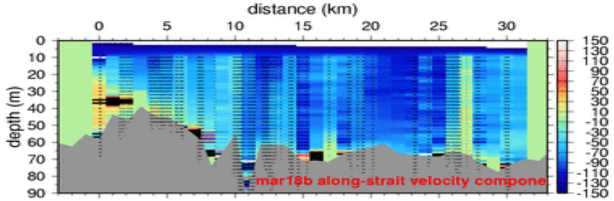

2-layer exchange flows (blocking of layered flows)

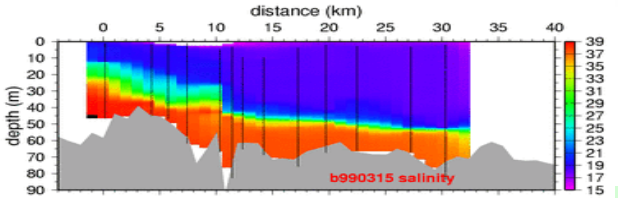

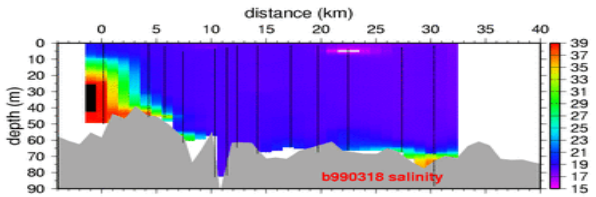

Bosphorus CTD measurements

normal lower layer blocked upper layer blocked

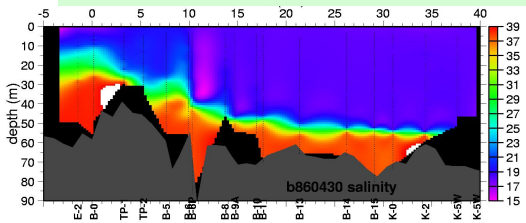

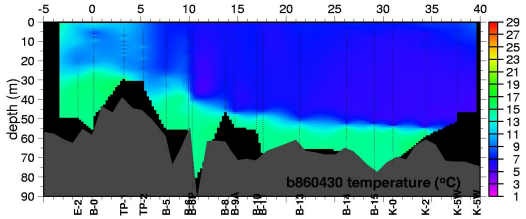

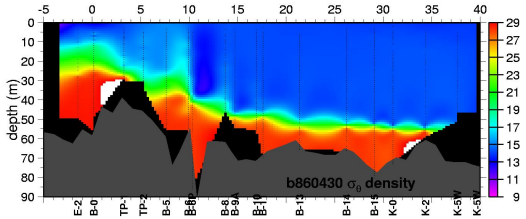

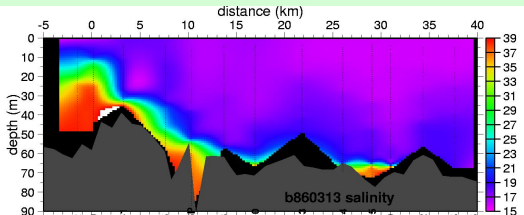

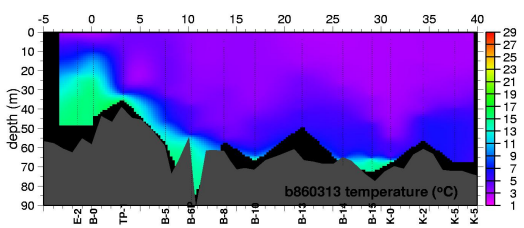

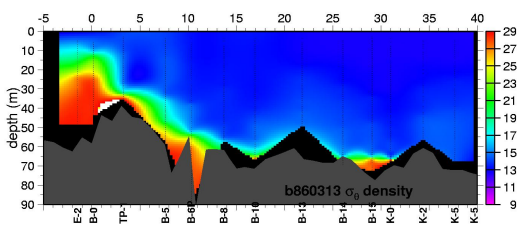

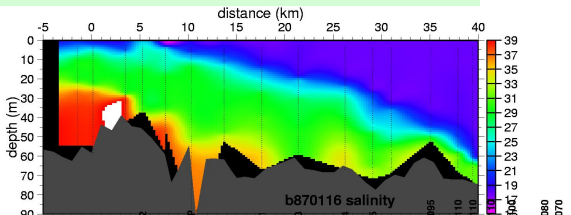

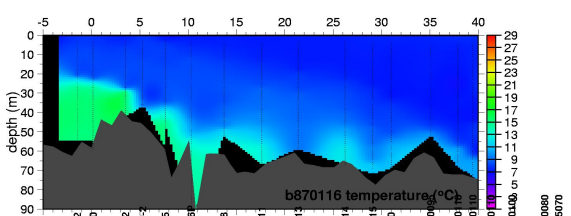

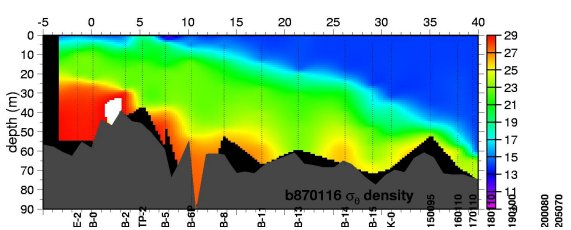

Simple linear model of TSS sea level oscillations at Marmara and Black Seas versus barotropic fluxes at Bosphorus and Dardanelles Straits ?

Özsoy et al., 1998

$$S_b \frac{\partial \eta_b}{\partial t} = Q_f - A_b u_b,$$

$$S_m \frac{\partial \eta_m}{\partial t} = A_b u_b - A_d u_d,$$

$$\frac{\partial u_b}{\partial t} = \frac{\Delta_{bm}}{\rho L_b} + \frac{g}{L_b}(\eta_b - \eta_m) - \lambda_b u_b,$$

$$\frac{\partial u_d}{\partial t} = \frac{\Delta_{ma}}{\rho L_d} + \frac{g}{L_d}(\eta_m - \eta_a) - \lambda_d u_d,$$

$$\frac{\partial^2 \eta_b}{\partial t^2} + \lambda_b \frac{\partial \eta_b}{\partial t} + \alpha_b \eta_b - \alpha_b \eta_m = \frac{1}{S_b}\left(\frac{\partial Q_f}{\partial t} + \lambda_b Q_f\right) - \beta_b \Delta_{bm}$$

$$\frac{\partial^2 \eta_m}{\partial t^2} + \lambda_d \frac{\partial \eta_m}{\partial t} + (\alpha_d + s\alpha_b)\eta_m - s(\lambda_d - \lambda_b)\frac{\partial \eta_b}{\partial t} - s\alpha_b \eta_b - s\alpha_d \eta_a = -(\lambda_d - \lambda_b)\frac{1}{S_m} Q_f - \beta_d \Delta_{ma} + s\beta_b \Delta_{bm}$$

$$\alpha_b = \frac{g A_b}{L_b S_b}, \quad \alpha_d = \frac{g A_d}{L_d S_m}, \beta_b = \frac{\alpha_b}{\rho g}, \quad \beta_d = \frac{\alpha_d}{\rho g}, s = \frac{S_b}{S_m}.$$

$$T_b = \frac{2\pi}{\sqrt{\alpha_b}} = \frac{2\pi}{\sqrt{\frac{g}{S_b}\frac{A_b}{L_b}}}, \quad T_m = \frac{2\pi}{\sqrt{\alpha_d + s\alpha_b}} = \frac{2\pi}{\sqrt{\frac{g}{S_m}\left(\frac{A_d}{L_d} + \frac{A_b}{L_b}\right)}}.$$

$$T_b = 14.7d, \; T_d = 1.9d$$

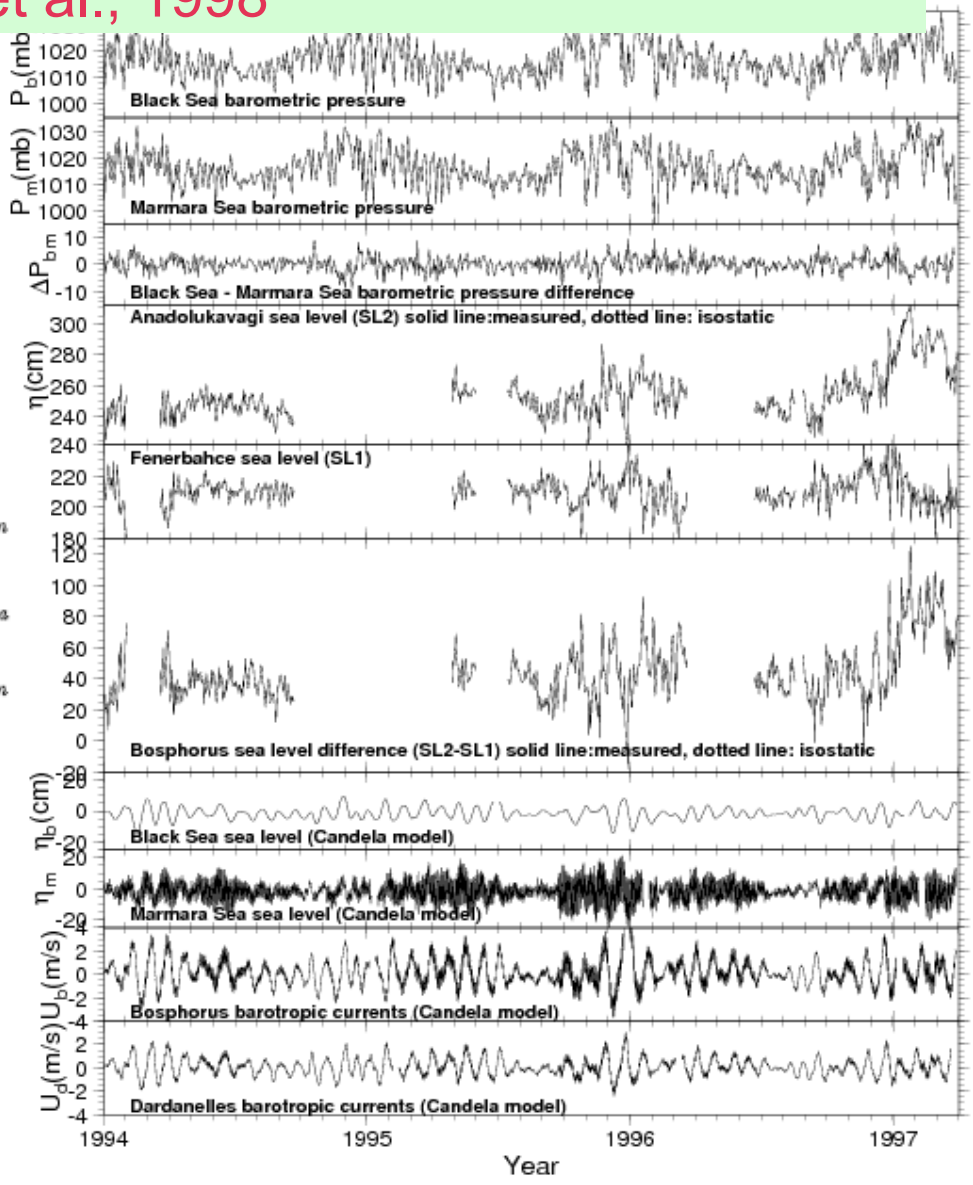

A simple two-layer model of the Bosphorus Exchange Flow
Özsoy, 1990; Özsoy et al., 1998.

Model integrated between two control sections and with
Black Sea water balance, free surface storage

$$S_b \frac{\partial \eta_b}{\partial t} = Q_f + Q_2 - Q_1$$

$$\frac{1}{2}\{u_{1s}^2\} = \frac{\Delta_{bs}}{\rho_1} + g(\eta_b - \eta_s)$$

$$\frac{1}{2}\{u_{1c}^2 - u_{1s}^2\} = \frac{\Delta_{sc}}{\rho_1} + g\eta_s - \int_{x_c}^{x_s} \frac{\tau_w}{\rho_1 y_1} dx - \int_{x_c}^{x_s} \frac{\tau_i}{\rho_1 y_1} dx$$

$$\frac{1}{2}\{u_{2c}^2 - u_{2s}^2\} = \frac{\Delta_{sc}}{\rho_2} + g\{\eta_s - \varepsilon(y_{1s} - y_{1c})\} + \int_{x_c}^{x_s} \frac{\tau_i}{\rho_1 y_2} dx + \int_{x_c}^{x_s} \frac{\tau_b}{\rho_2 y_2} dx$$

$$\frac{u_{1c}^2}{\varepsilon g y_{1c}} + \frac{u_{2c}^2}{\varepsilon g y_{2c}} = 1$$

$$\frac{u_{1s}^2}{\varepsilon g y_{1s}} + \frac{u_{2s}^2}{\varepsilon g y_{2s}} = 1$$

$$y_{1c} + y_{2c} = y_o$$

$$y_{1s} + y_{2s} + H_s = \eta_s + y_o$$

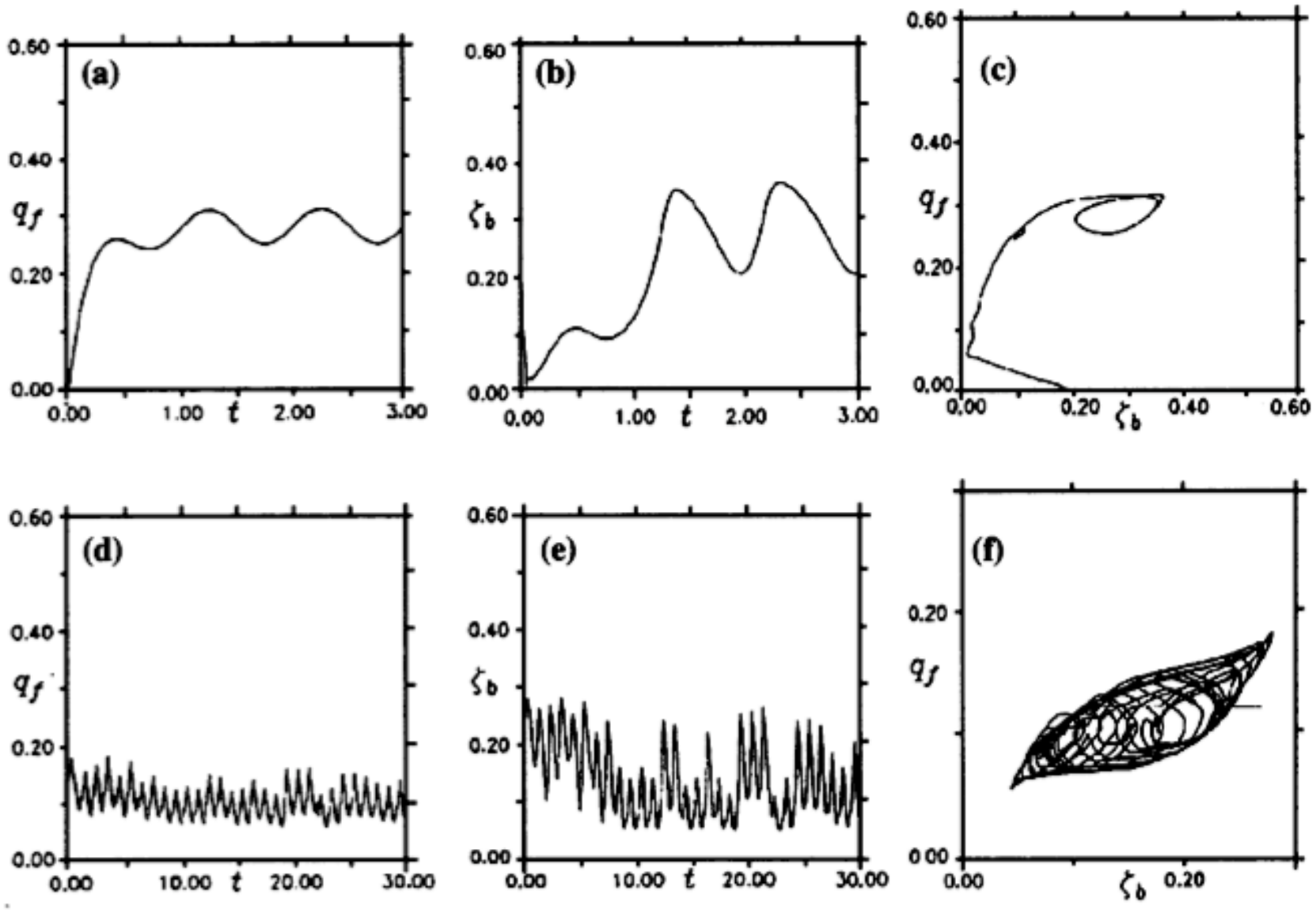

Figure 4 – Top: a three-year run of the seasonal model with (a) forcing q_f, and (b) the sea-level response, and (c) q_f versus ζ_b. Bottom: a thirty year simulated run of the seasonal model, with (d) synthetic fresh water inflow q_f, (e) the sea-level response ζ_b, and (f) q_f *versus* ζ_b (after ÖZSOY, 1990).

2D STRAIT MODEL

WIDTH-INTEGRATED, TIME DEPENDENT, NON-HYDROSTATIC, TURBULENT

$$\frac{\partial \zeta}{\partial t} - \frac{1}{B} J(\psi, \zeta) + \frac{\zeta}{B^2} J(B, \zeta) = \frac{g}{\rho_o} \frac{\partial \rho}{\partial x} - \frac{1}{B} \nabla \cdot B \nu_{ik} \nabla \zeta$$

$$- S_f \frac{\zeta}{B} |\nabla \psi| + \ldots \text{additional terms} \ldots$$

$$\frac{\partial T}{\partial t} - \frac{1}{B} J(\psi, T) = -\frac{1}{B} \nabla \cdot B K^T_{ik} \nabla T$$

$$\frac{\partial S}{\partial t} - \frac{1}{B} J(\psi, S) = -\frac{1}{B} \nabla \cdot B K^S_{ik} \nabla S$$

$$\frac{\partial C}{\partial t} - \frac{1}{B} J(\psi, C) = -\frac{1}{B} \nabla \cdot B K^C_{ik} \nabla C$$

$$\nabla \cdot \frac{1}{B} \nabla \psi = \zeta$$

and supplemented by an equation of state $\rho = \rho(T, S)$. Here $B(x, z)$ is the width of the strait, ν_{ik}, K_{ik} are the eddy viscosity and diffusion coefficients, the velocity field and the vorticity are given by $\vec{u} = \hat{j} \times \nabla \psi / B$, $\zeta = \hat{j} \cdot \nabla \times \vec{u}$, and the Jacobian is defined as $J(a, b) = a_x b_z - b_x a_z$.

Richardson number dependent mixing or Smagorinsky type mixing are implemented. Boundary conditions - radiation and basin conditions.

Strait with separated contraction and sill

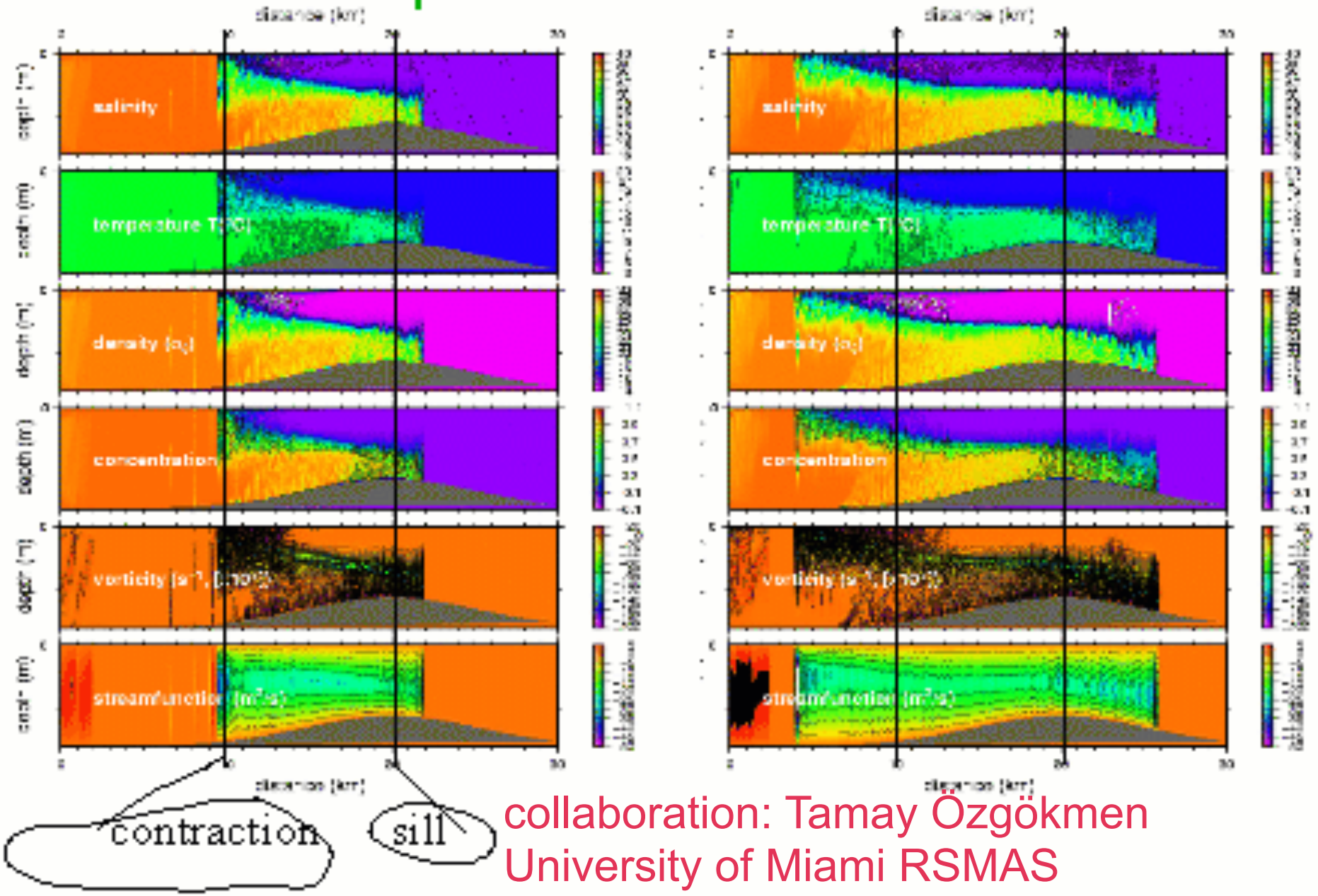

collaboration: Tamay Özgökmen
University of Miami RSMAS

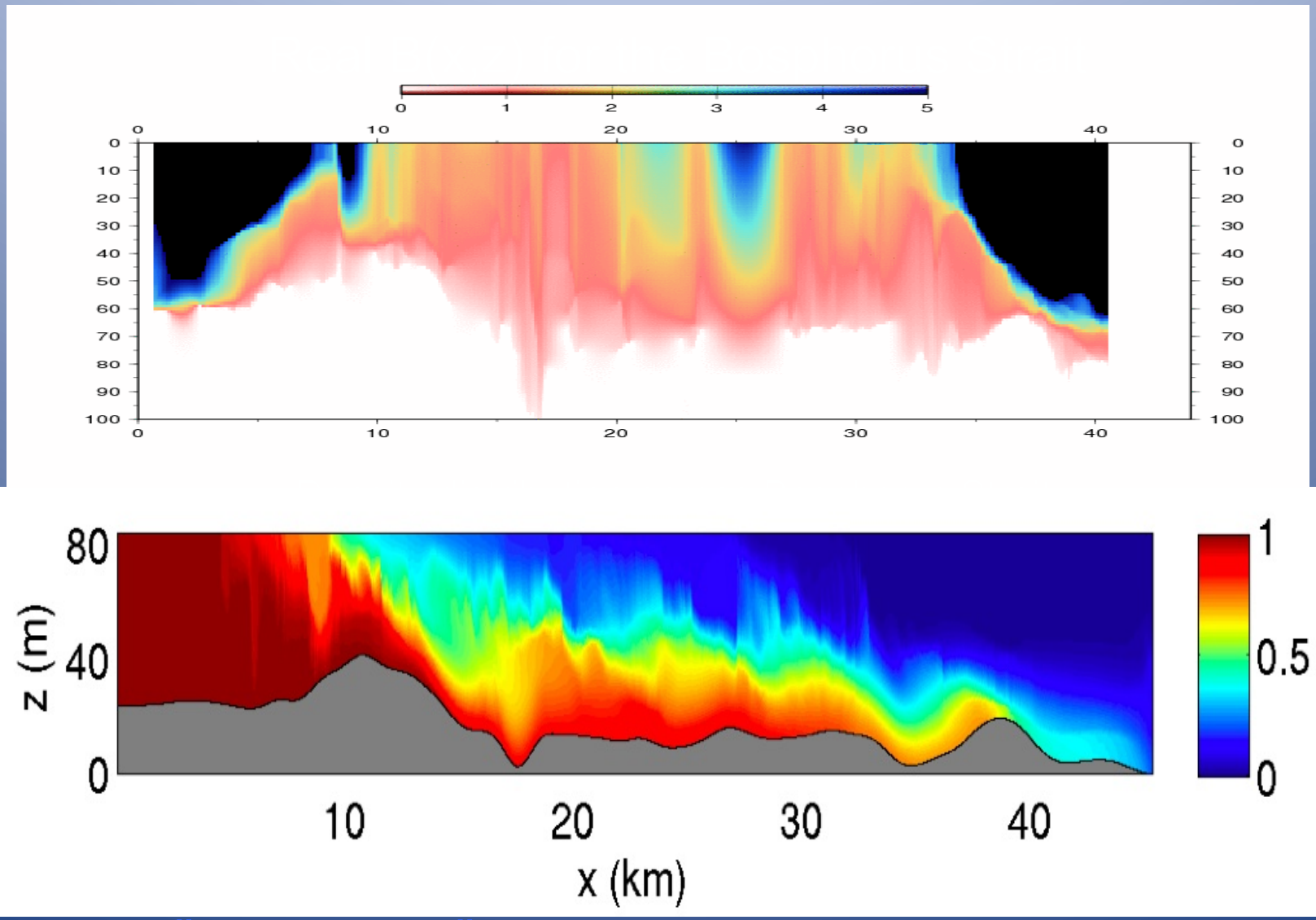

Ilıcak, Özgökmen, Özsoy, Fischer, 2009. Non-hydrostatic Modeling of Exchange Flows Across Complex Geometries, Ocean Modelling

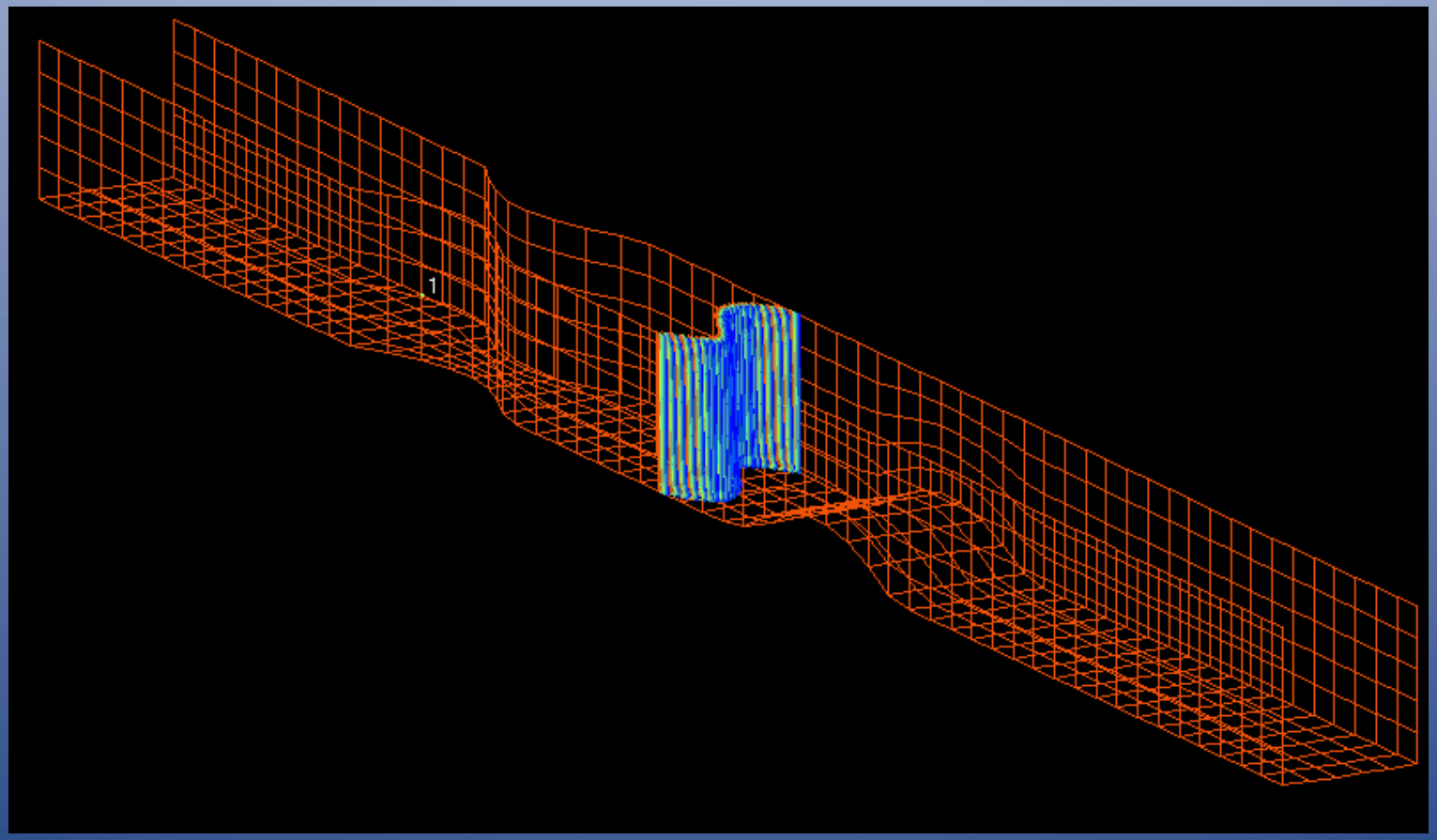

Tamay Özgökmen (RSMAS, Miami)

Adil Sözer (2013)

Numerical Modeling of the Bosphorus Exchange Flow Dynamics, PhD thesis, Institute of Marine Sciences, Middle East Technical University, Erdemli, Mersin, Turkey.

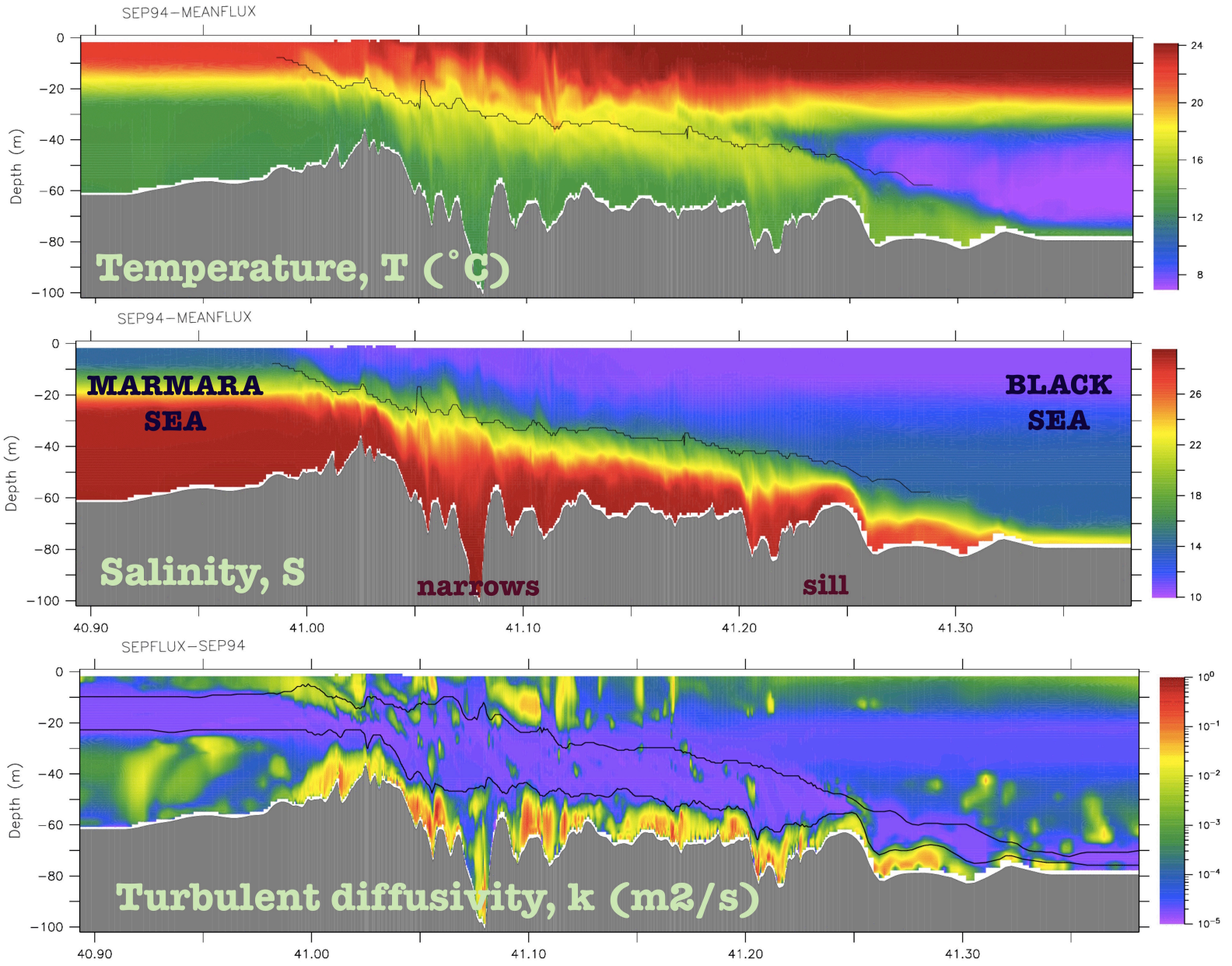

Details of the properties of flow through the Bosphorus along the Bosphorus Strait according to the model of Sözer (2013) – PhD study.

COMPARISON OF TWO DIFFERENT MODELS with OBSERVATIONS
ROMS and MITgcm

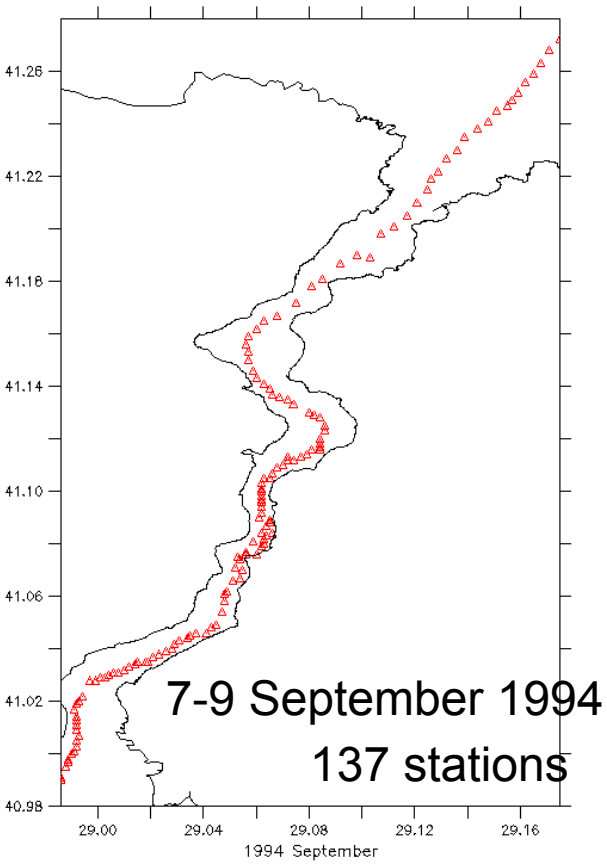

Model vs observations on the cruise path

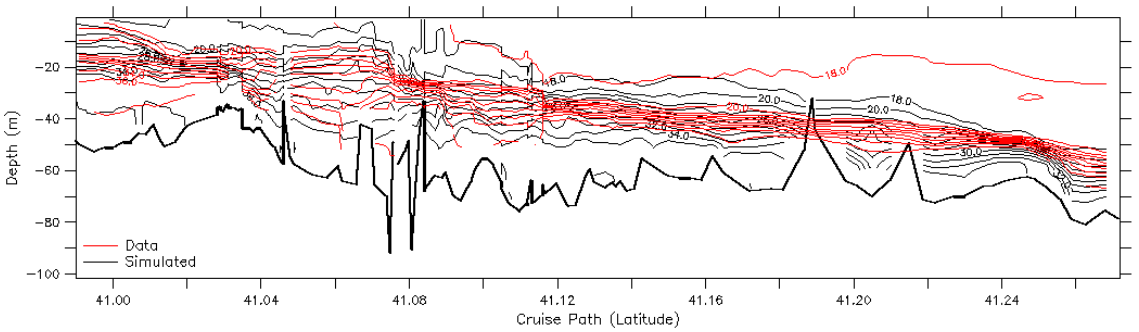

ROMS, Salinity

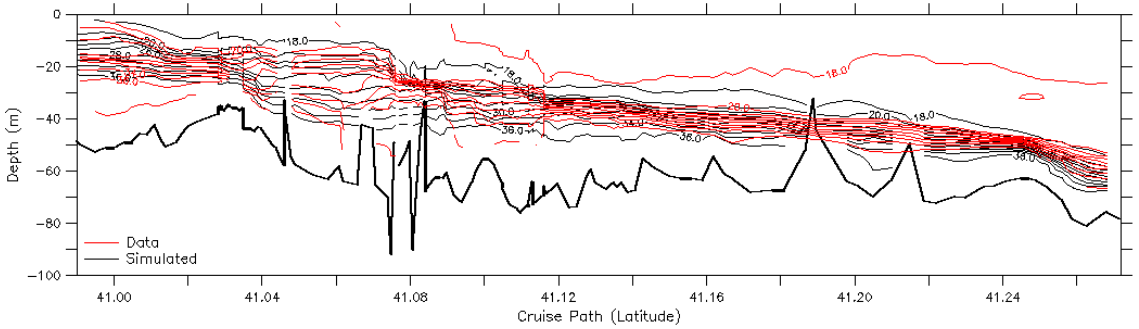

MITgcm, Salinity

COMPARISON OF TWO DIFFERENT MODELS with OBSERVATIONS
ROMS and MITgcm

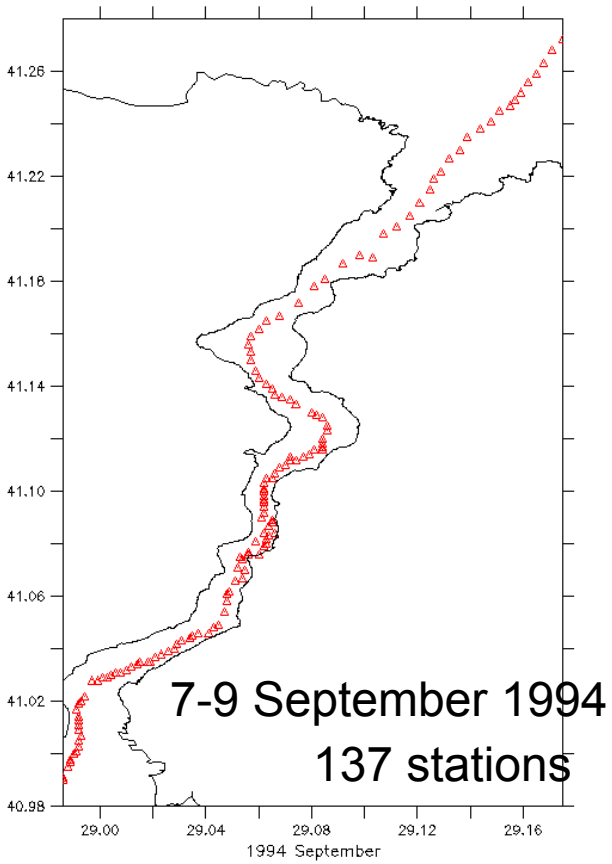

Model vs observations on the cruise path

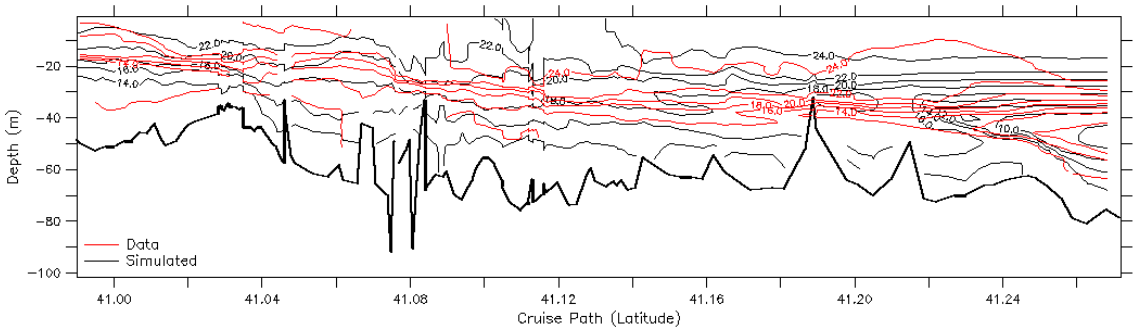

ROMS, Temperature

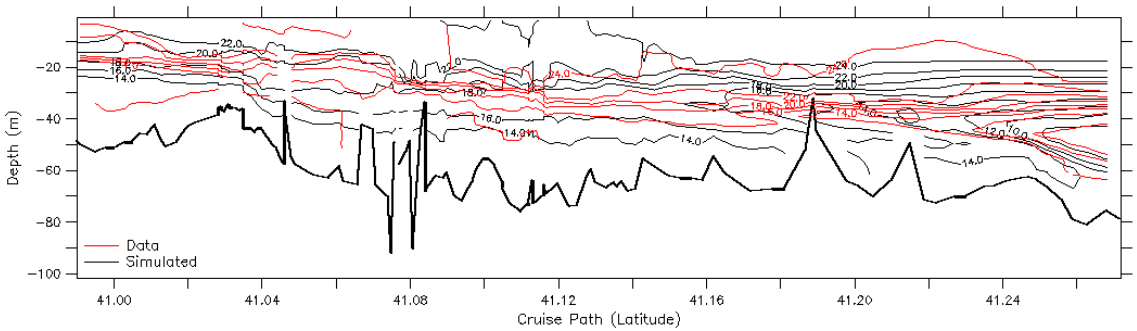

MITgcm, Temperature

TWO-LAYER FROUDE-NUMBER

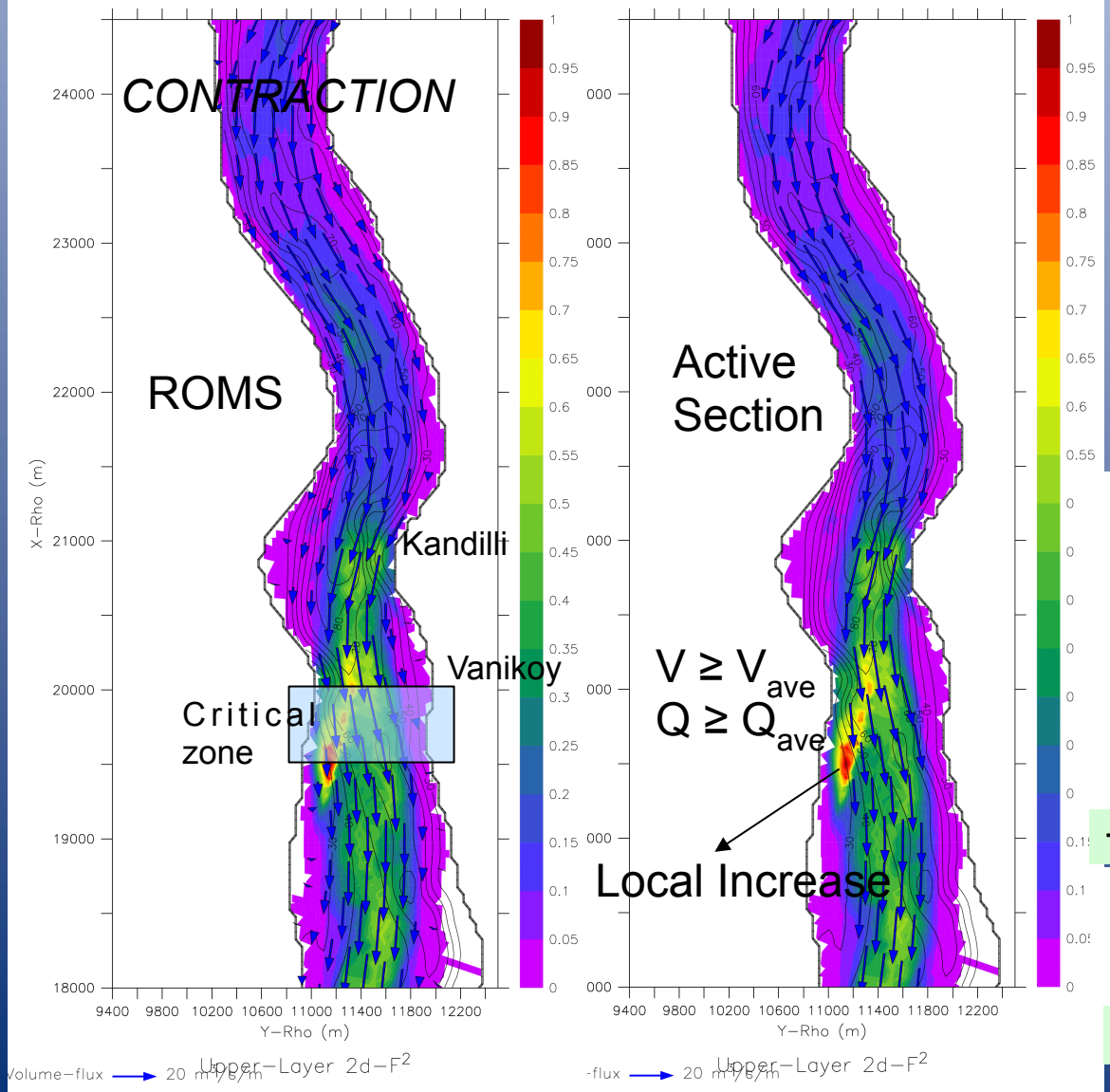

Recirculation

Eddy at the Contraction

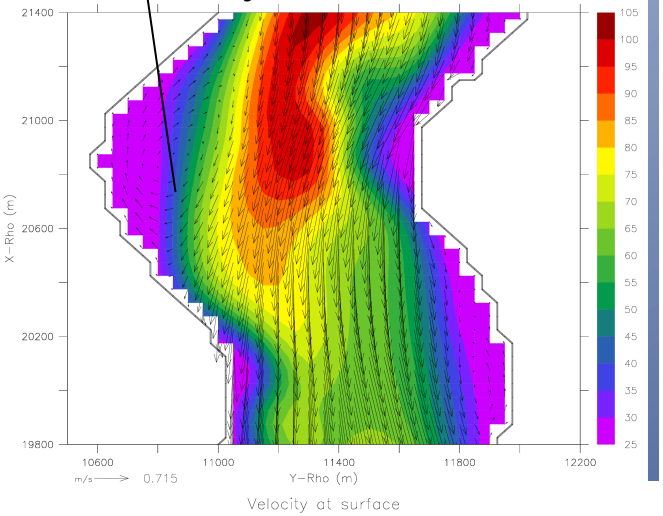

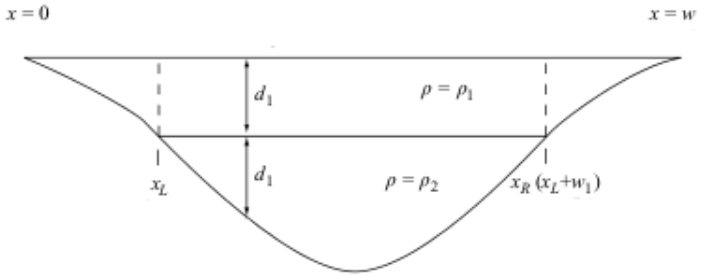

Transverse variation in velocity*

$$G_w^2 = \frac{1}{\frac{1}{w_I}\int_0^w \frac{g' D_1}{V_1^2}\,dx} + \frac{1}{\frac{1}{w_I}\int_{x_L}^{x_R} \frac{g' D_2}{V_2^2}\,dx} = 1.$$

* Pratt 2008

TWO-LAYER FROUDE-NUMBER

SOUTH-EXIT

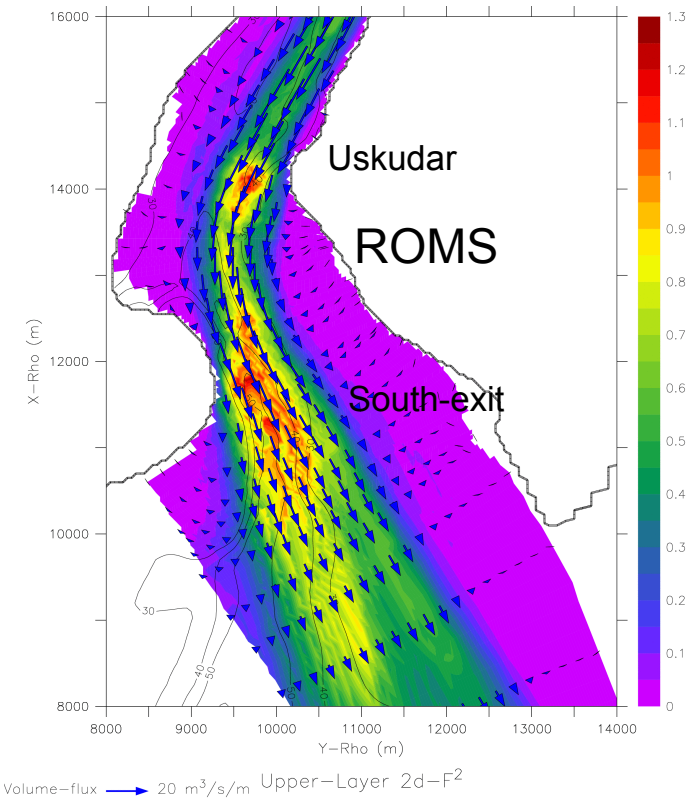

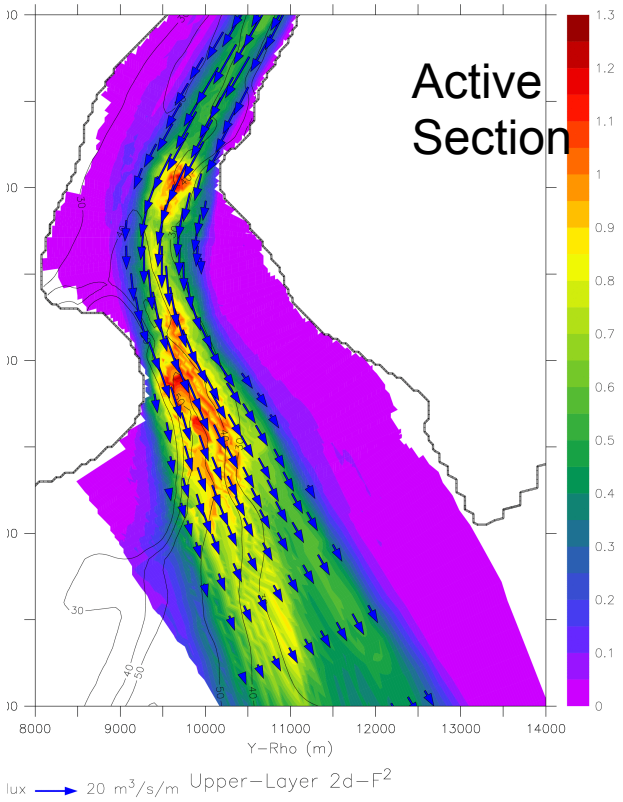

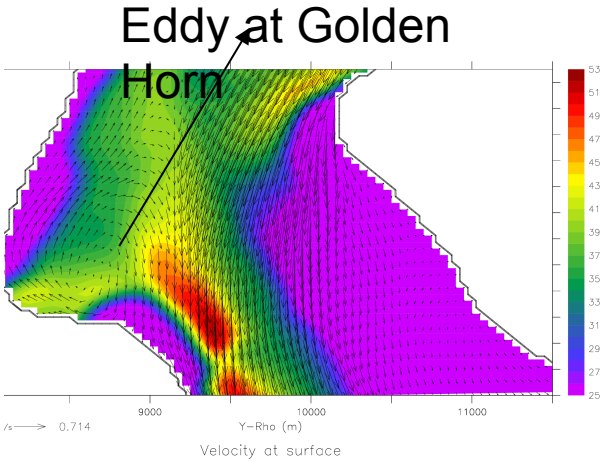

TWO-LAYER FROUDE-NUMBER

NORTH SILL

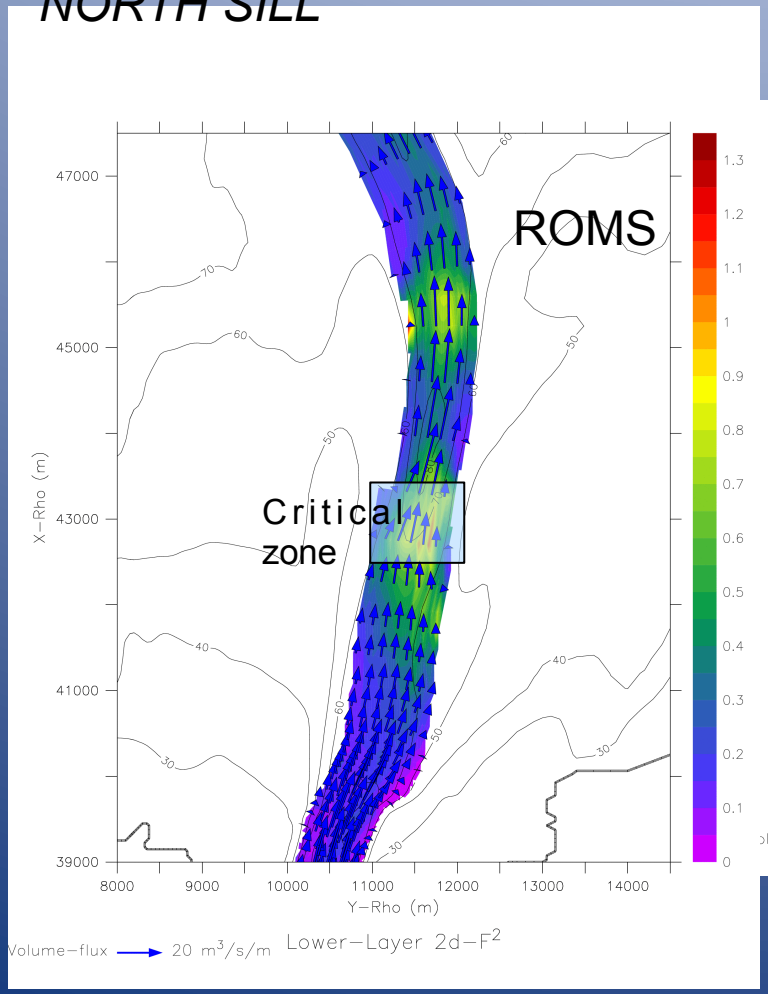

South Sill

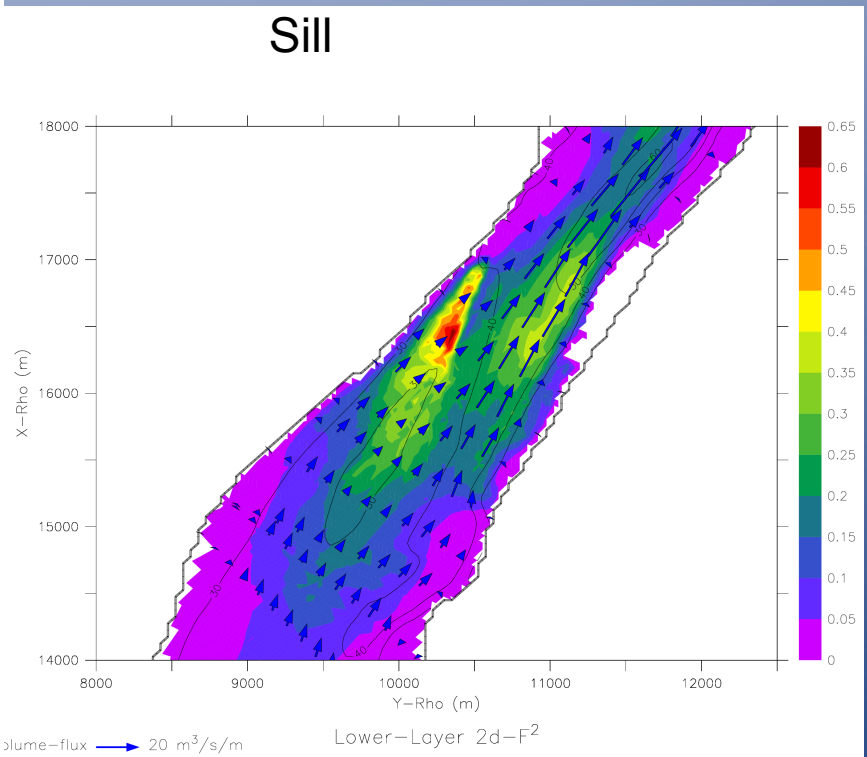

TWO-LAYER FROUDE-NUMBER

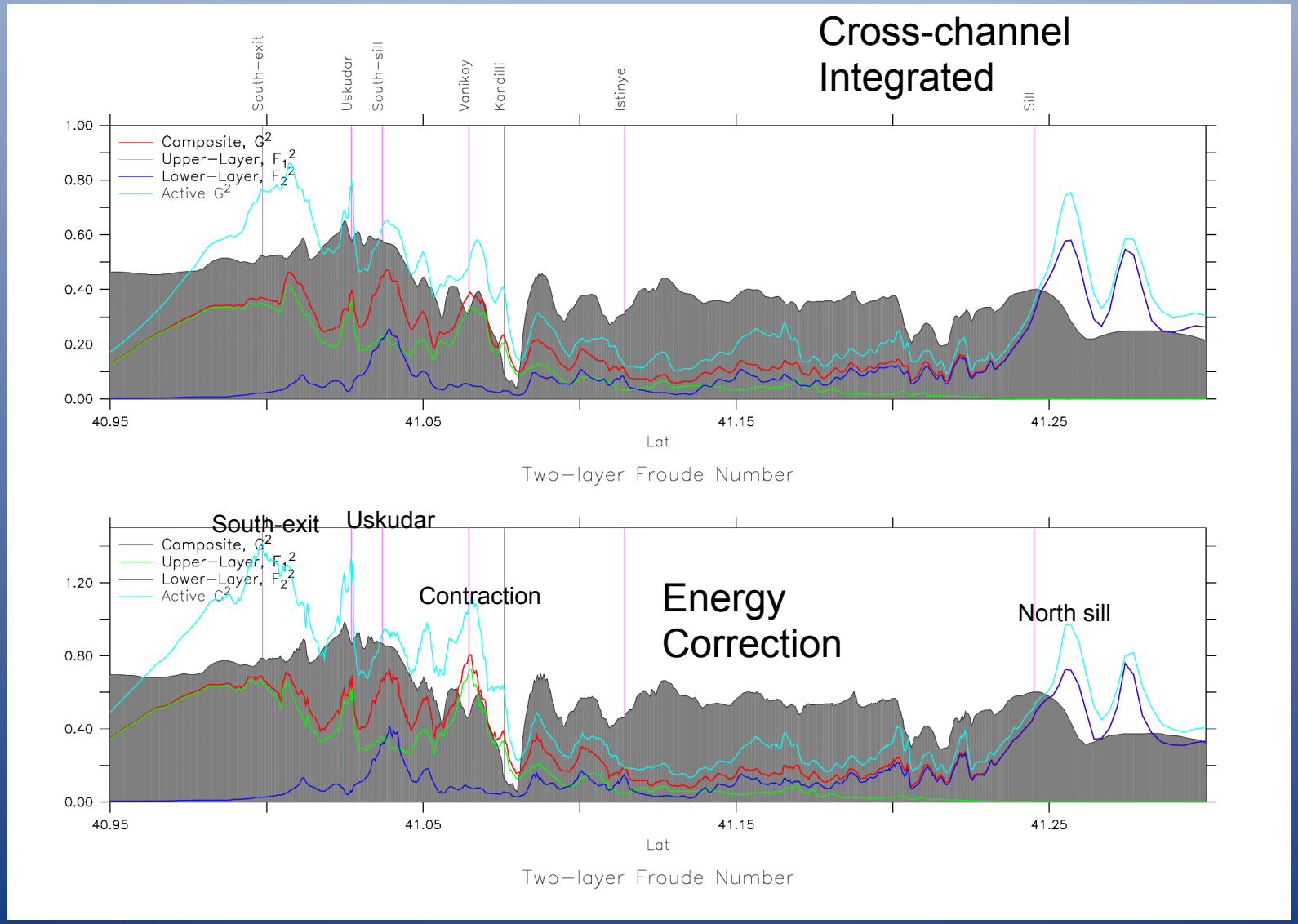

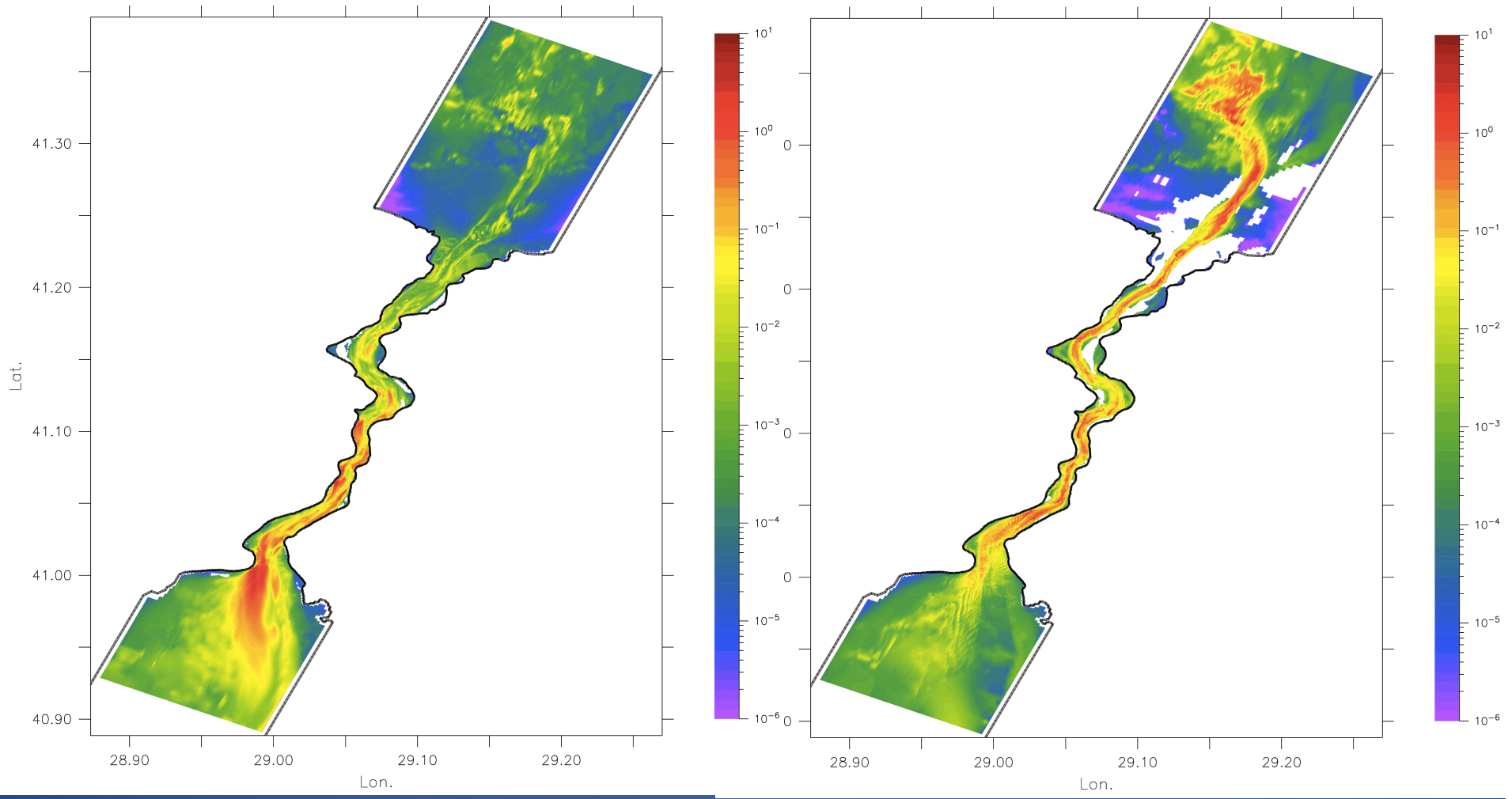

Horizontal distribution of mechanical energy dissipation (W/m^2) in the (a) upper and (b) lower layers

Model results versus ADCP and sea level measurements
Sözer (2012) 3-D model results
Tutsak (2012) Analyses from 4years of measurements
Özsoy and Latif (1994-2000) R/V BİLİM on board ADCP measurements
Merz (1917-1918) measurements)

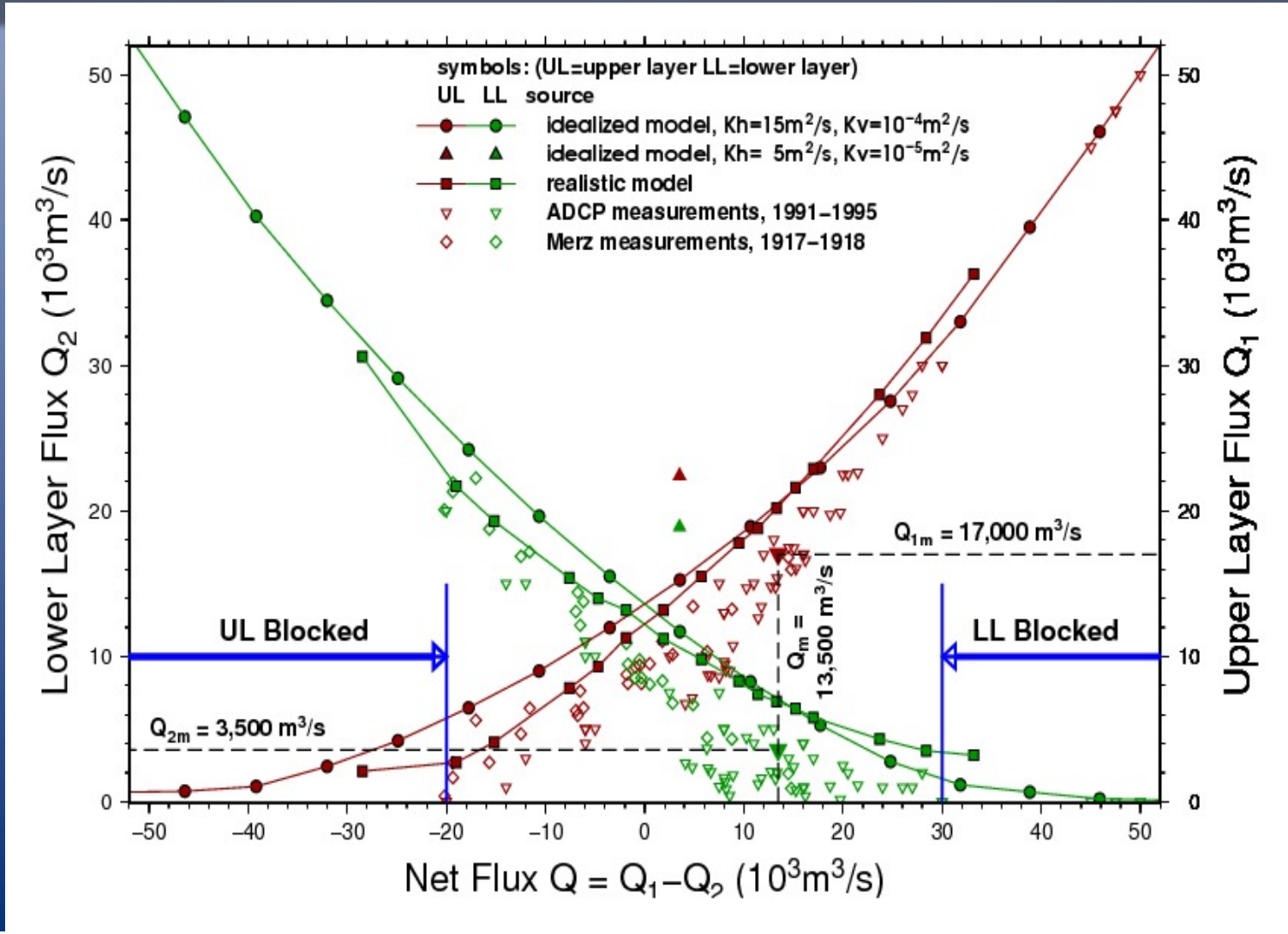

Bosphorus and prototype Canal İstanbul coupled model predictions (Sözer, 2013)

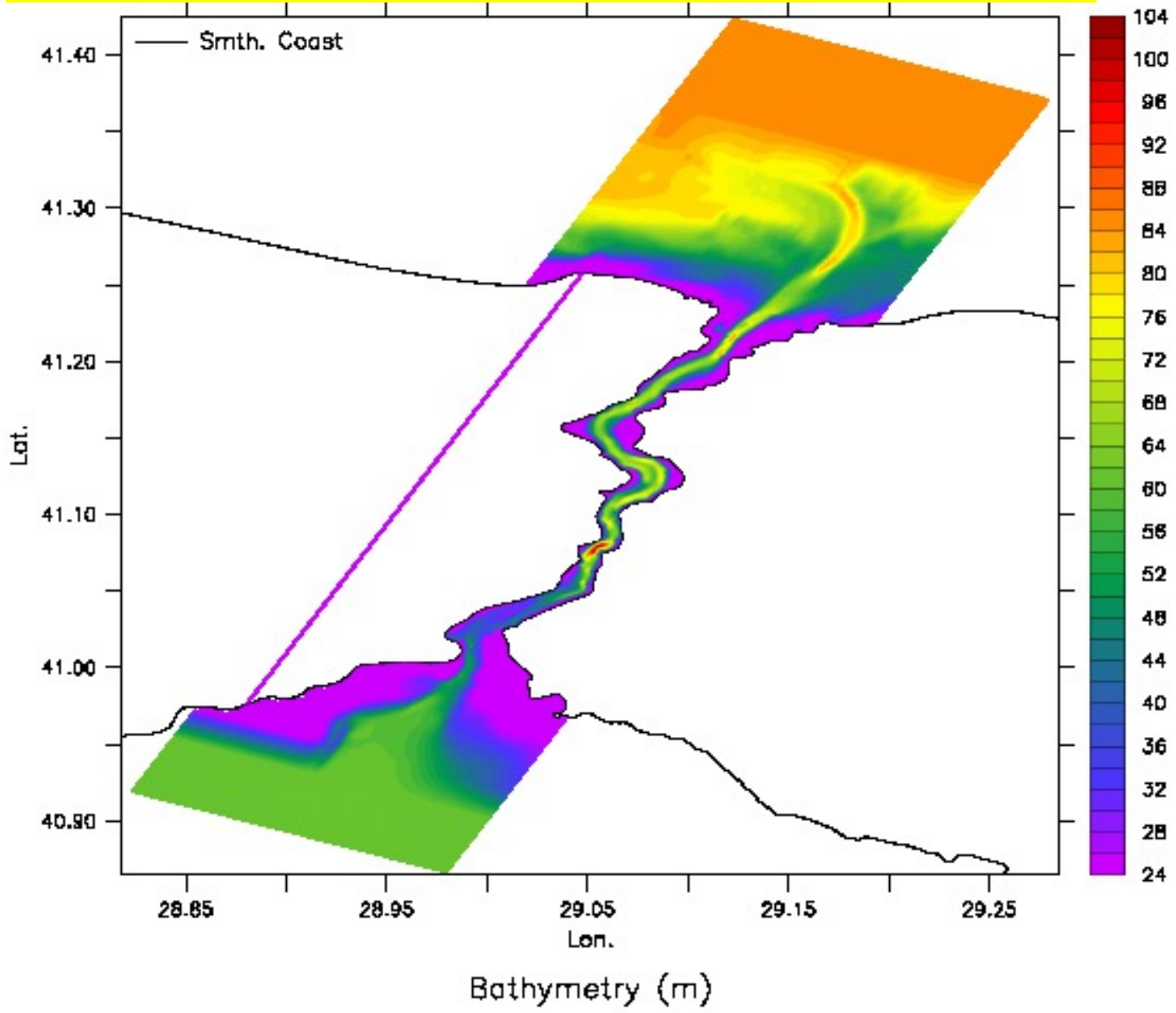

Bosphorus and Canal İstanbul currents (Sözer, 2013)

Bosphorus

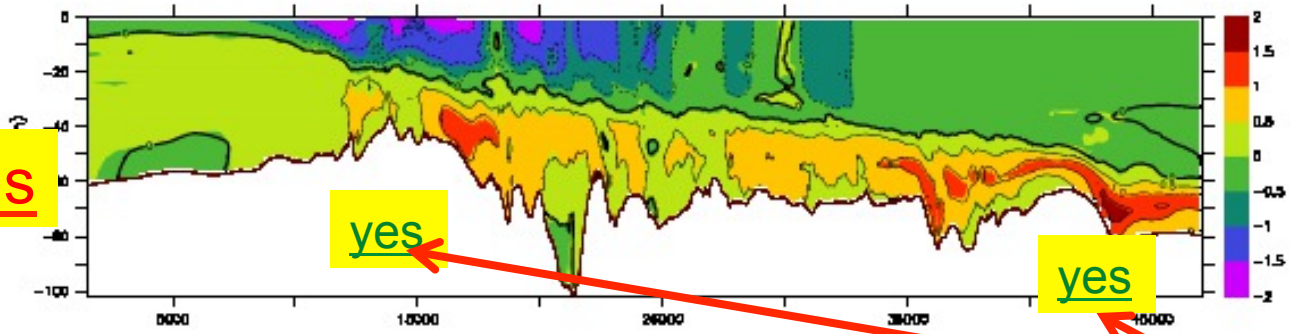

yes

yes

'hydraulic jump' !

yes

Canal İstanbul

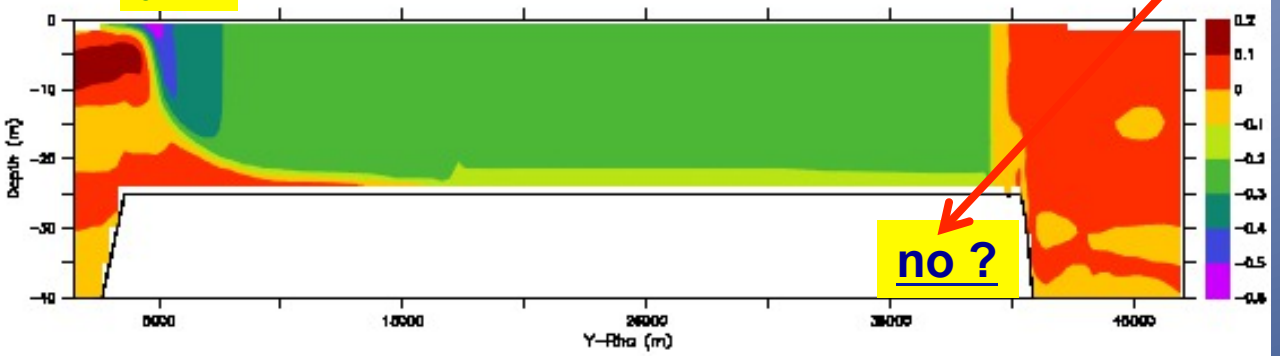

no ?

Sea level variation between Black Sea and the Marmara

Marmara Sea

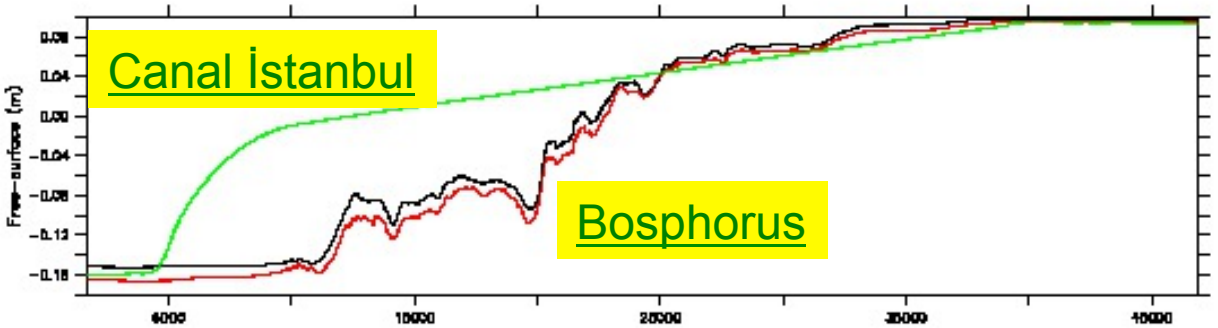

Canal İstanbul

Bosphorus

Black Sea

Turkish Strait System

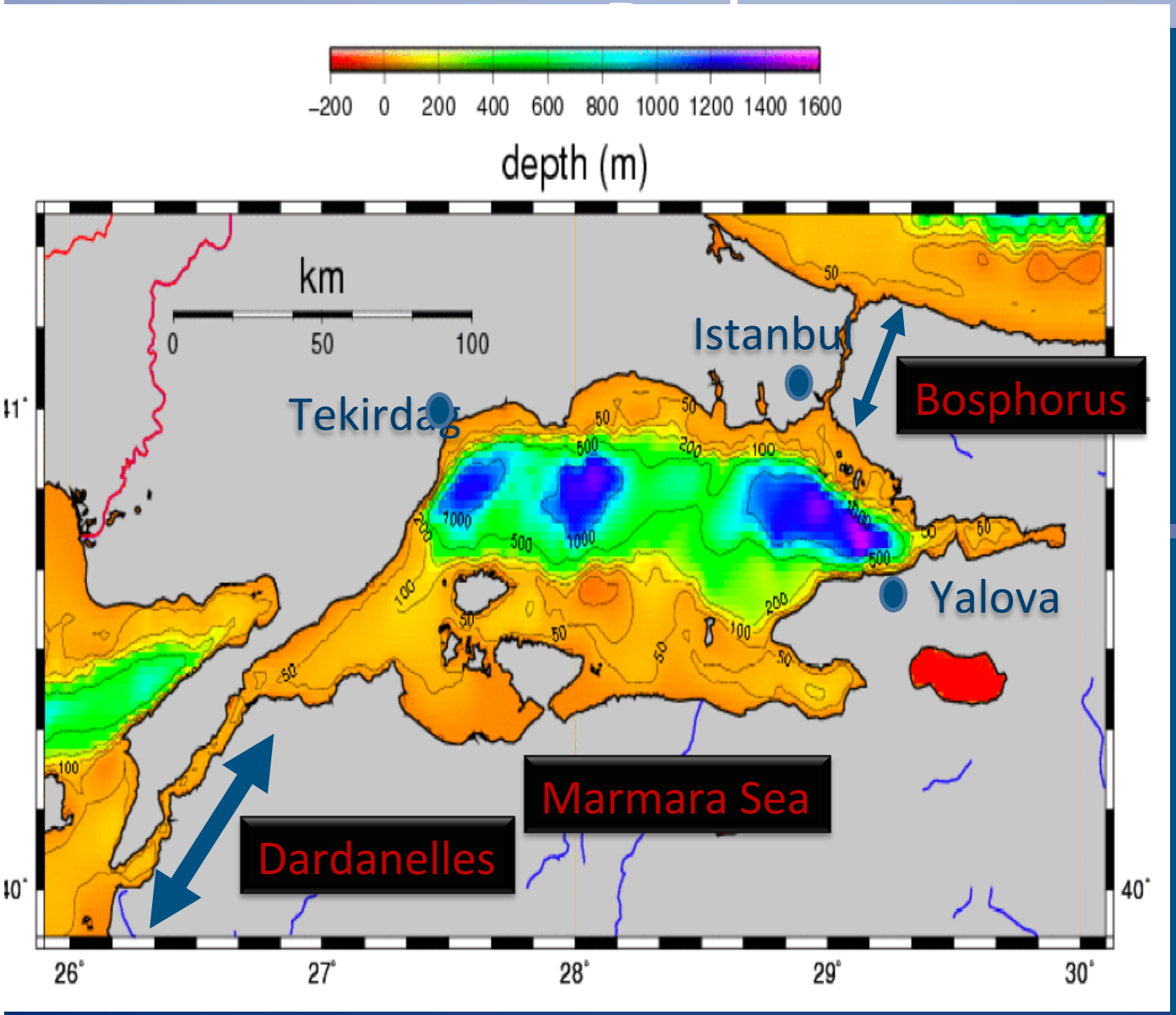

- ✓ Rugged coastline
- ✓ Islands and embayment
- ✓ Large shallow southern area
- ✓ Narrow band of shelf
- ✓ 3 depressions

	Bos	Dar	Mar
L (km)	31	62	250
W (km)	1.5	4	70
D (m)	35	55	300

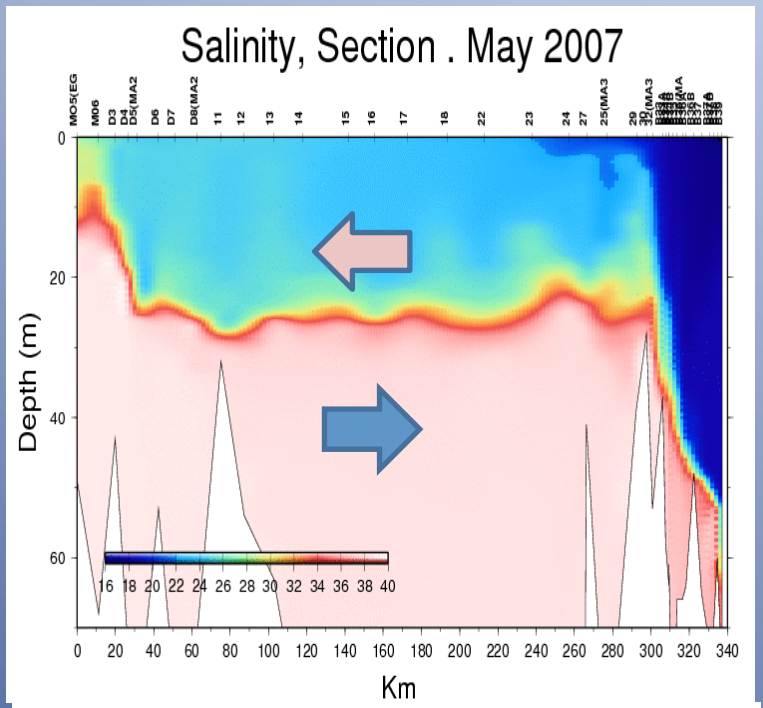

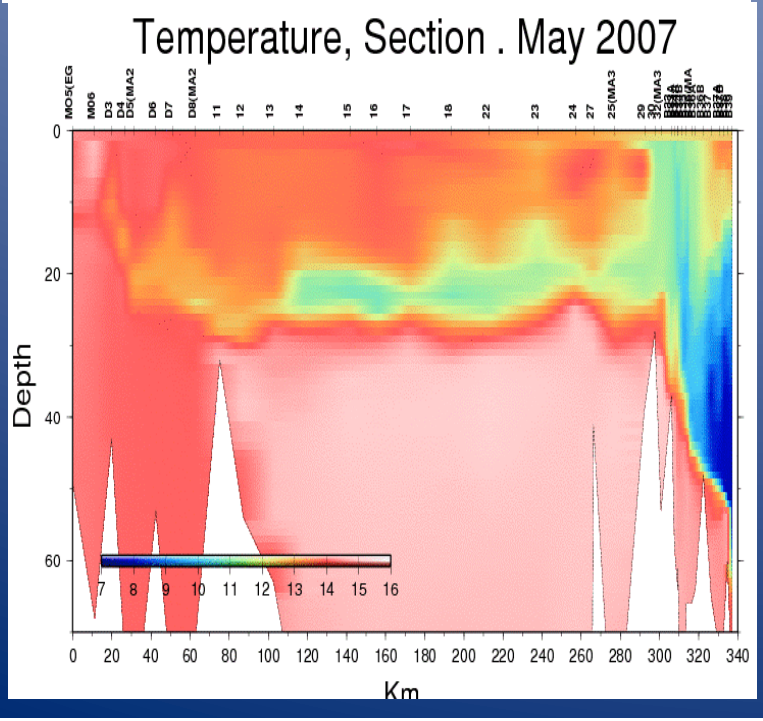

variation across the TSS

The salinity and temperature distribution along the Turkish Strait System (R/V BİLİM May 2007 Cruise)

Circulation Observations

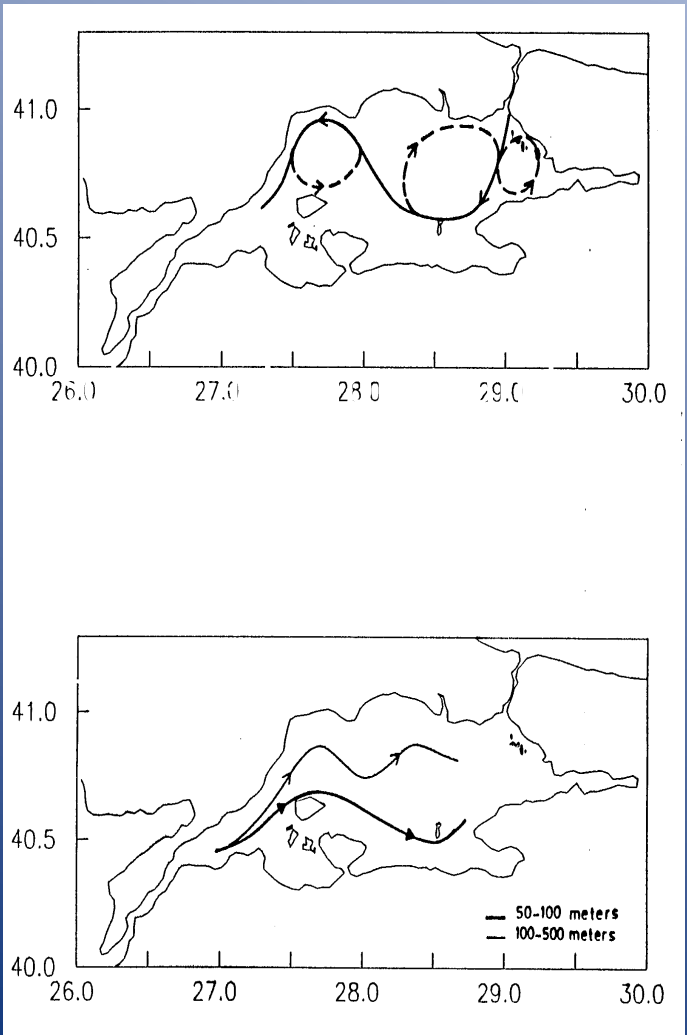

Beşiktepe et al., 1994

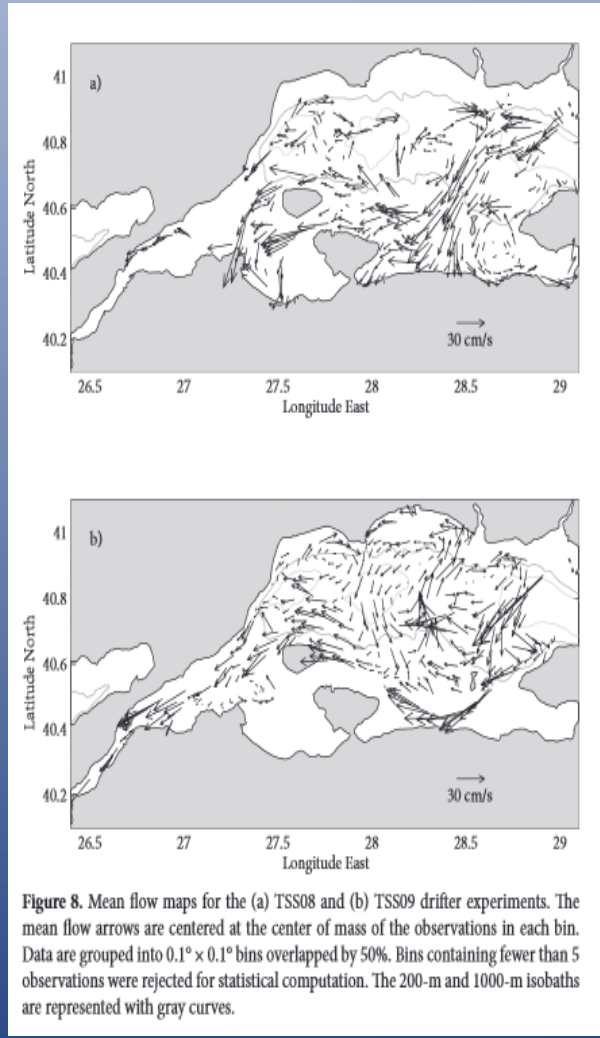

Figure 8. Mean flow maps for the (a) TSS08 and (b) TSS09 drifter experiments. The mean flow arrows are centered at the center of mass of the observations in each bin. Data are grouped into 0.1° × 0.1° bins overlapped by 50%. Bins containing fewer than 5 observations were rejected for statistical computation. The 200-m and 1000-m isobaths are represented with gray curves.

Gerin et al., 2013

- ✓ fresh surface waters from the Black Sea into the Aegean Sea
- ✓ salty deep waters form Aegean Sea into the Black Sea

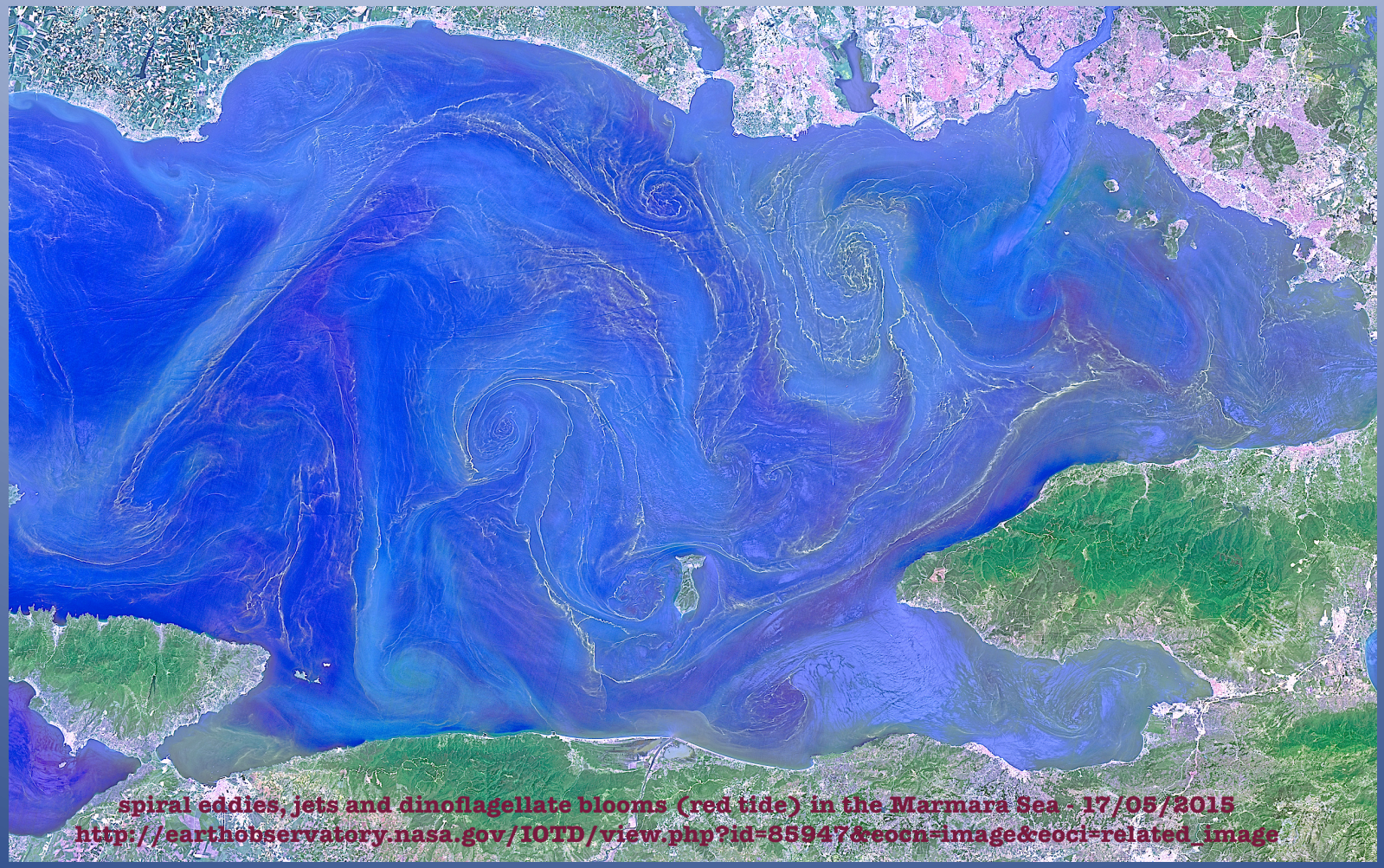

17 May 2015 satellite image of red tide (or harmful algal bloom, HAB)
(http://earthobservatory.nasa.gov/IOTD/view.php?id=85947&eocn=image&eoci=moreiotd)

Murat Gündüz and Emin Özsoy (2014, 2015)

Inter-annual variability of upper layer blocking of the Dardanelles strait and its connection with the fish catch in the Aegean sea (1979-2013)

Blocking of the Upper Layer Flow in the Dardanelles Strait and its Influence on Fish Catches

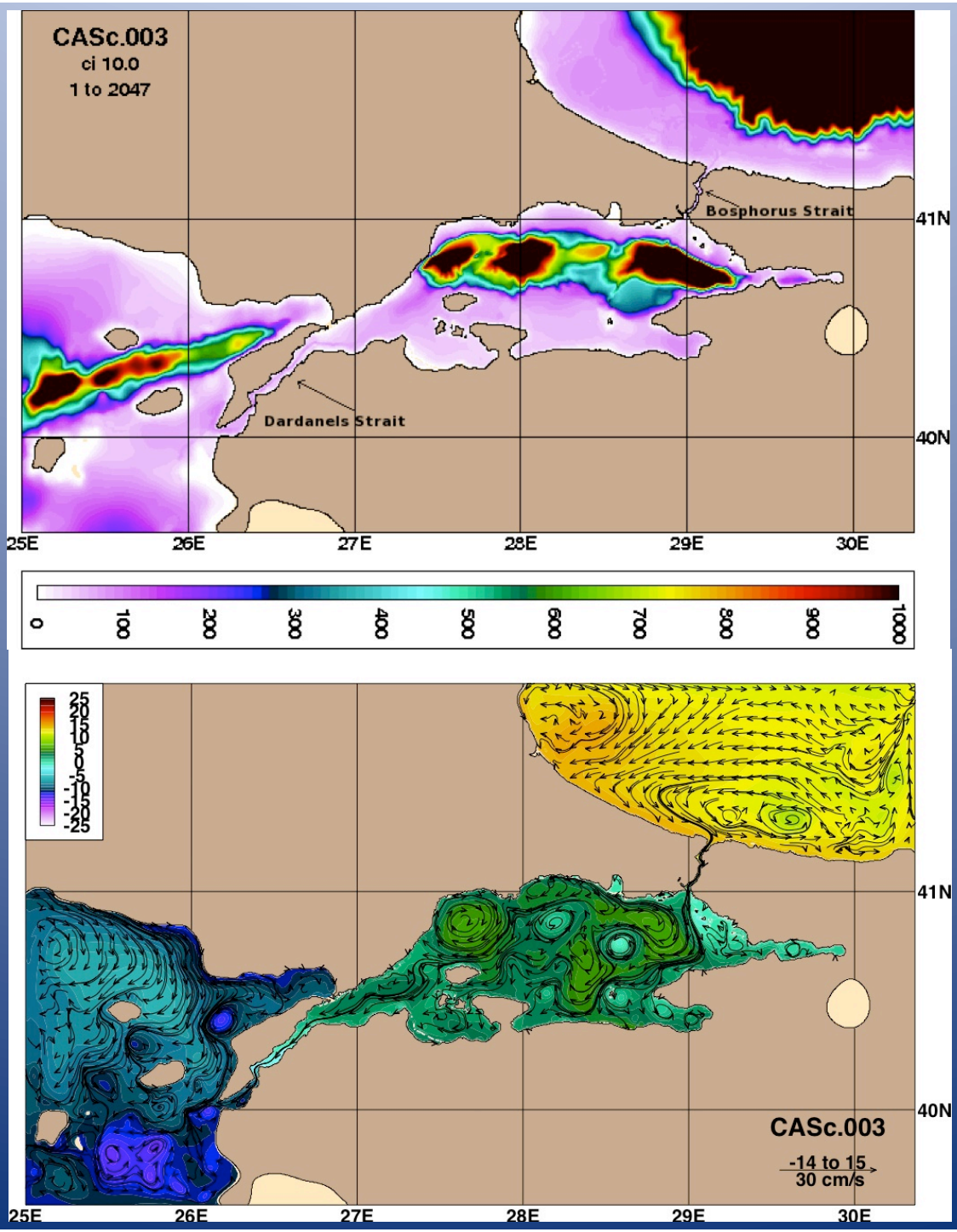

Murat Gündüz, 2009

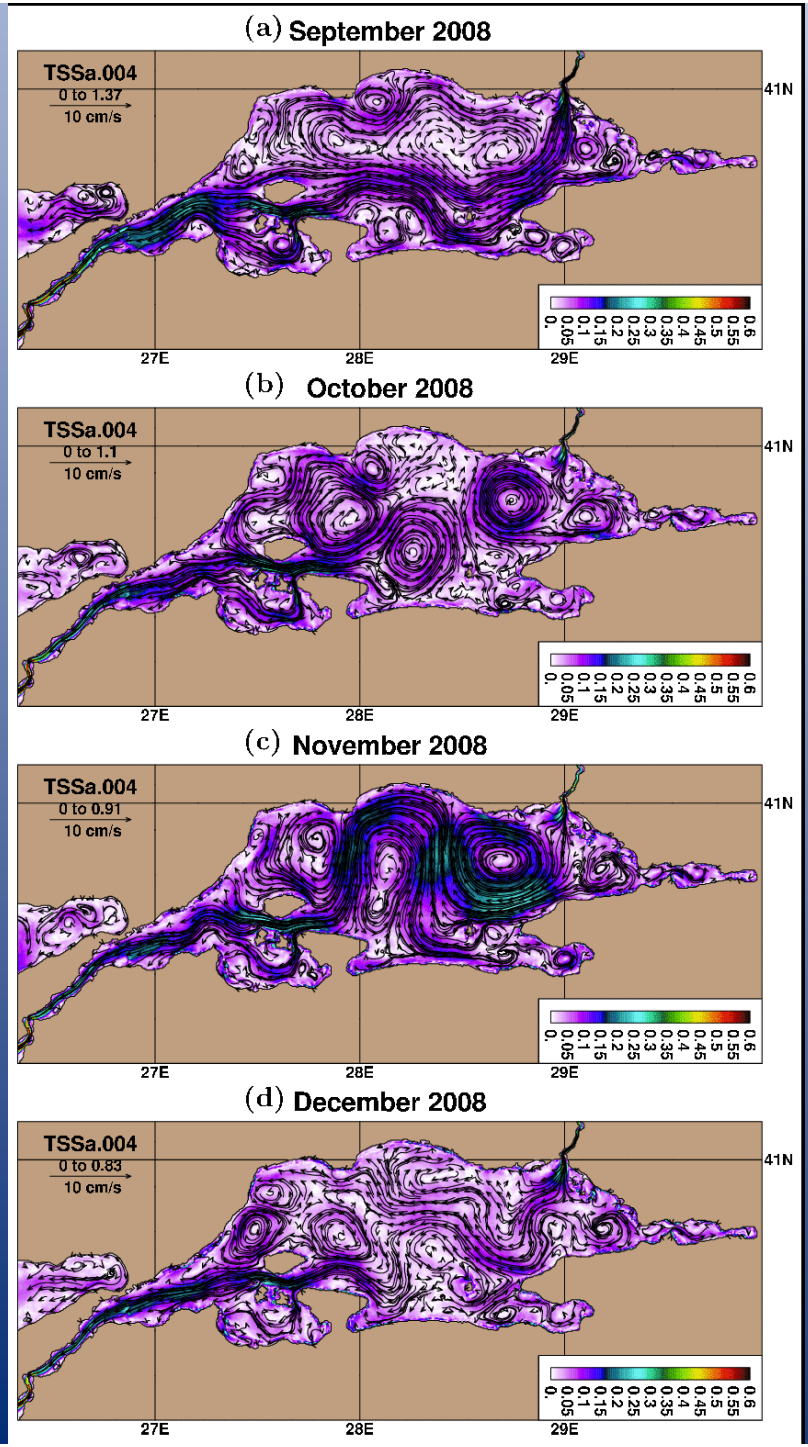

Quasi-permanent feature of the Marmara Sea circulation is the S-shaped jet flow.

The jet flow successfully reproduced in September. It is very organized in this month.

But it breaks up to form small eddies as in the case of October and November.

In December, the jet flow become to be organized again.

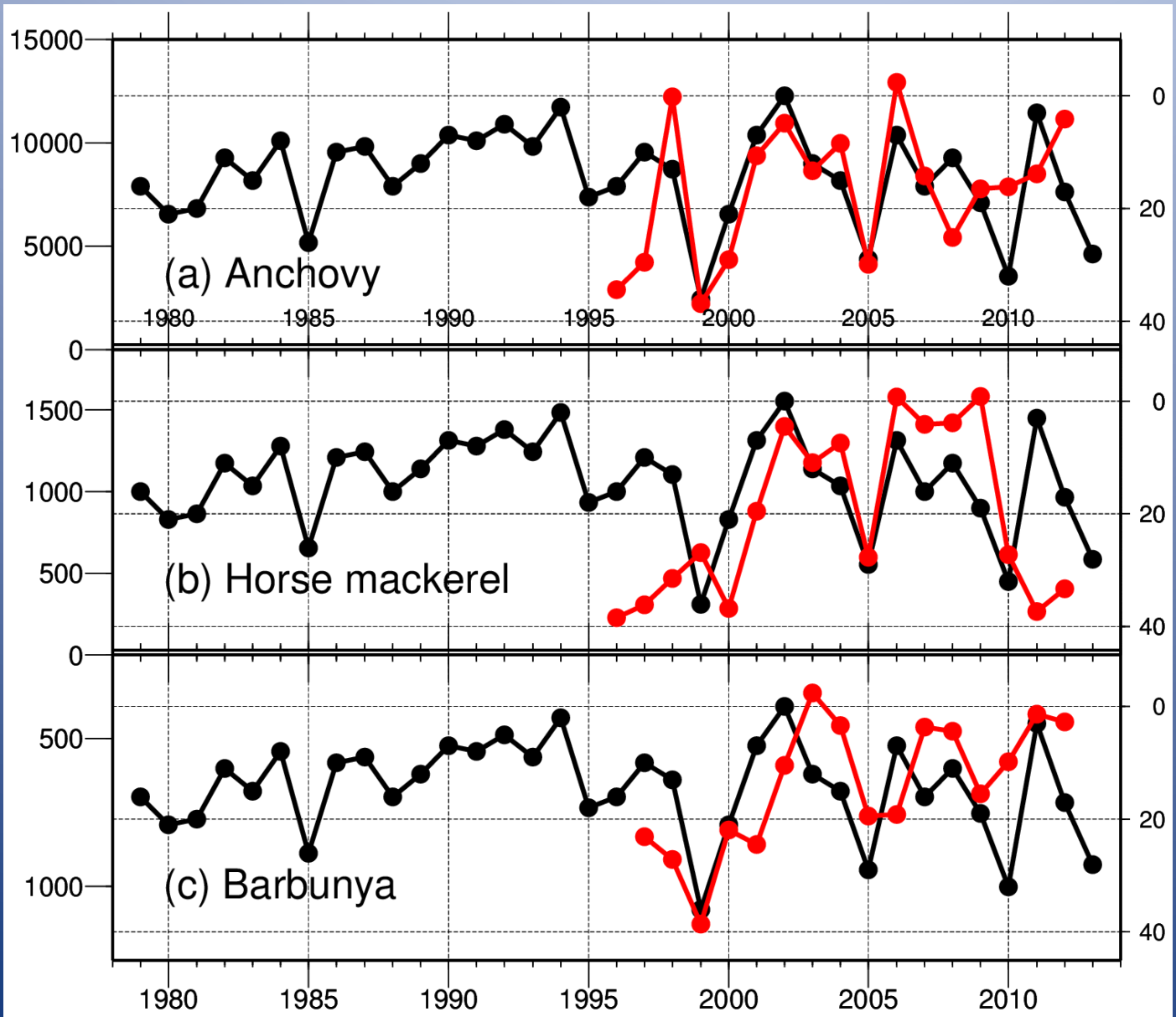

Annual mean number of blocking events (black line, right axis) and fish catches in tons (red line, left axis) in the Aegean Sea for
(a) Horse mackerel
(b) Anchovy
(c) Atlantic Bonito

Sannino, Sözer and Özsoy (2014)

A High-Resolution Modelling Study of the Turkish Straits System (2014, 2015)

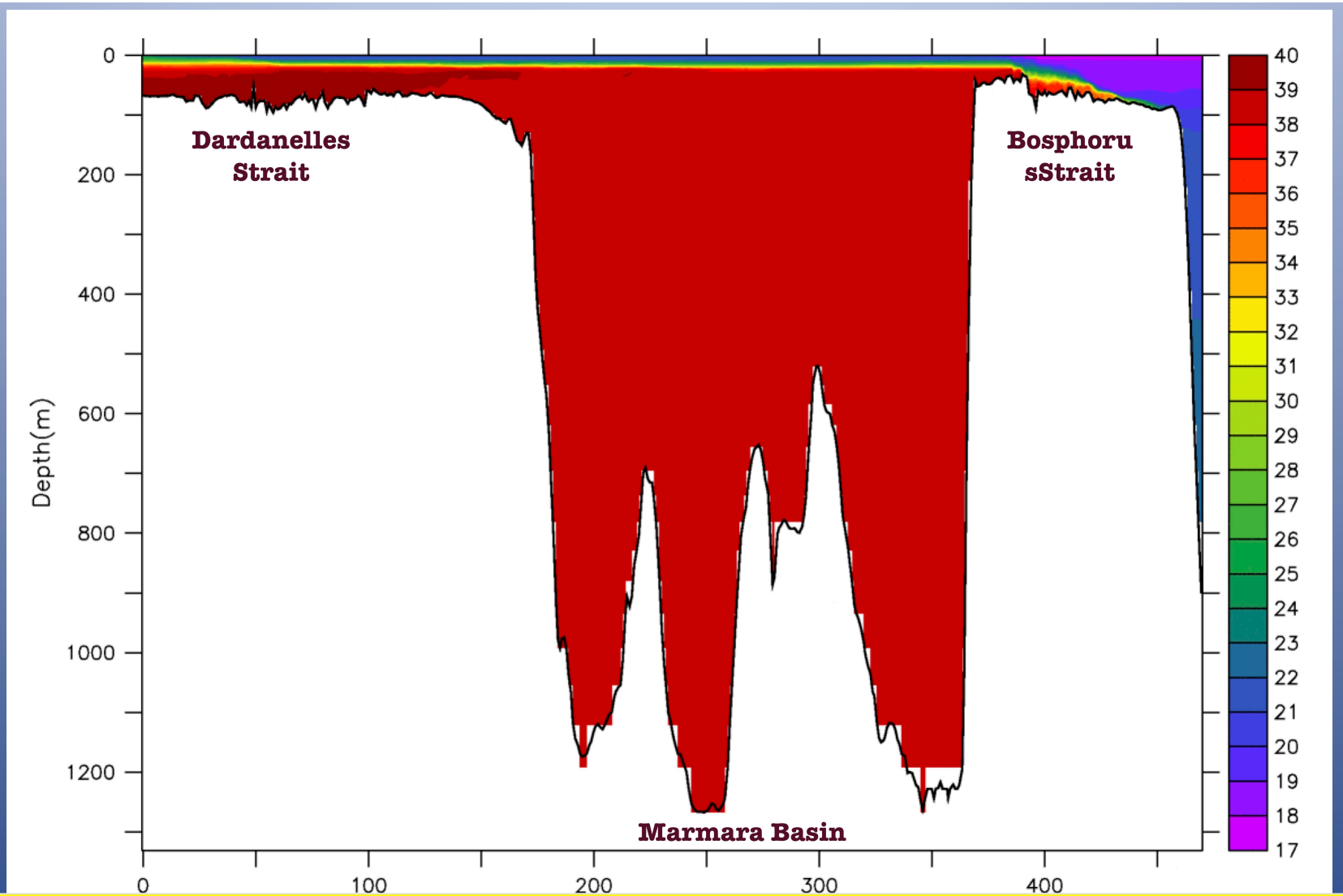

Model result from the work of Sannino, Sözer and Özsoy (2014) showing salinity on a southwest to northeast transect along the thalweg. The thin upper layer in the upper 25m carries water of Black Sea origin, flowing towards the Aegean Sea, while the lower layer flow first fills the Marmara Sea and then outflow to the Black Sea through the Bosphorus.

Gianmaria Sannino (ENEA), Adil Sözer, Emin Özsoy (ODTÜ-DBE)
Yüksek Enerji Çevre Dinamiği: Türk Boğazlar Sistemi'nde Süreçler
TURBO / DEEP (TÜBİTAK – İtalya Dışişleri Bakanlığı İkili İşbirliği Projesi)
Supported by the EU initiative PRACE
(Partnership for Advanced Computing in Europe) for supercomputing

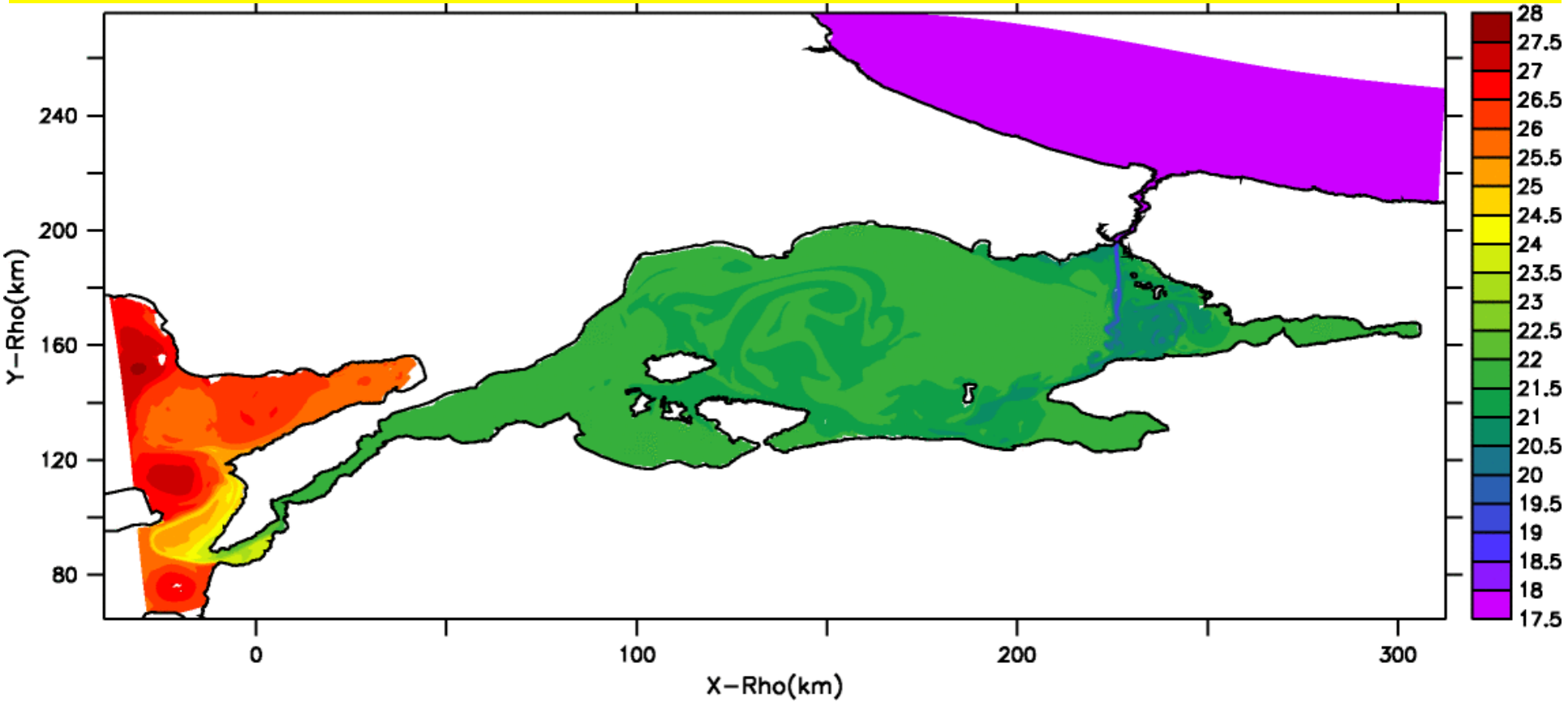

MITgcm non-hydrostatic model (curvilinear variable grid)
Δx = 35-500m, Δy = 60-1000m, Grid Size = 2184*648*72

Q=-9600 m³/s, day=67, range=2.2 cm

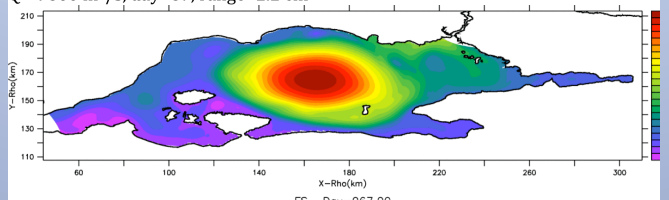

Q=0 m³/s, day=100, range=2.7cm

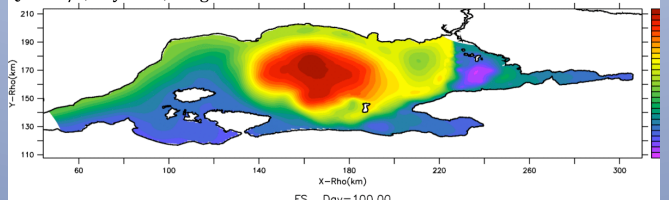

Q=5600 m³/s, day=66, range=4.5 cm

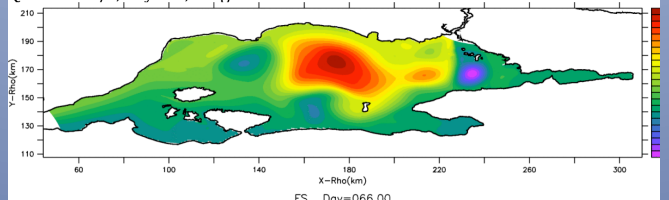

Q=9600 m³/s, day=22, range=4.8 cm

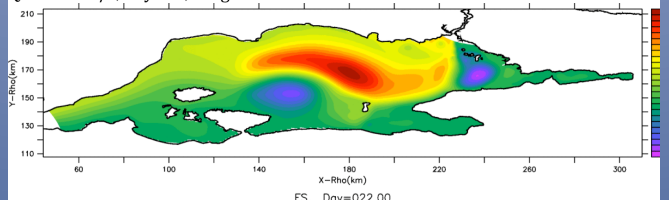

Q=18000 m³/s, day=65, range=6.4 cm

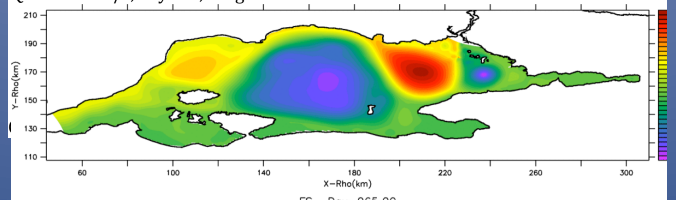

Q=50000 m³/s, day=125, range=12.0 cm

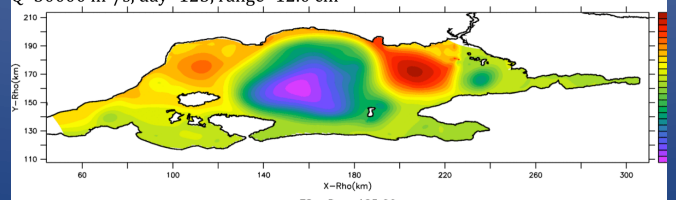

Figure 3. The free surface variations in the Marmara Sea for varying net barotropic volume flux values of Q = -9600, 0, 5600, 9600, 18000 and 50000 m³/s.

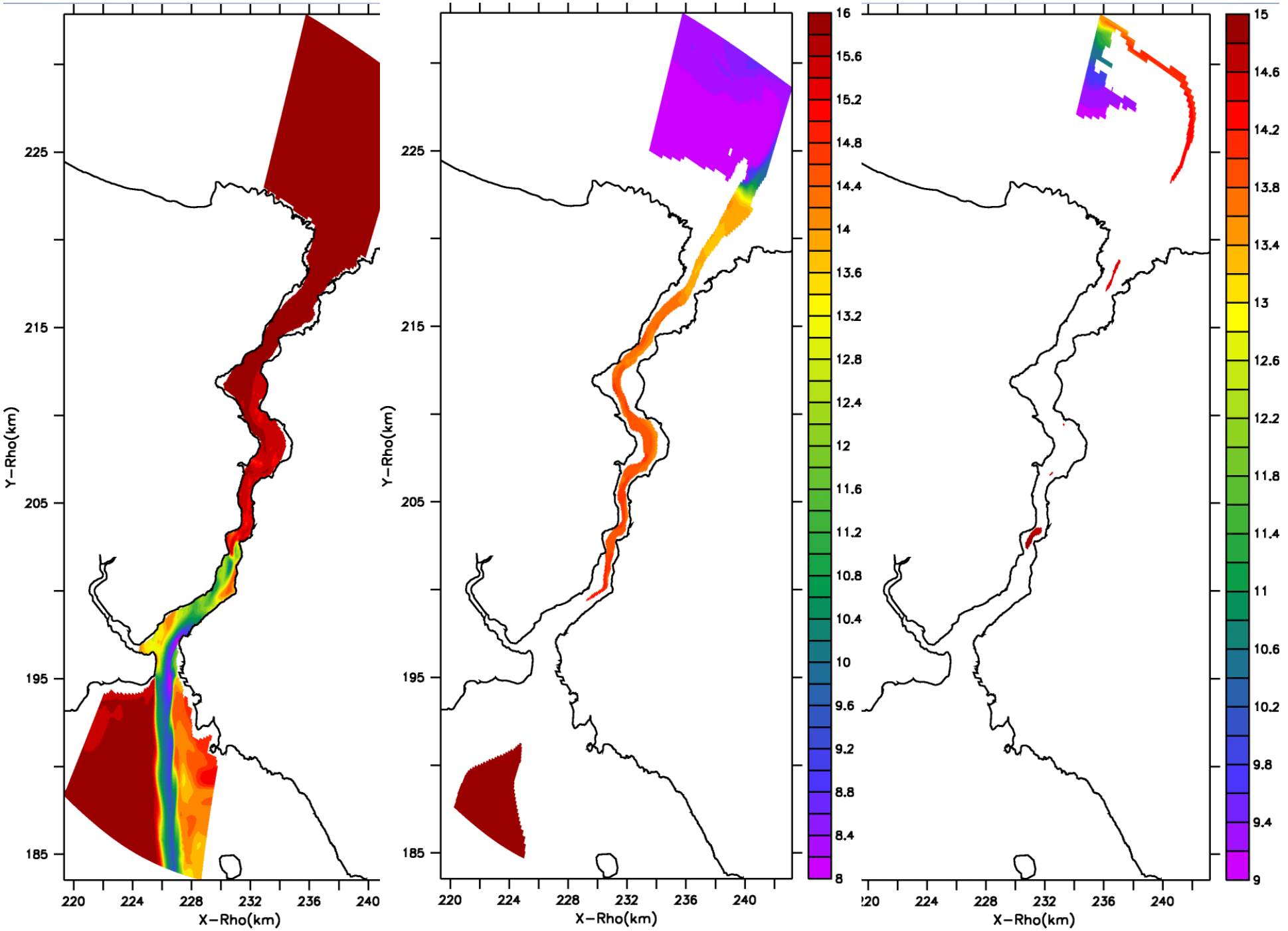

Temp, Z=−5.4m, Day=035.0

Temp, Z=−51m, Day=035.00

Temp, Z=−73.9m, Day=035.00

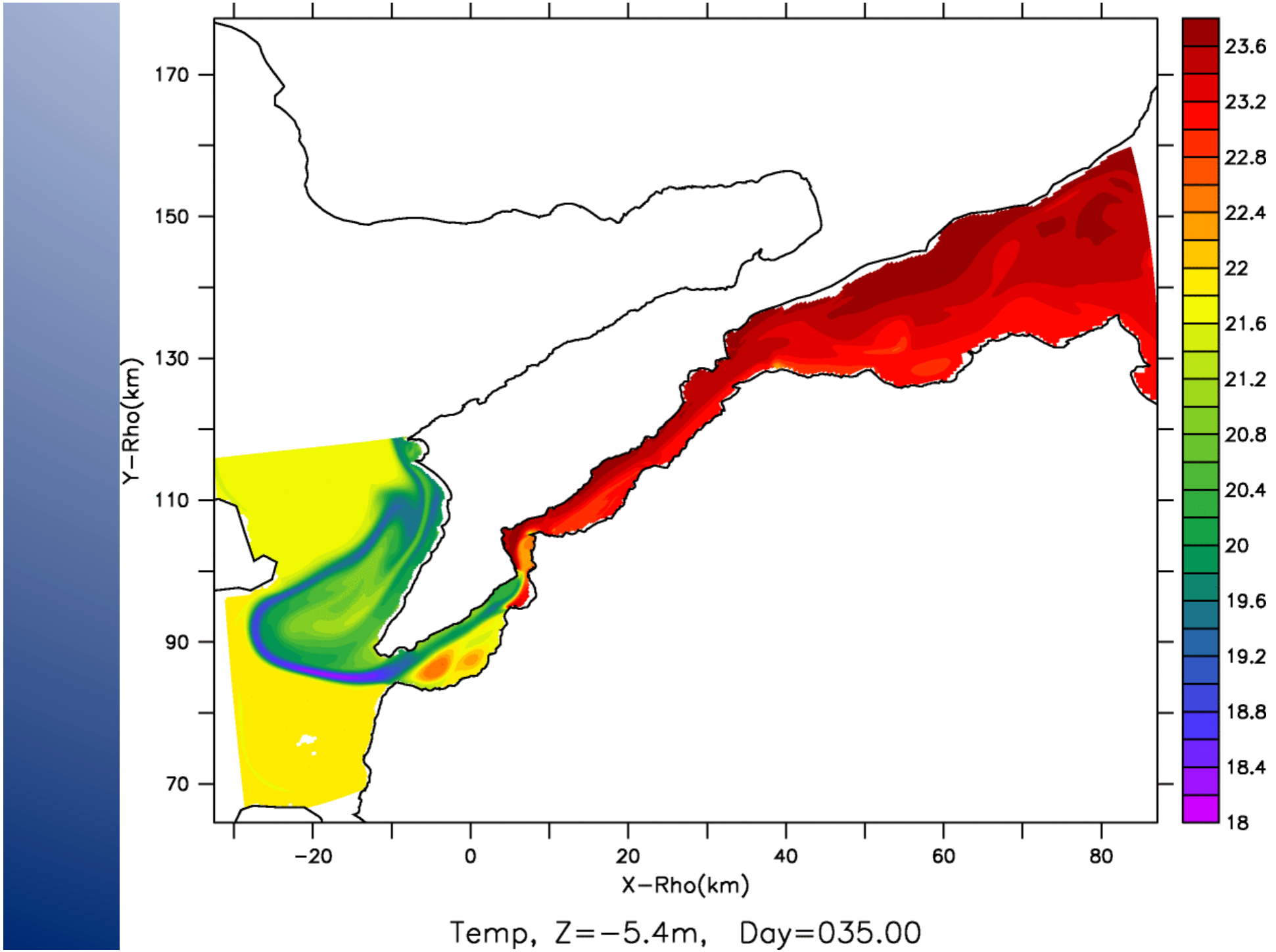
170
150
130
110
90
70
Y−Rho(km)
−20
0
20
40
60
80
X−Rho(km)
23.6
23.2
22.8
22.4
22
21.6
21.2
20.8
20.4
20
19.6
19.2
18.8
18.4
18
Temp, Z=−5.4m, Day=035.00

Bosphorus fluxes based on measurements and different model results

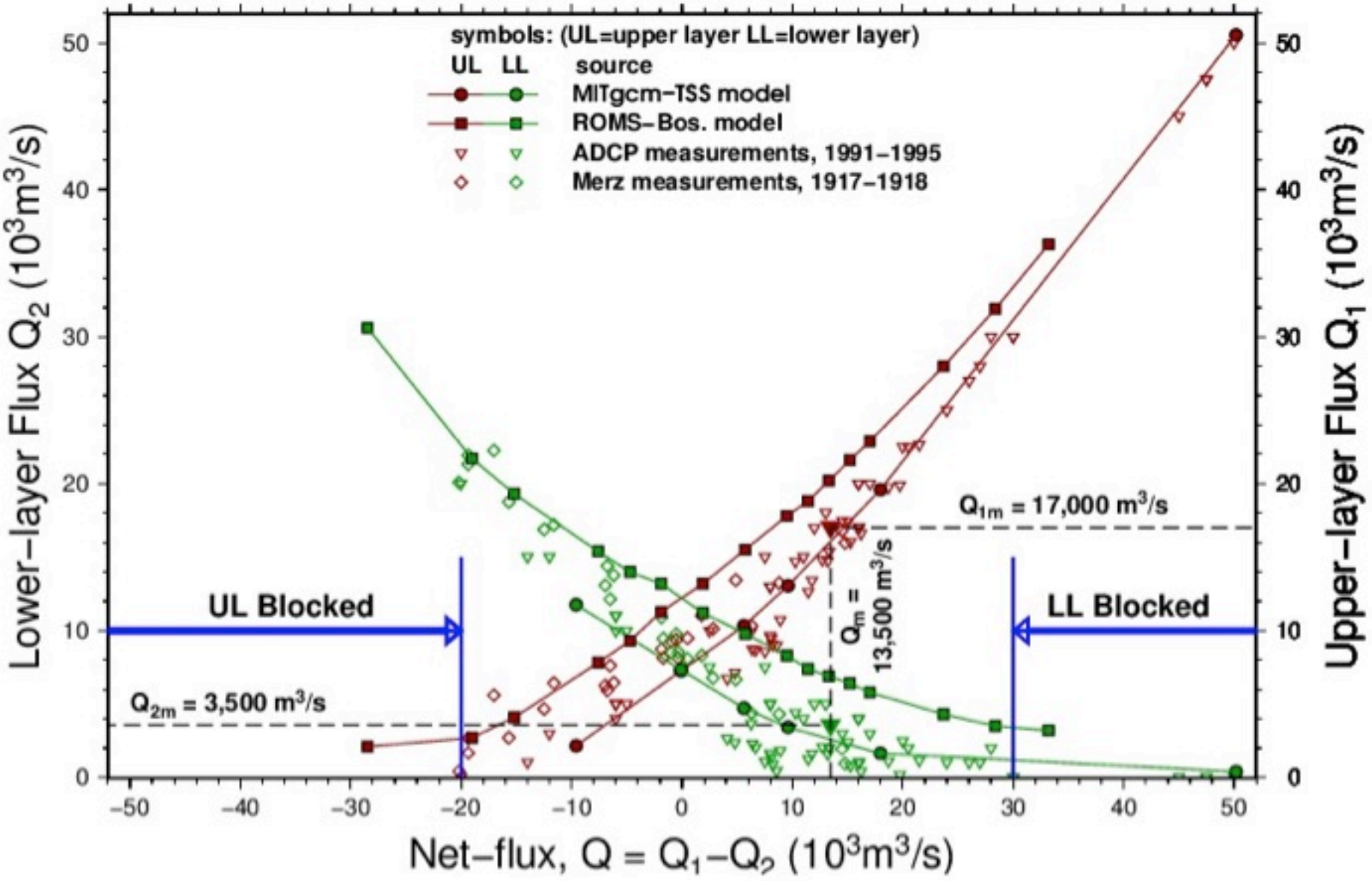

Özgür Gürses, PhD study

Modeling the Turkish Straits System: Assessment of the dynamics based on multi-resolution inter-basin coupling

Özgür Gürses, Ali Aydoğdu, Nadia Pinardi, Emin Özsoy (2015)

An Idealized Turkish Strait System in a Finite Element Ocean circulation model

Finite Element Ocean Circulation Model (FEOM)
Özgür Gürses (PhD study)

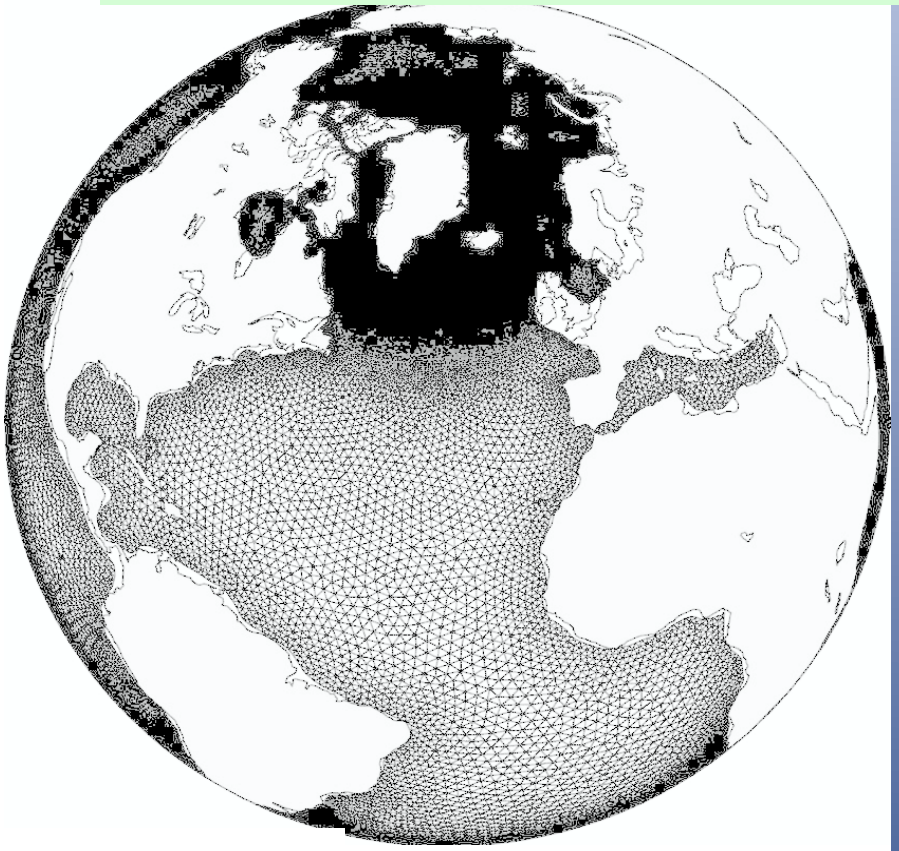

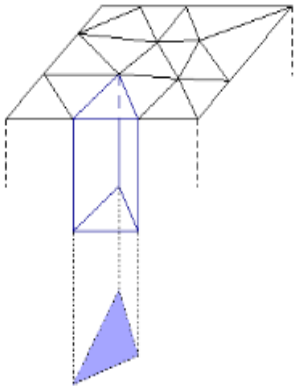

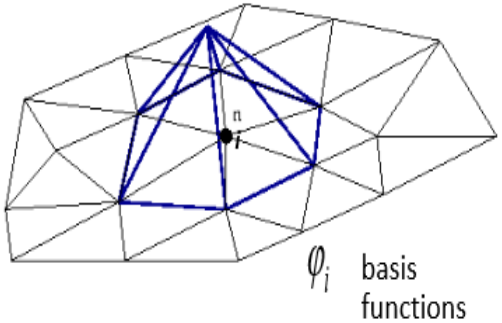

developed at Alfred Wegener Institute (Danilov et. al. 2004, Wang et. al 2014)

- ✓ Triangular (2D) and tetrahedral (3D) elements in a regional configuration
- ✓ Solves the primitive equations (momentum and vertically integrated continuity equation) on the sphere
- ✓ Tracer equations for salinity and temperature
- ✓ Finite element discretization: P_1-P_1 scheme (continuous linear basis functions)

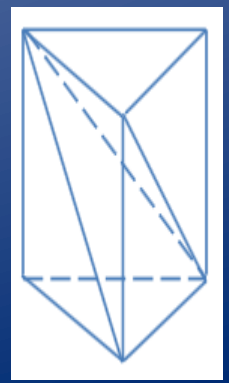

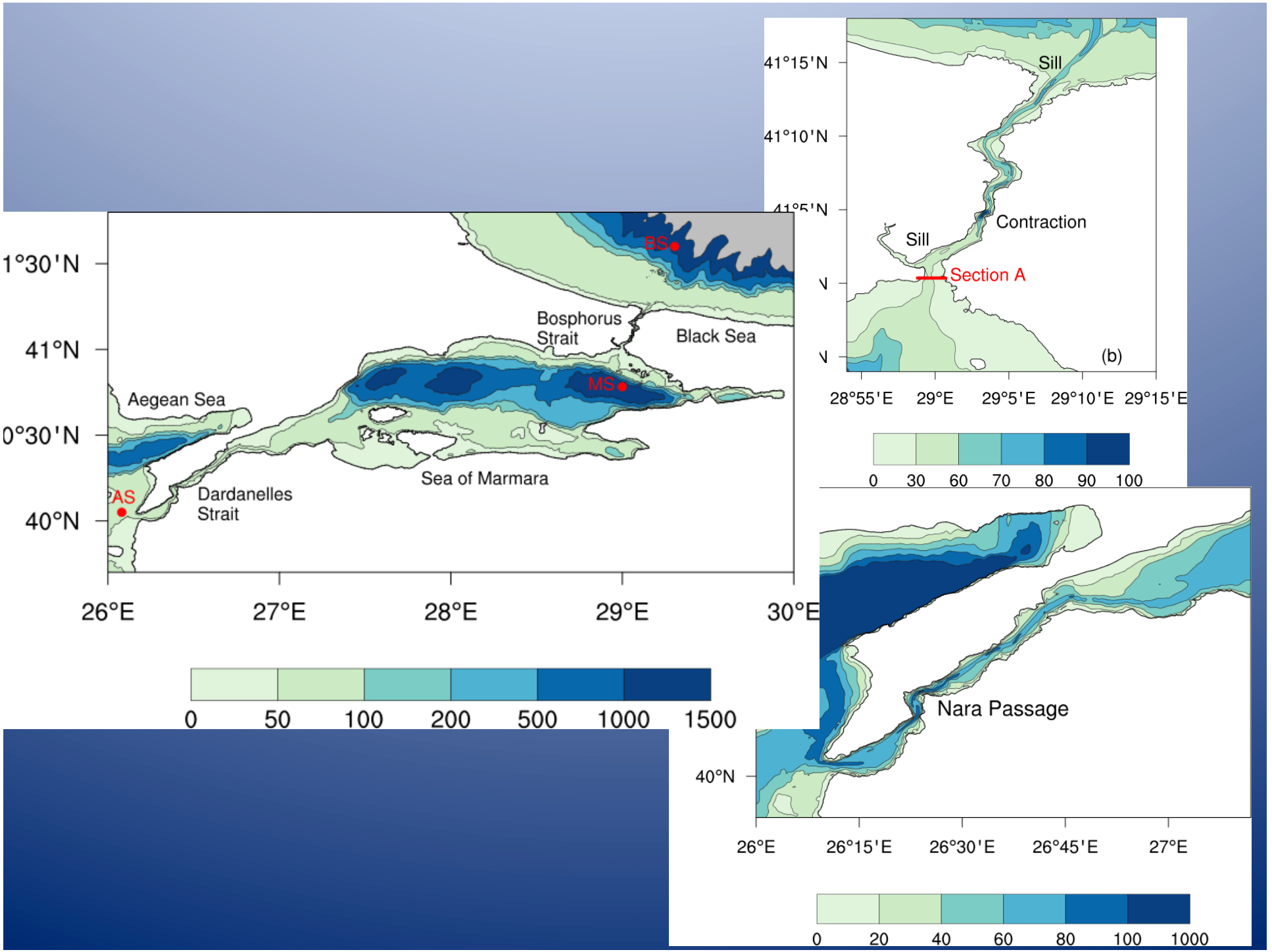
41°15'N
41°10'N
Sill
Contraction
Sill
Section A
(b)
28°55'E
29°E
29°5'E
29°10'E
29°15'E
0
30
60
70
80
90
100
1°30'N
41°N
0°30'N
40°N
BS
Bosphorus
Strait
Black Sea
MS
Aegean Sea
AS
Dardanelles
Strait
Sea of Marmara
26°E
27°E
28°E
29°E
30°E
0
50
100
200
500
1000
1500
Nara Passage
40°N
26°E
26°15'E
26°30'E
26°45'E
27°E
0
20
40
60
80
100
1000

Discretization

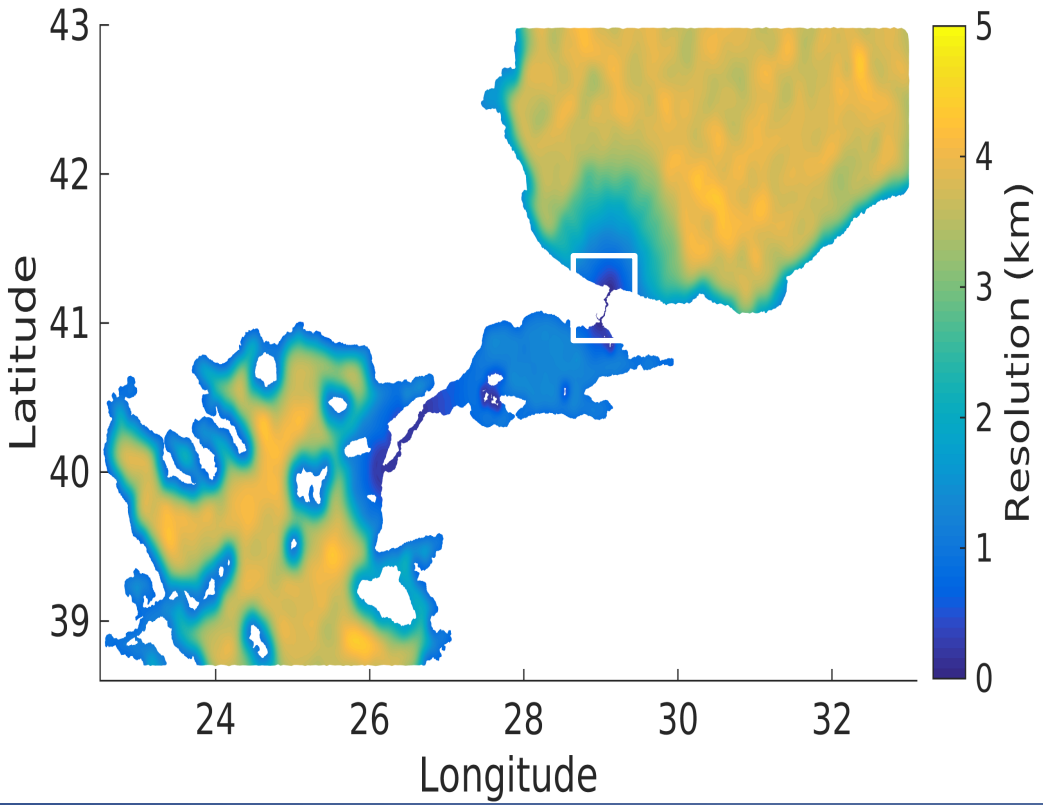

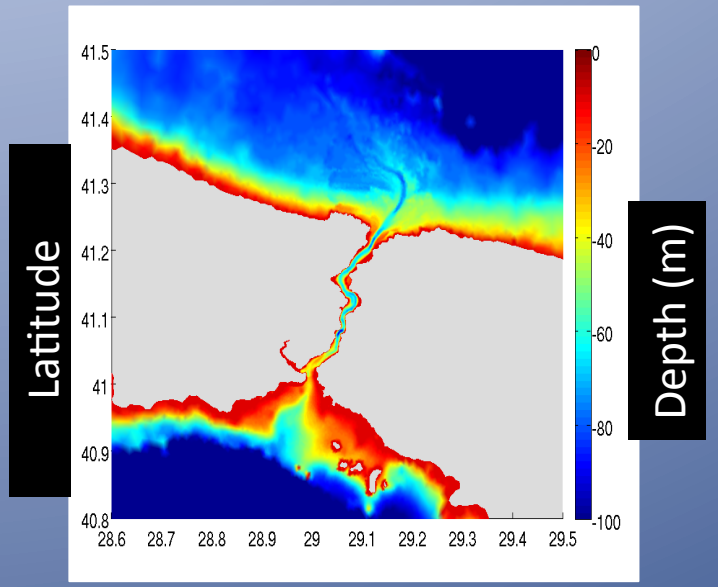

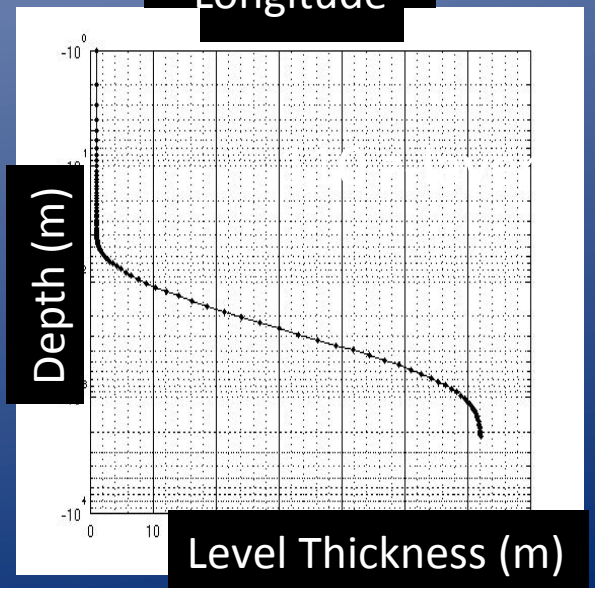

NUMBER of NODES	
2D	77000
3D	~3 mil

SPATIAL RESOLUTION	
BOS	65 m
DAR	100 m
MAR	1.5 km
BS/AS	5 km

Model Setup

- ✓ Initial Condition:

  Lock Exch. : 3 profiles from each basin

  Hindcast : temperature, salinity and initial velocity fields are extracted from the lock-exchange run

- ✓ Atmospheric Forcing : ECMWF

  Domain : 22°W 33°E - 38°˜ 43°N

  Frequency : 6-hourly

  Resolution : 0.125°x0.125°

- ✓ Lateral boundaries are closed with no-slip condition

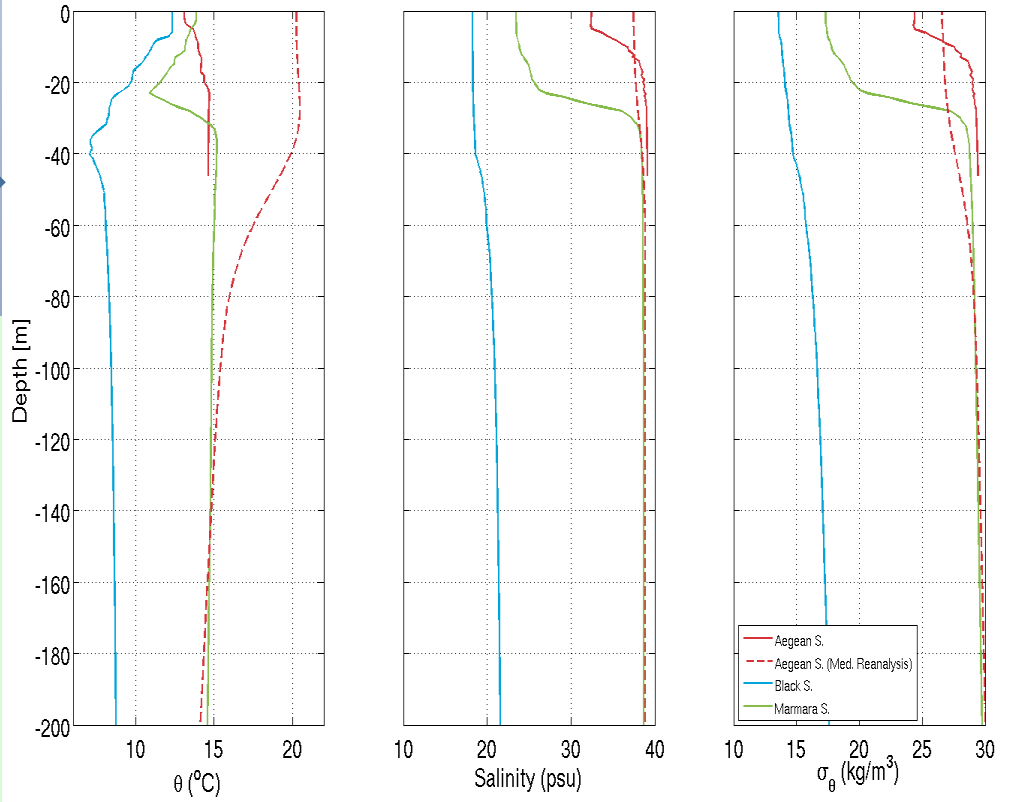

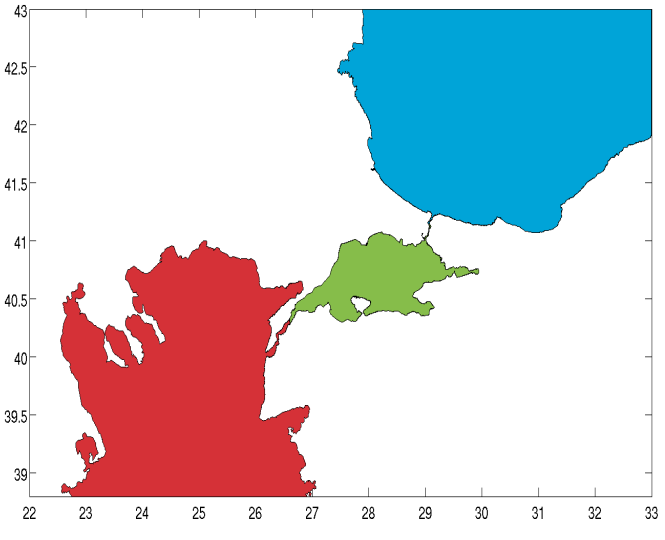

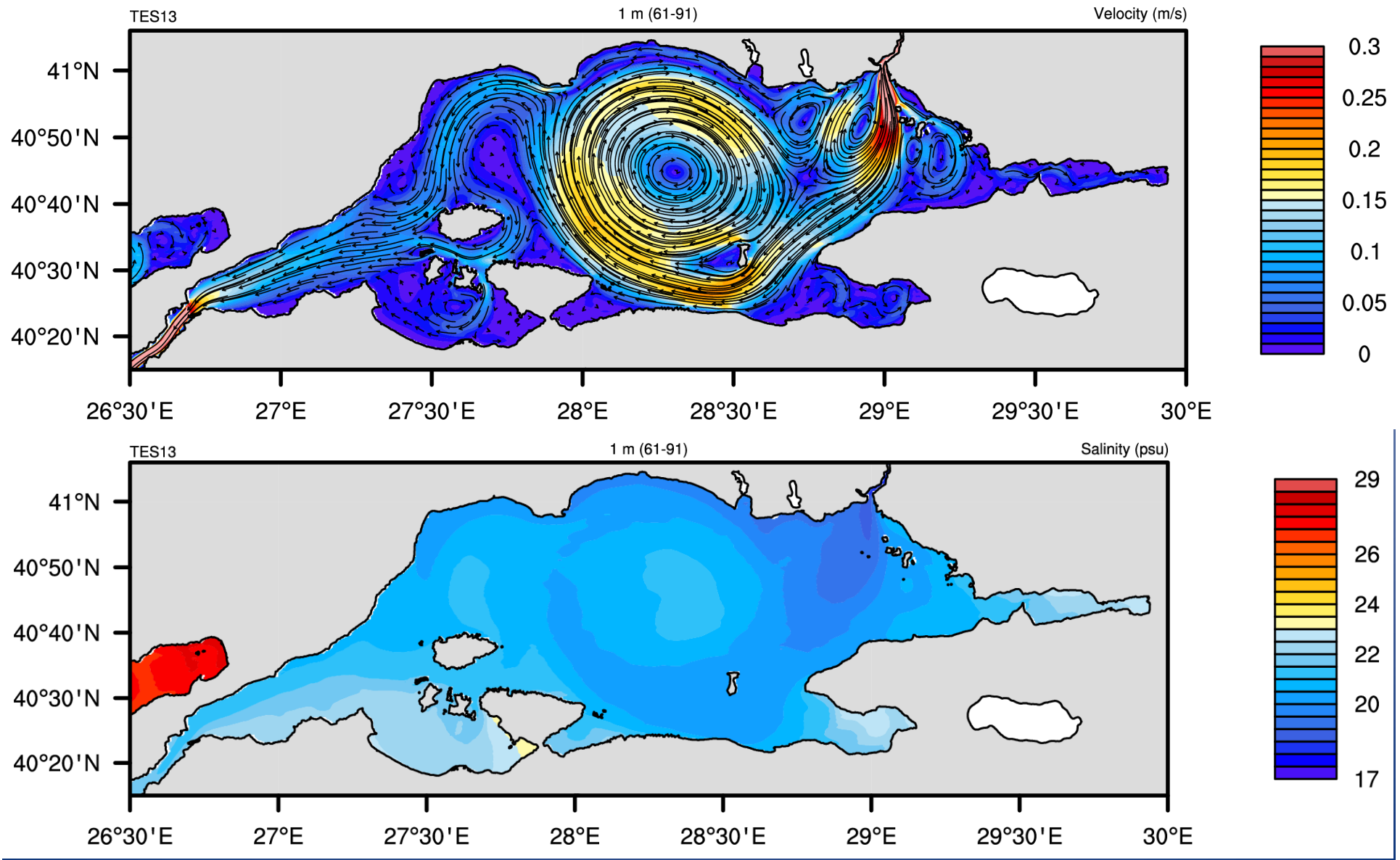
TES13
1 m (61-91)
Velocity (m/s)
41°N
40°50'N
40°40'N
40°30'N
40°20'N
26°30'E
27°E
27°30'E
28°E
28°30'E
29°E
29°30'E
30°E
0.3
0.25
0.2
0.15
0.1
0.05
0
TES13
1 m (61-91)
Salinity (psu)
41°N
40°50'N
40°40'N
40°30'N
40°20'N
26°30'E
27°E
27°30'E
28°E
28°30'E
29°E
29°30'E
30°E
29
26
24
22
20
17

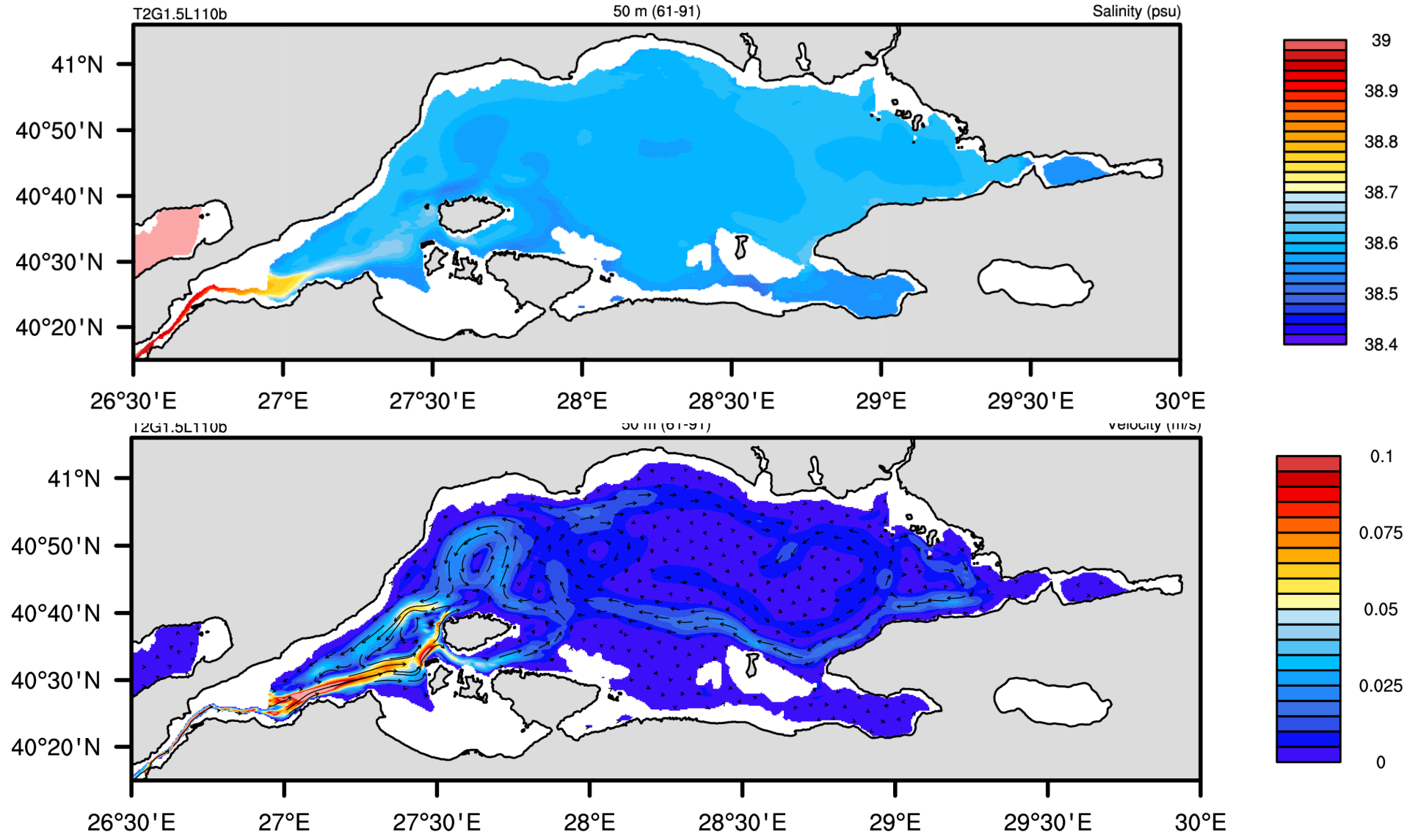
T2G1.5L110b
50 m (61-91)
Salinity (psu)
41°N
40°50'N
40°40'N
40°30'N
40°20'N
26°30'E
27°E
27°30'E
28°E
28°30'E
29°E
29°30'E
30°E
39
38.9
38.8
38.7
38.6
38.5
38.4
0.1
0.075
0.05
0.025
0

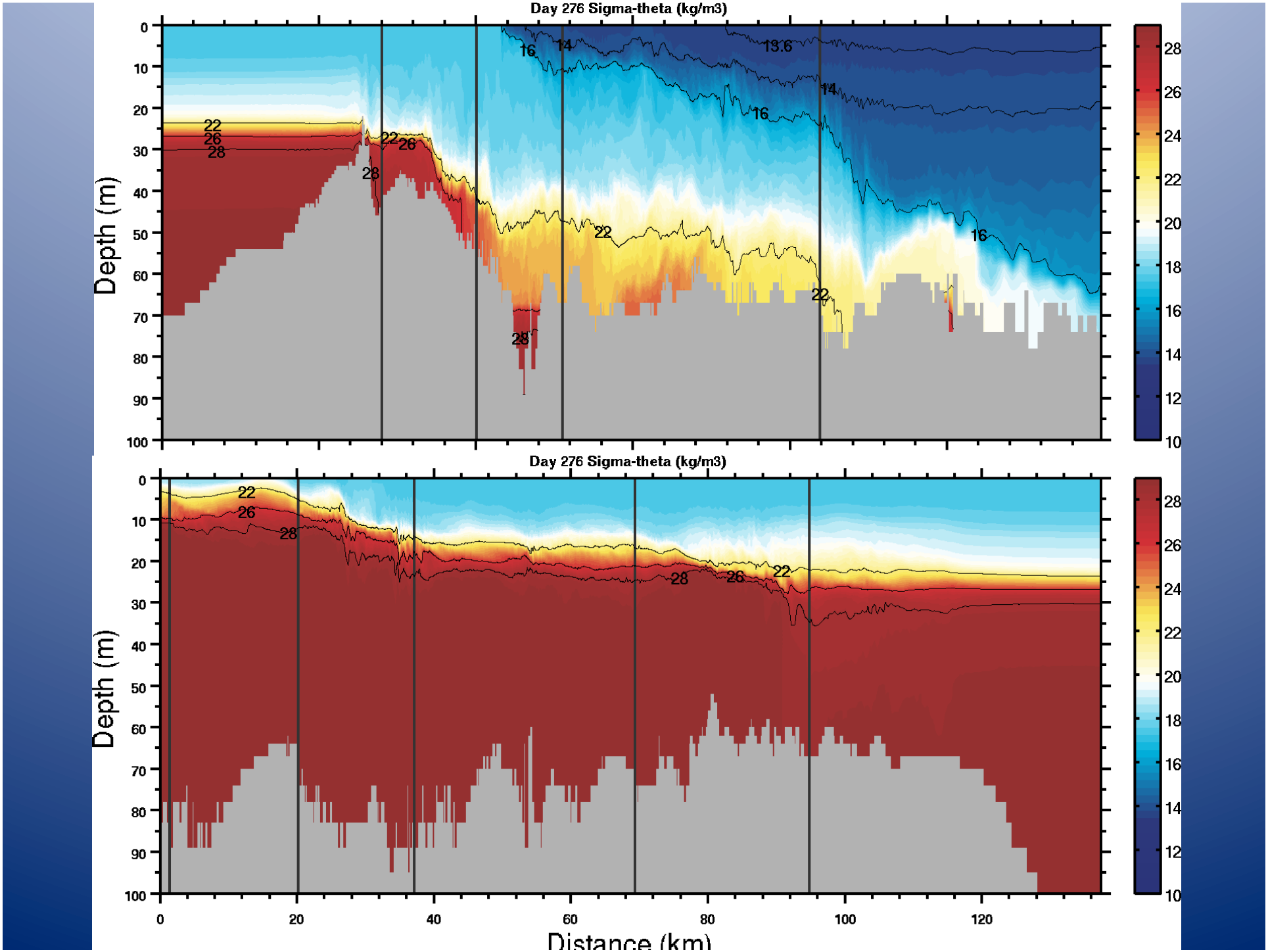
Day 276 Sigma-theta (kg/m3)
Depth (m)
Distance (km)
Day 276 Sigma-theta (kg/m3)
Depth (m)
Distance (km)

The image cannot be displayed. Your computer may not have enough memory to open the image, or the image may have been corrupted. Restart your computer, and then open the file again. If the red x still appears, you may have to delete the image and then insert it again.

Marmara Sea (April 2008)

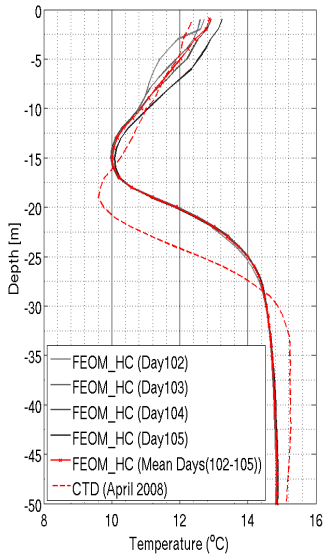

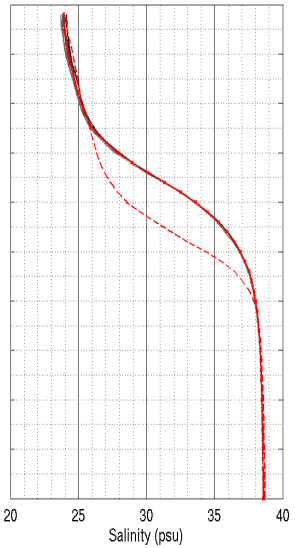

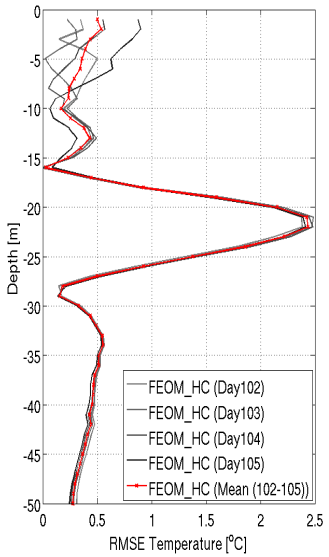

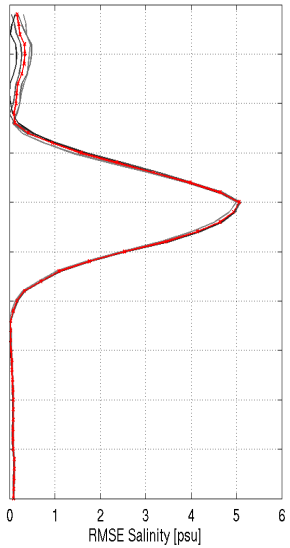

HC1

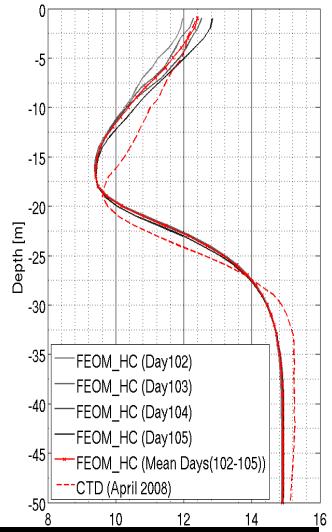

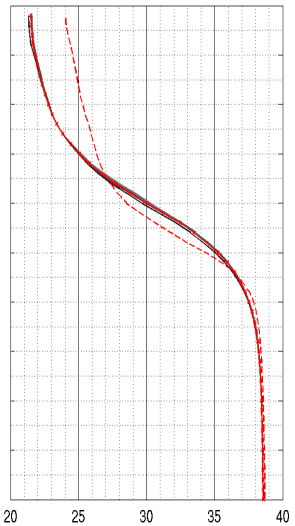

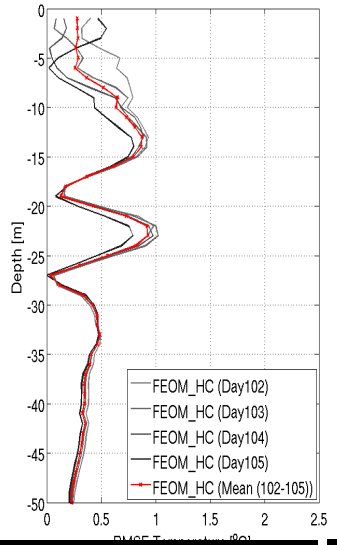

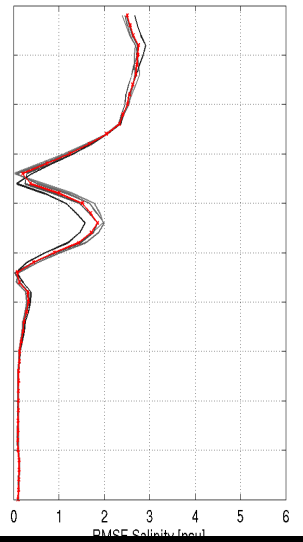

HC2

Temperature (°C) **Salinity (psu)** **RMSE Temperature (°C)** **RMSE – Salinity (psu)**


Başakşehir
Büyükçekmece
Büyükçekmece
Küçükçekmece
Istanbul
Caferaga-WERA
Maltepe
Adalar
Marmara Trough
Senköy-WERA
Çınarcık
© 2015 Basarsoft
WERA Container
Receive Antenna Array
Walking Pedestrians
WERA Container
Receive Antenna Array
Walking Pedestrians

Mixing on the Black Sea Shelf
of the Bosphorus
Michael C. Gregg and Emin Özsoy
(1999)

Dissipation W/kg
Vertical diffusivity m^2/s

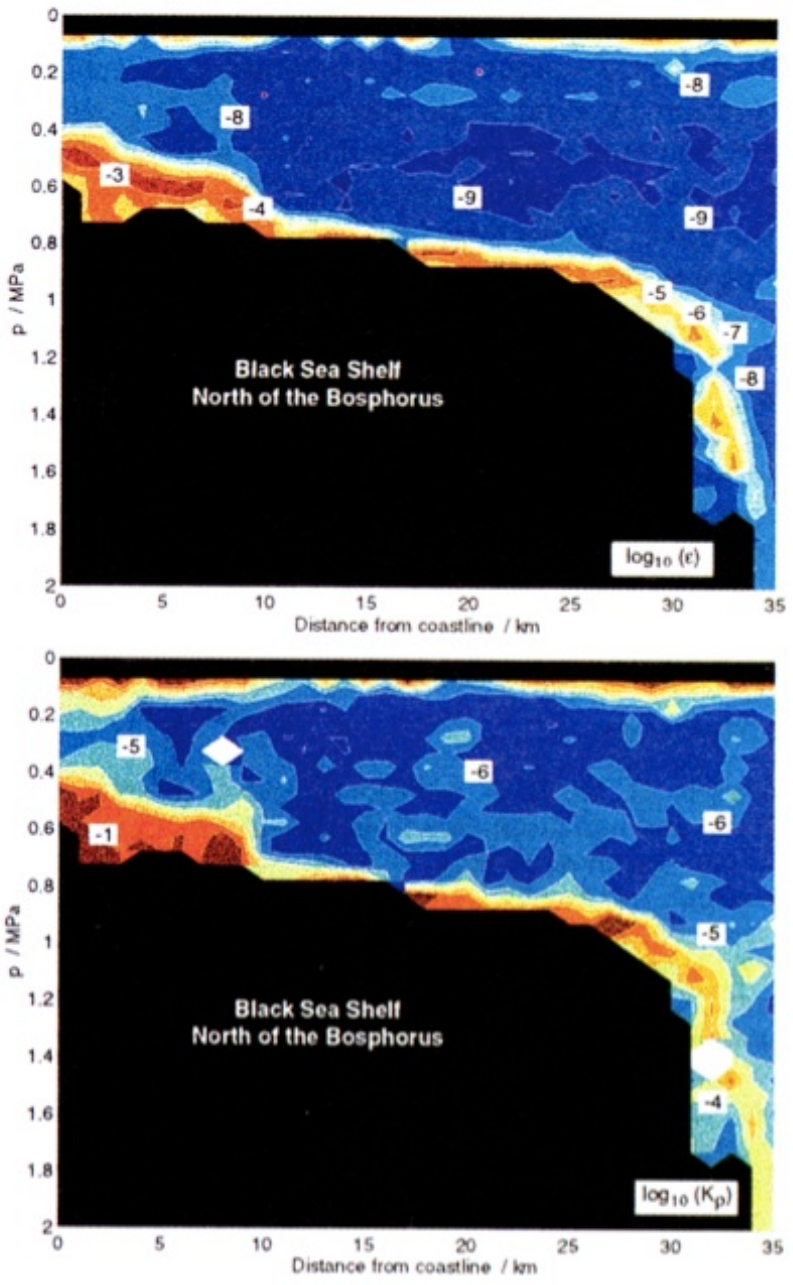

Figure 6. Contours of 1-km-averages of $\log_{10}(\epsilon)$ and $\log_{10}(K_\rho)$.

Emin Özsoy, Robinson Hordoir, Nathalie Toque, Hazem Nagy, Adil Sözer
(2014, 2015)

Model Development for the Black Sea Circulation and Mixing with Applications (2010-2014)

The Black Sea:

- an ‘almost’ closed basin, constrained by the exchange of water at the Turkish Straits System,
- catchment area covering almost half of the European continent
- large rivers and land runoff carry water and pollutants into the sea
- The hydrological cycle of water originating from the European-Black Sea and the Euro-Mediterranean regions is completed by the fluxes of water through the Turkish Straits System
- air-sea exchange is all too significant in the climate sensitive region of seas trapped between lands - medi terra nean character

The Catchment Area - Black Sea Drainage Basin

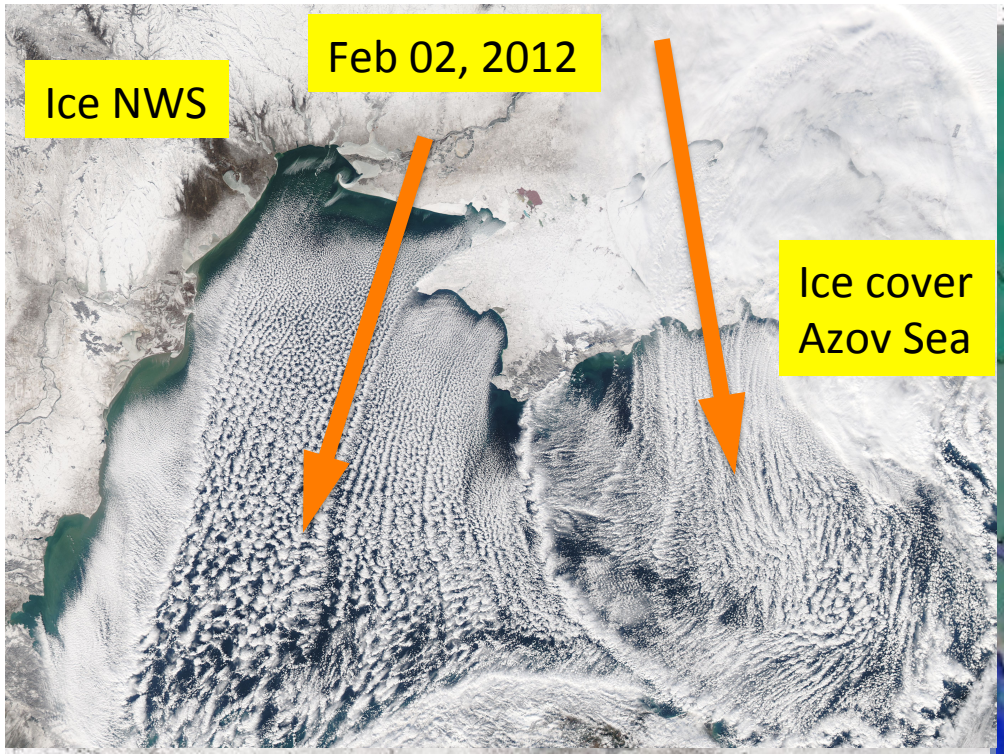

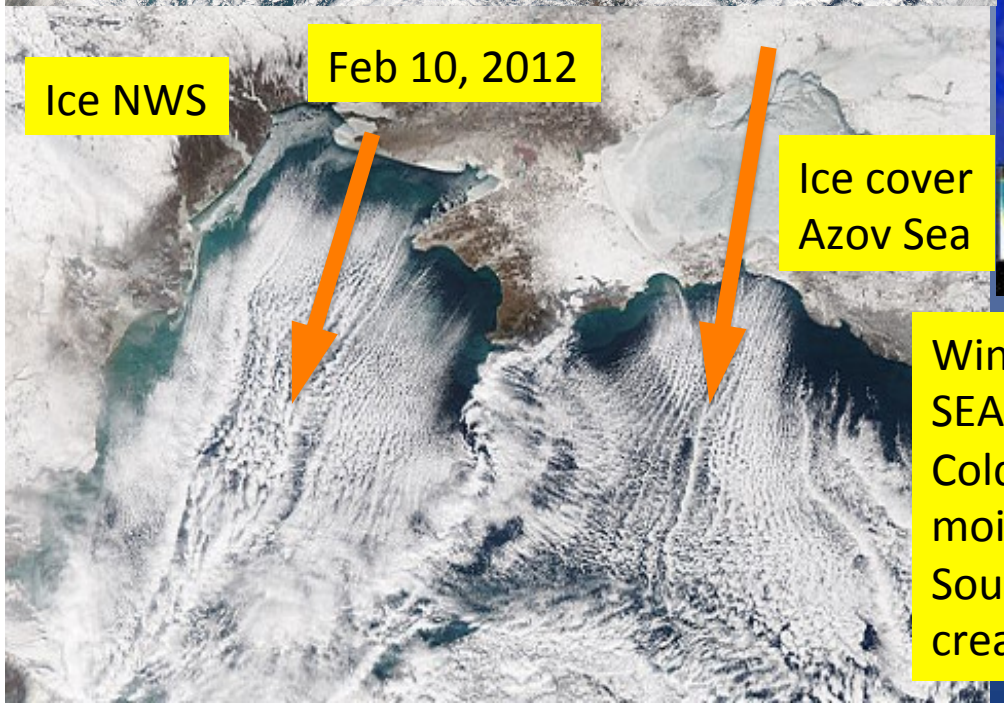

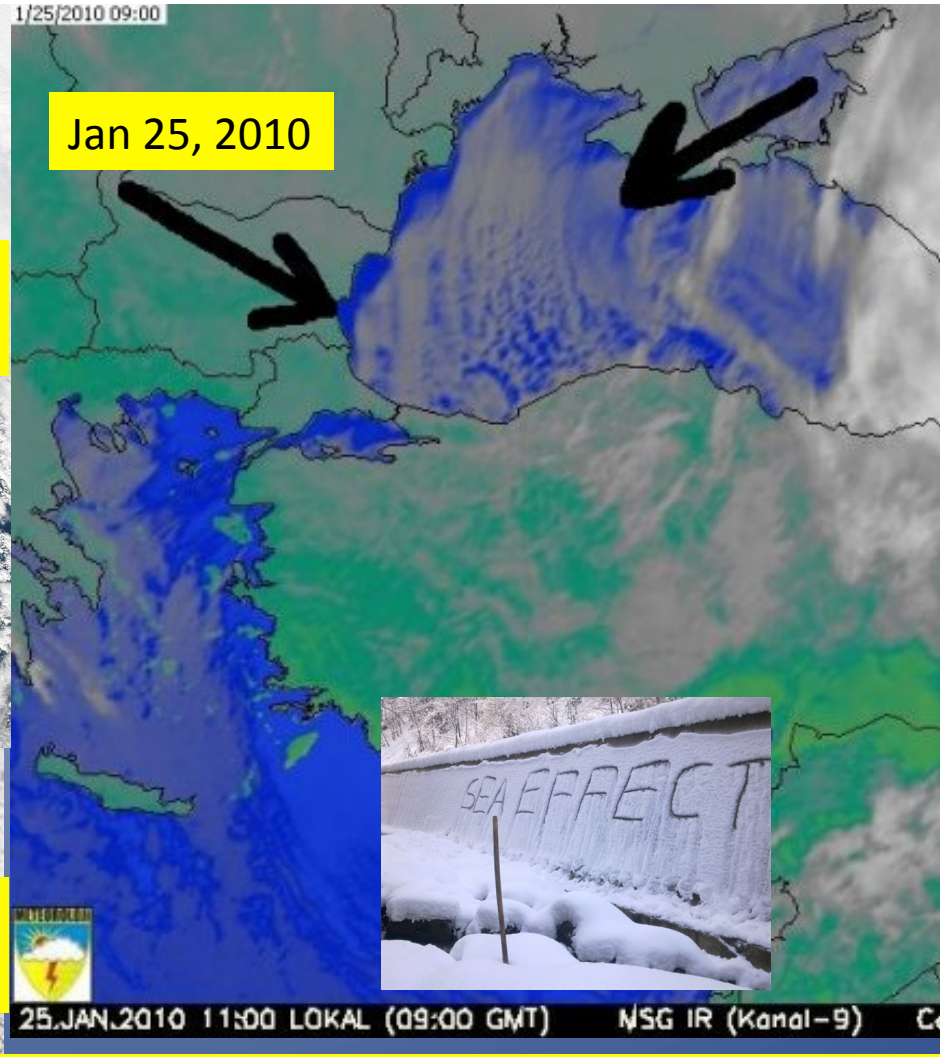

Wintertime moisture transport
SEA EFFECT
Cold dry winds from the north picking up moisture from the warm Black Sea
Southward moisture transport from the Black Sea creates snow blizzards in the absence of a storm…

72hr accumulated Precipitation on 18 Sep 2012 (metuwrf forecast)

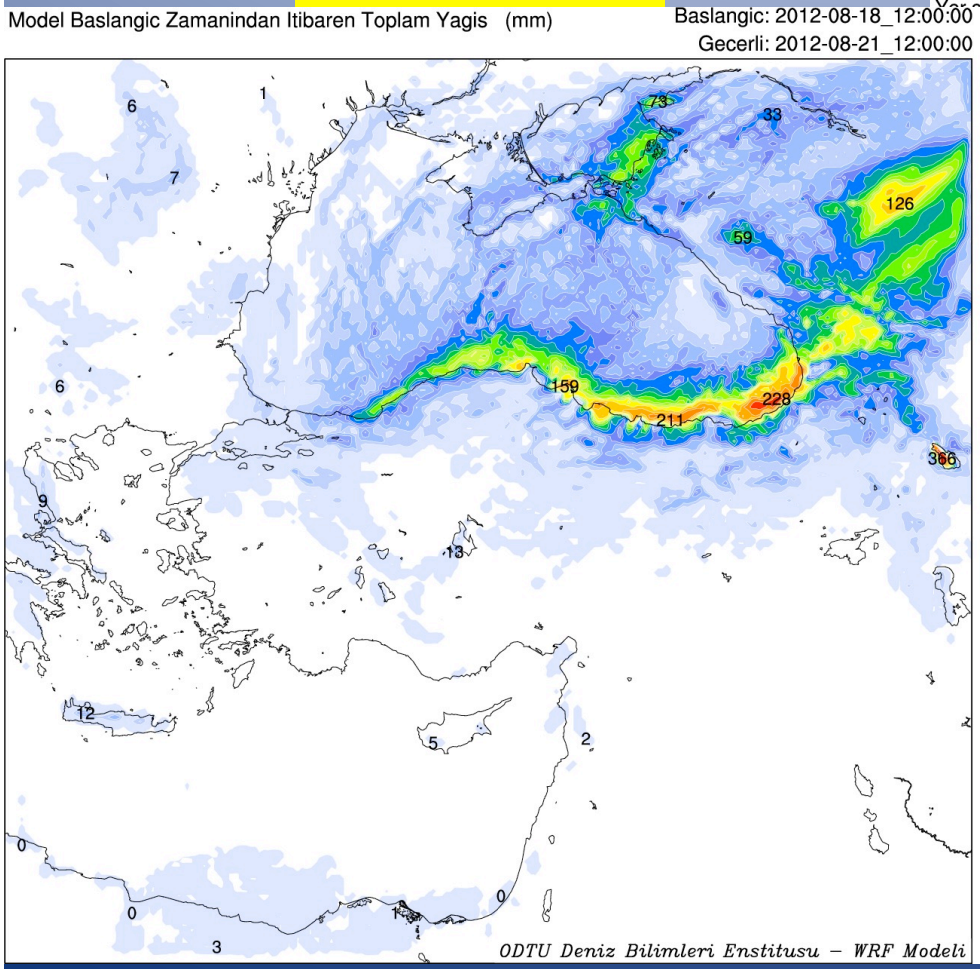

72 hr surface winds and relative humidity on 18 Sep 2012 (metuwrf forecast)

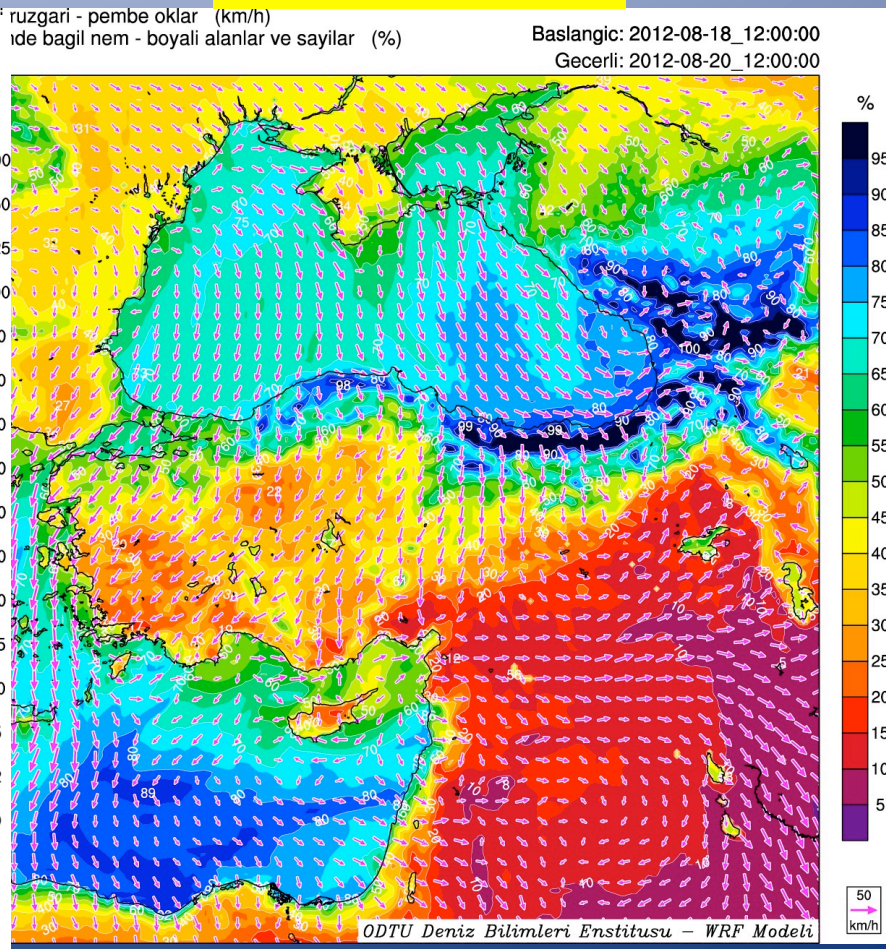

Skiron winds
on 12 Sep 2012

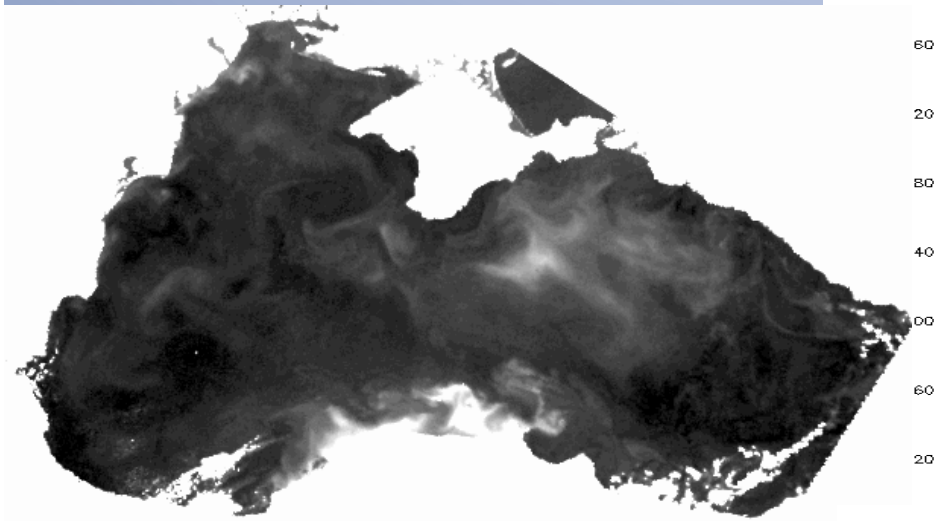

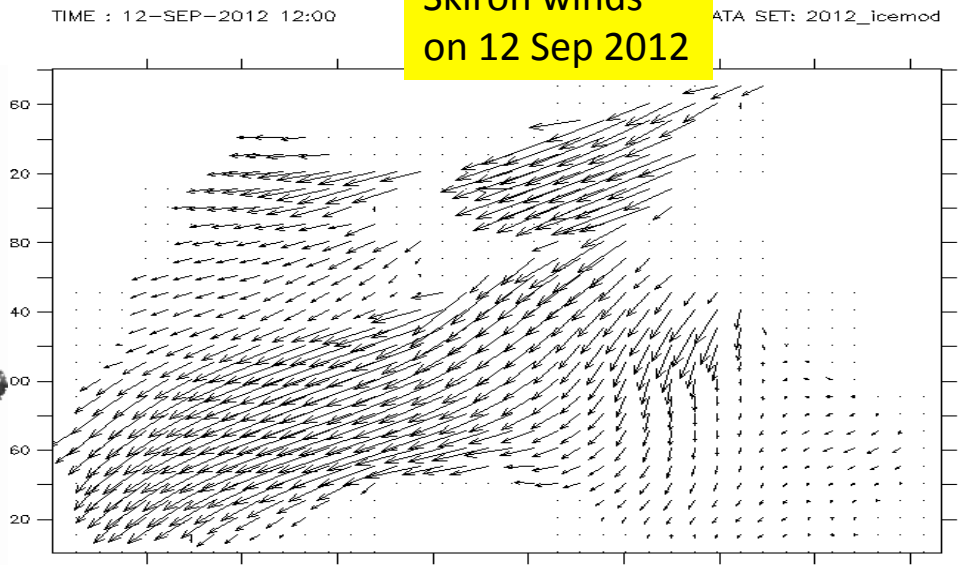

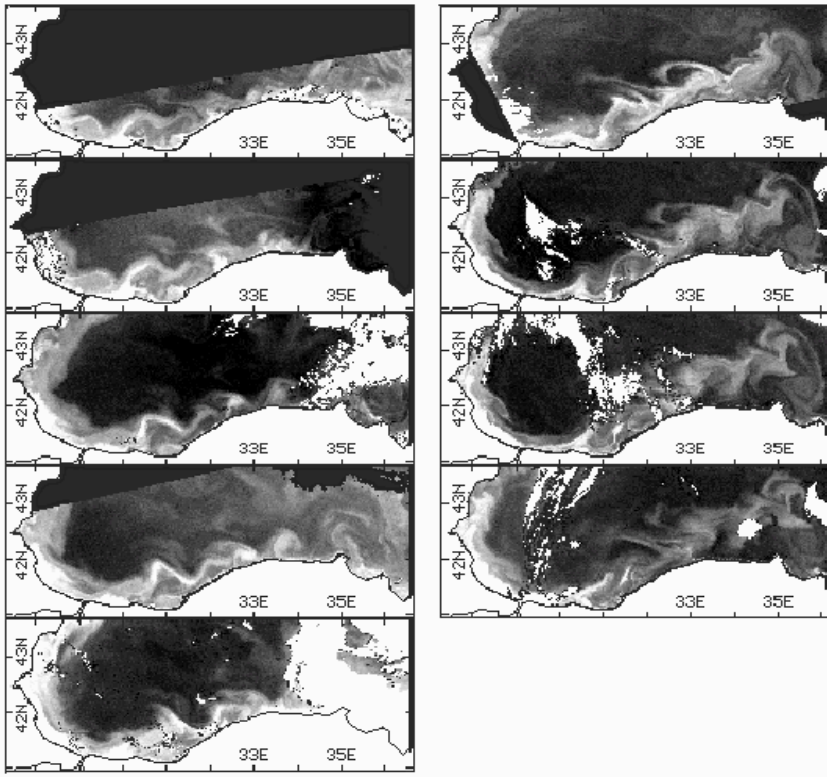

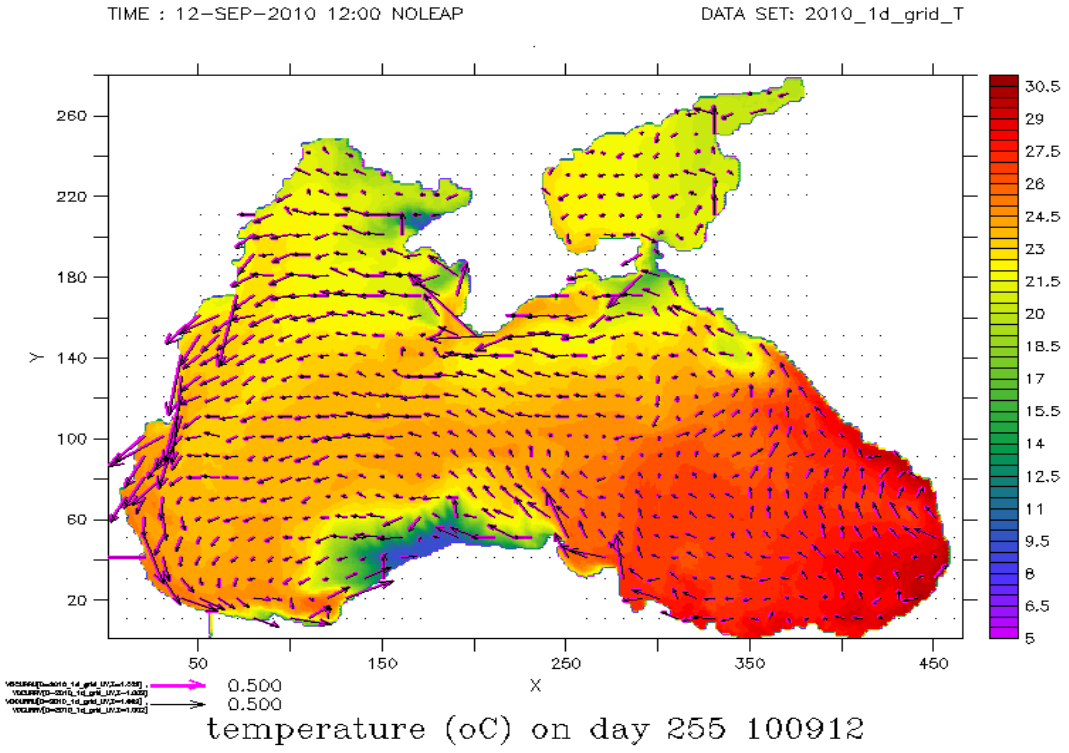

İNEBOLU Sea Surface Temperature SST

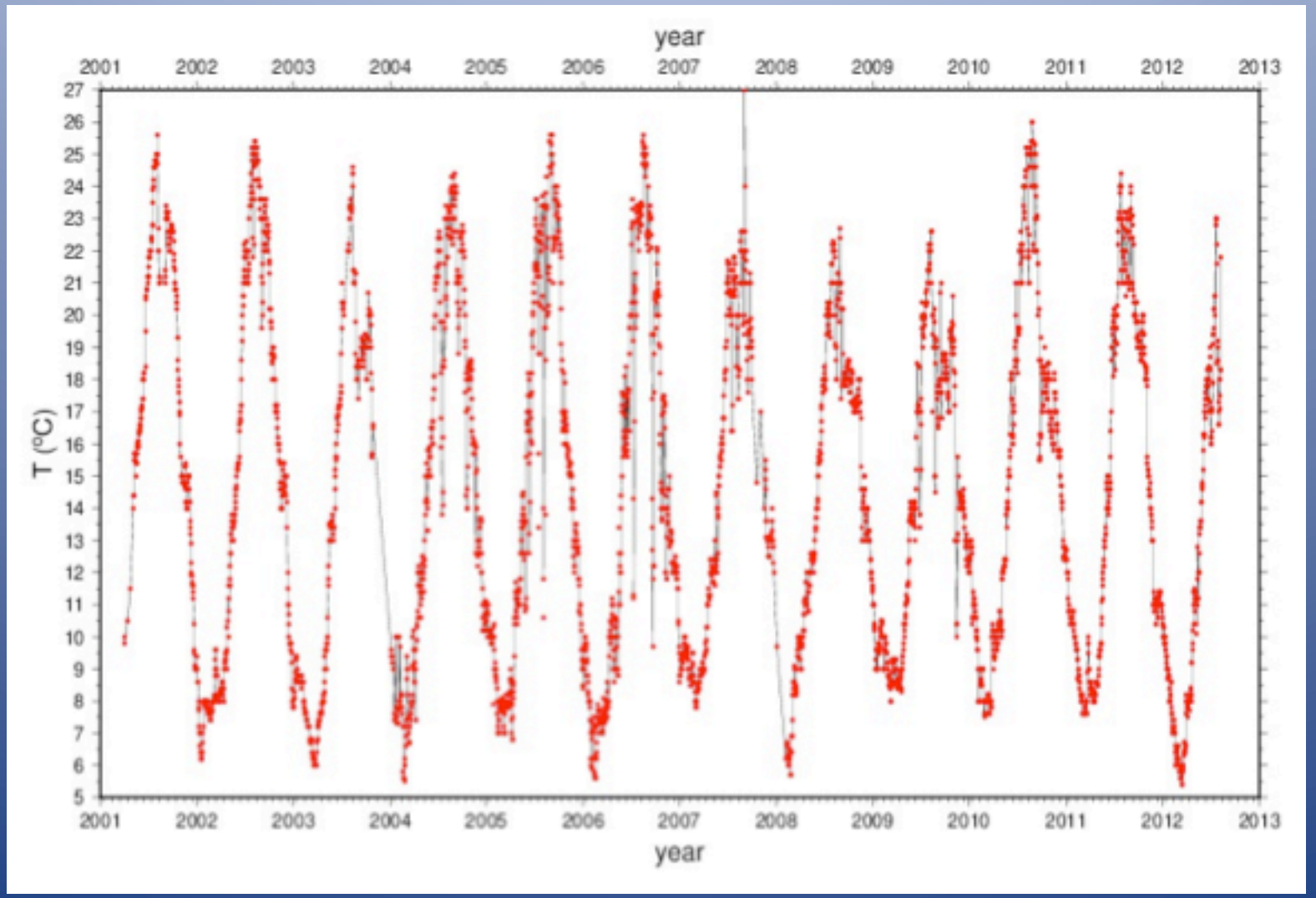

İNEBOLU Sea Surface Temperature SST

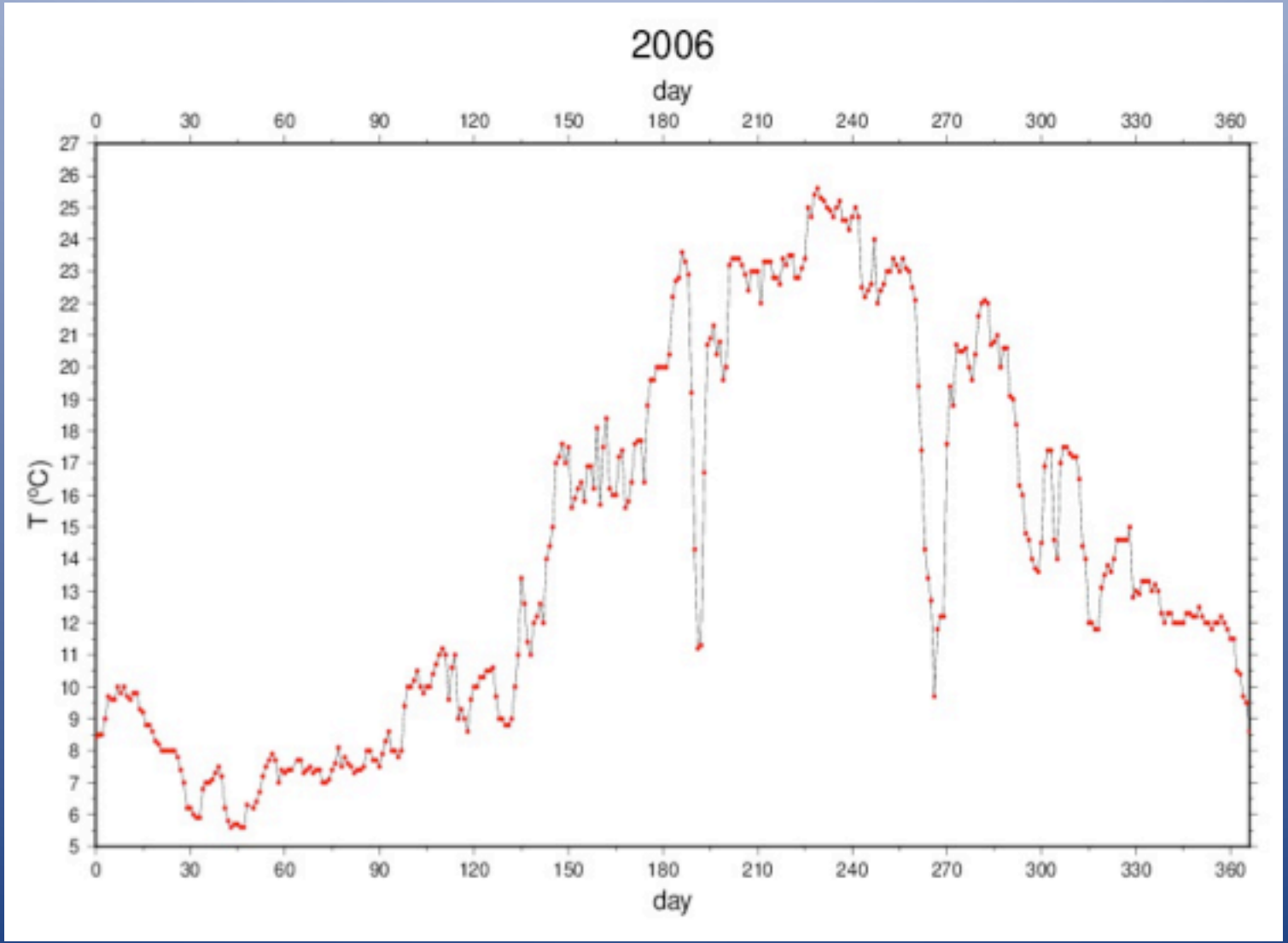

same pattern repeated 2008-2014 !

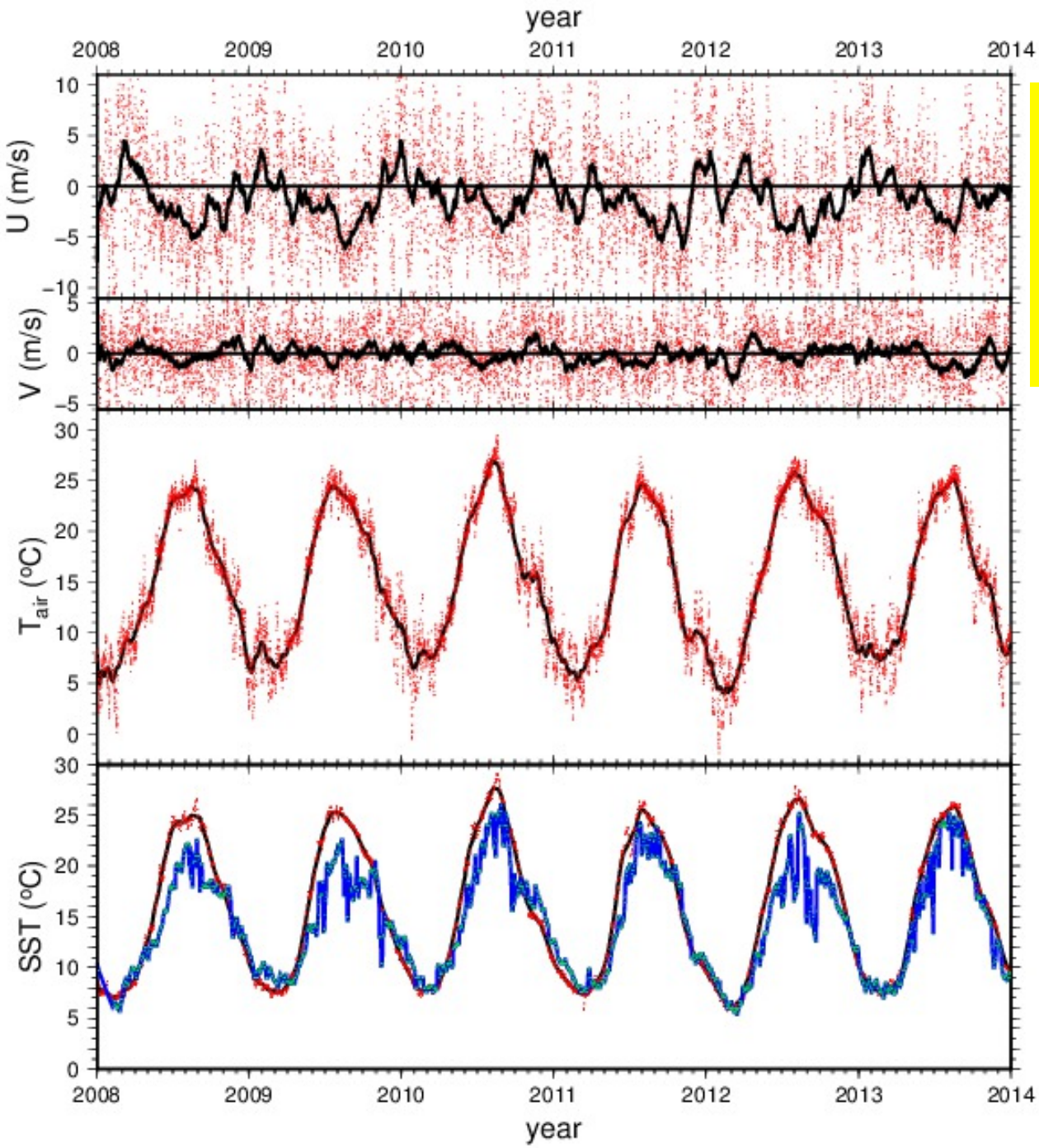

İnebolu winds
low pass filtered
aligned with
the coast
U -alongshore
V -crosshore

ECMWF SST
near inebolu

İnebolu SST
blue – observed
black – ECMWF

Dizzying fish by the upwelling collected by the people of İnebolu !

Photos Sinan Çevik

‘Marine Layer’ (atmospheric inversion) at İnebolu coastal upwelling area, Black Sea

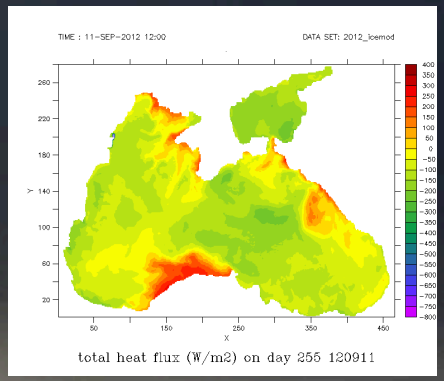

Photo Sinan Çevik

The Black Sea 2nd NEMO configuration, IMS-METU (DIFFERENCES FROM 1st IN RED!)
(Robinson Hordoir, Adil Sözer, Hazem Nagy, Emin Özsoy)

NEMO 3.4

Model of the Black sea with the Azov sea

Domain: 40.92°-47.30°N, 27.43°-42.00°E

Horizontal resolution Δx=2.5km

Z coordinate, partial steps, vertical resolution: 60 levels

(adjusted to topography and density variations)

Dynamical time step:

240s, number of barotropic time steps: 100, time step: 2.4s (for large K_h, A_h =400 m^2/s)

240s, number of barotropic time steps: 600, time step: 0.4s (for small K_h, A_h = 10 m^2/s)

Bathymetry: GEBCO 2008, max. depth in model grid 2201m

Surface atmospheric forcing: U. Athens - IASA Skiron, 0.05° horizontal-resolution

1hr temporal resolution - core bulk formulation

Runoff: Danube, Dniestr, Dniepr, Don, Kuban + Turkish rivers (total 12 rivers)

No geothermal flux at the bottom

Open boundary condition: Vertical profiles of temperature and salinity and η=0

at 1 point wide strait of the Bosphorus

Initial conditions: July 1992 temperature and salinity objectively analyzed data set

Laplacian lateral diffusion for the tracer (rn_aht_0 = runs with 400 and 10 m^2/s)

Laplacian lateral mixing for the momentum (rn_ahm_0 = runs with 400 and 10 m^2/s)

Generic Length Scale model (gls), No Double Diffusion Mixing model – yet!

List of the keys: key_mpp_mpi, key_ldfslp, key_dynspg_ts, key_trabbl, key_lim3, key_iomput,

key_bdy, key_zdfgls,, key_nosignedzero, key_BSEA_LIM3

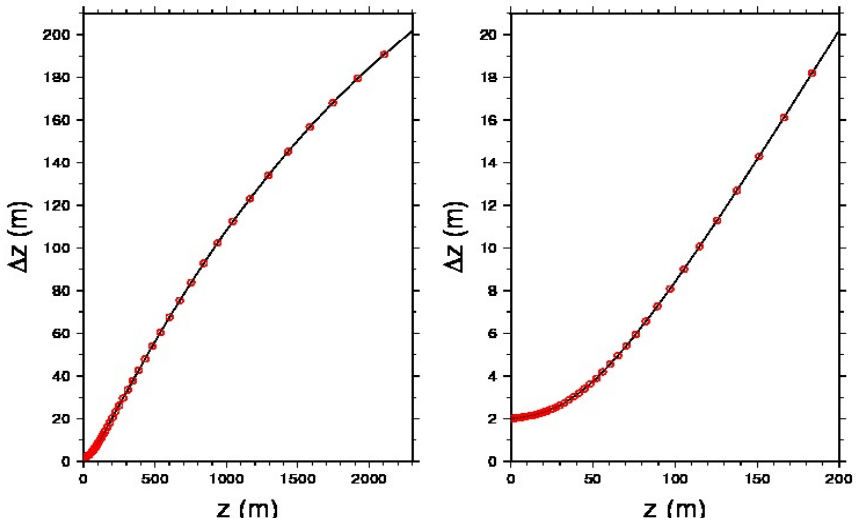
Δz (m)
z (m)
Δz (m)
z (m)

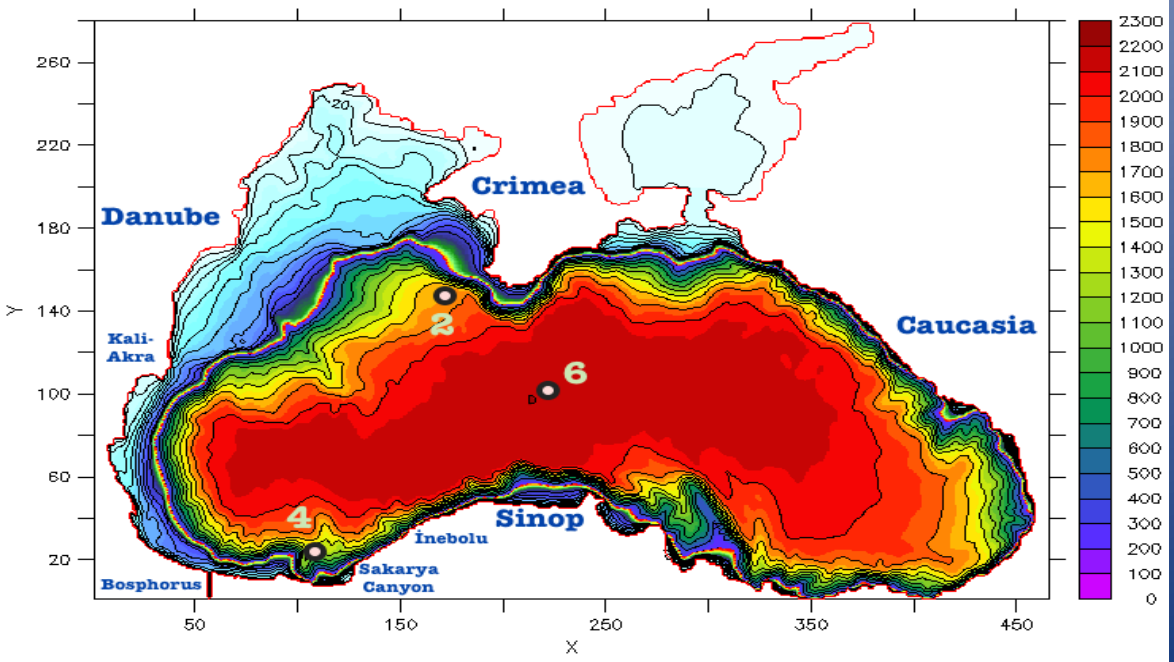
Danube
Crimea
Caucasia
Kali-
Akra
Sinop
Inebolu
Sakarya
Canyon
Bosphorus
2
4
6
Y
X
depth (m)

Initial conditions 02-26 July 1992 CoMSBlack Survey

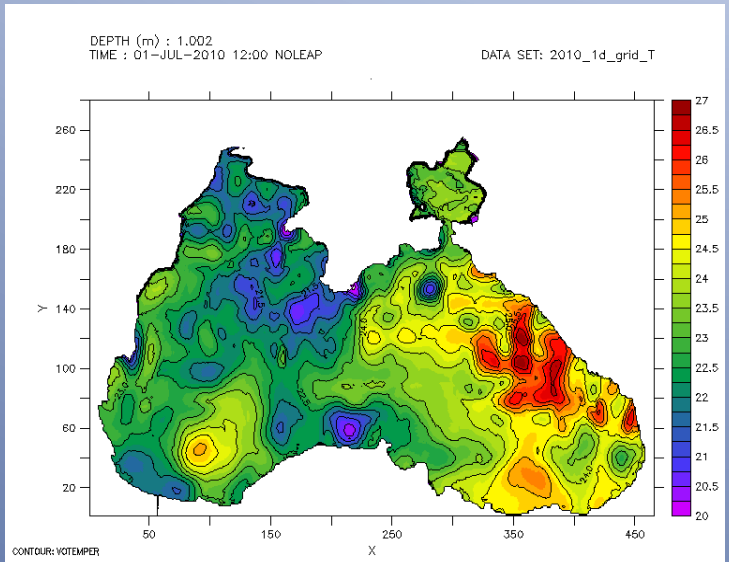

surface temperature (oC) July 1992

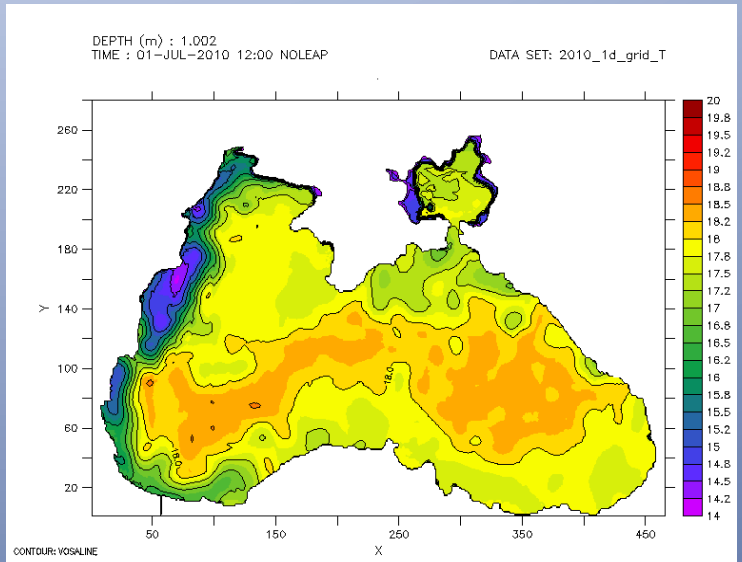

surface salinity July 1992

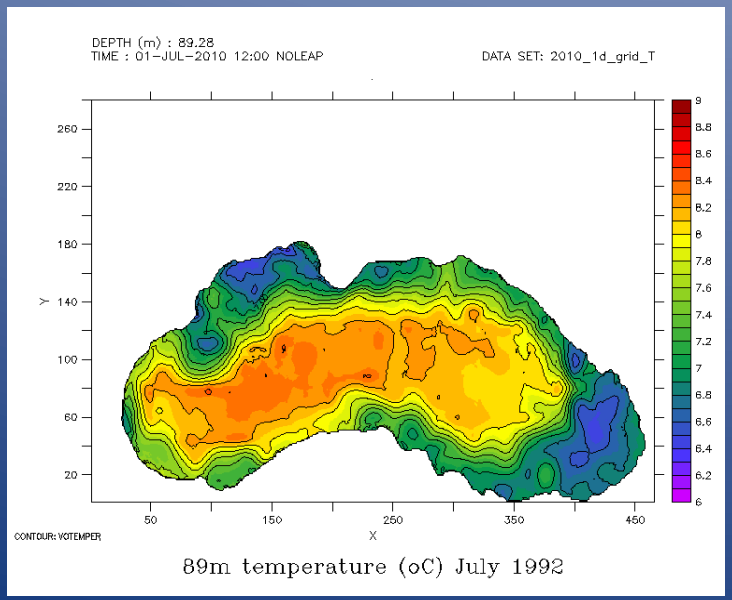

89m temperature (oC) July 1992

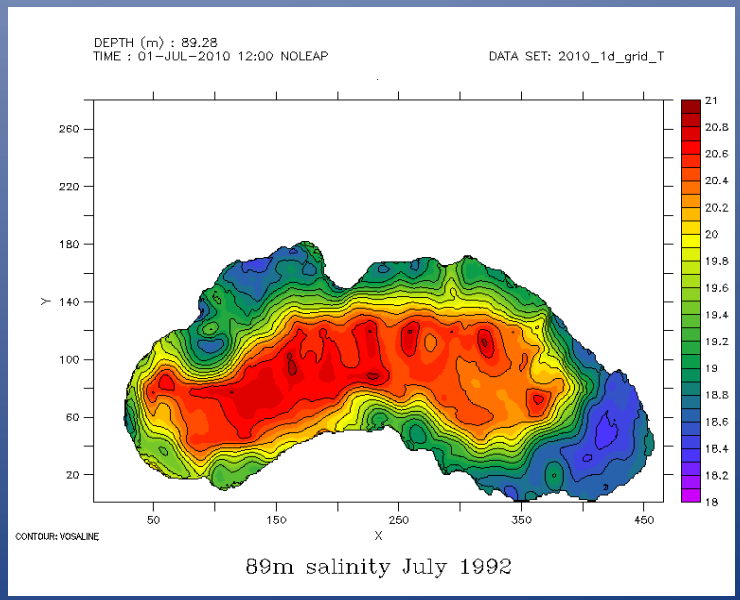

89m salinity July 1992

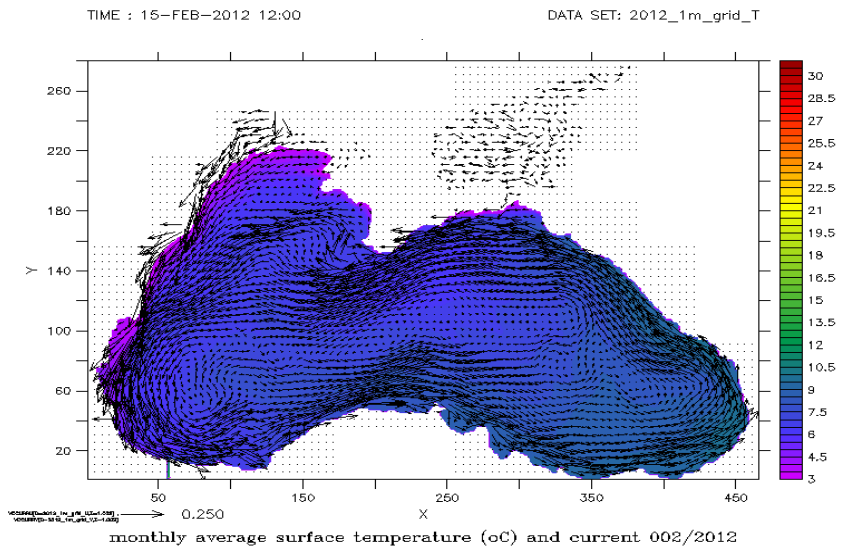

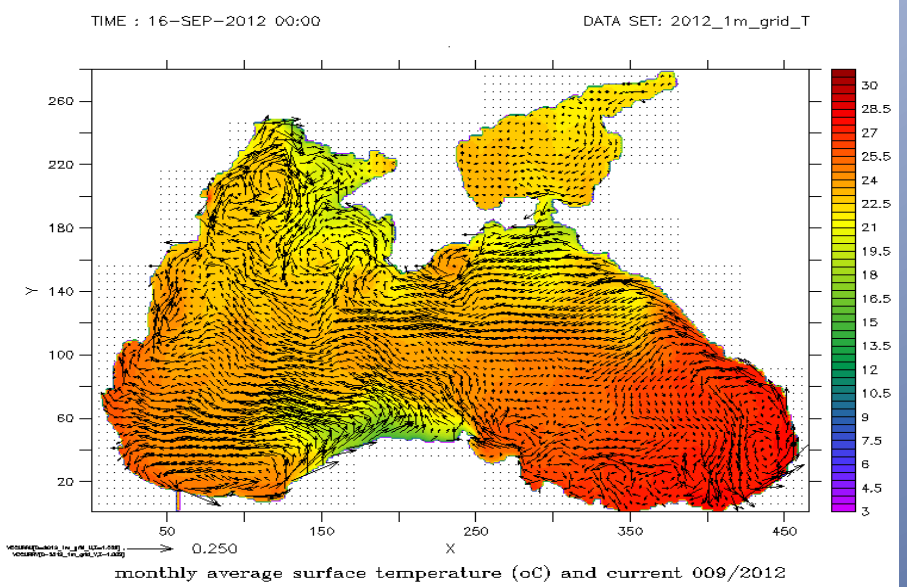

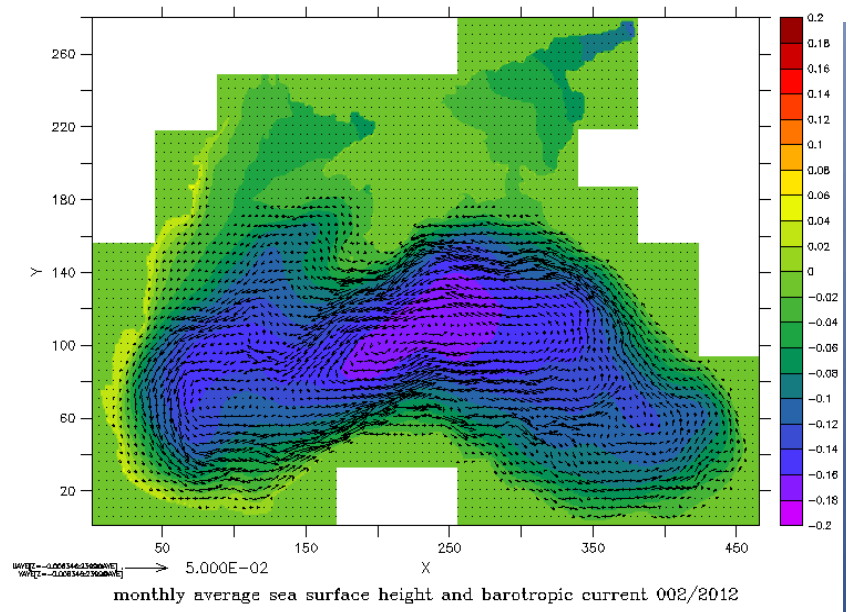

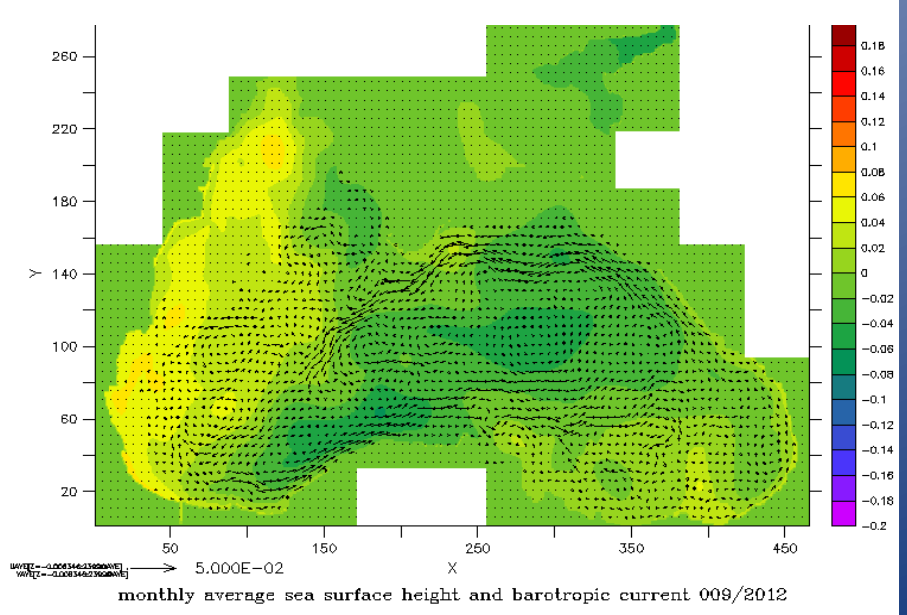

Monthly average circulation in February 2011 (lhs) and September 2011 (rhs), displayed in terms of surface salinity and currents (top row), surface temperature and currents (middle row) and sea surface height and barotropic currents (bottom row).

Satellite SST
on 12 Sep 2012

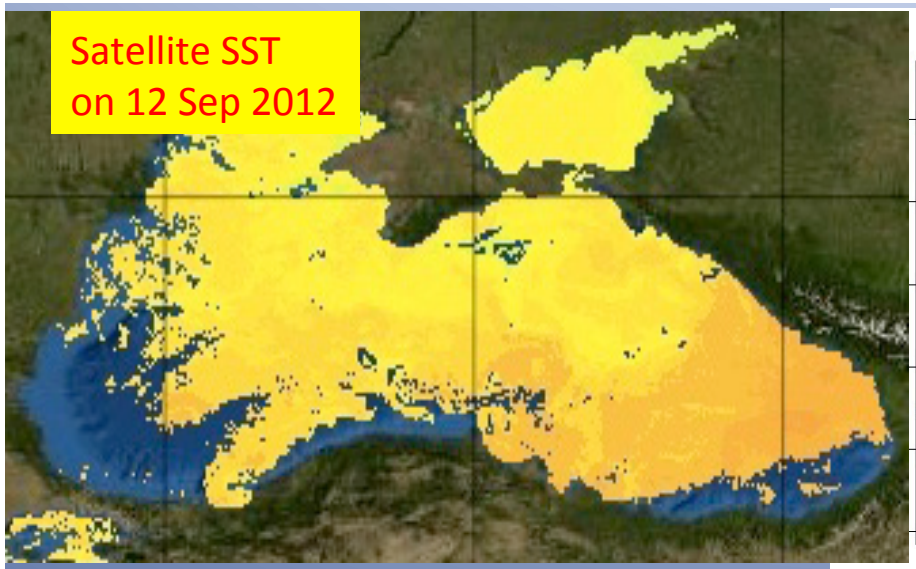

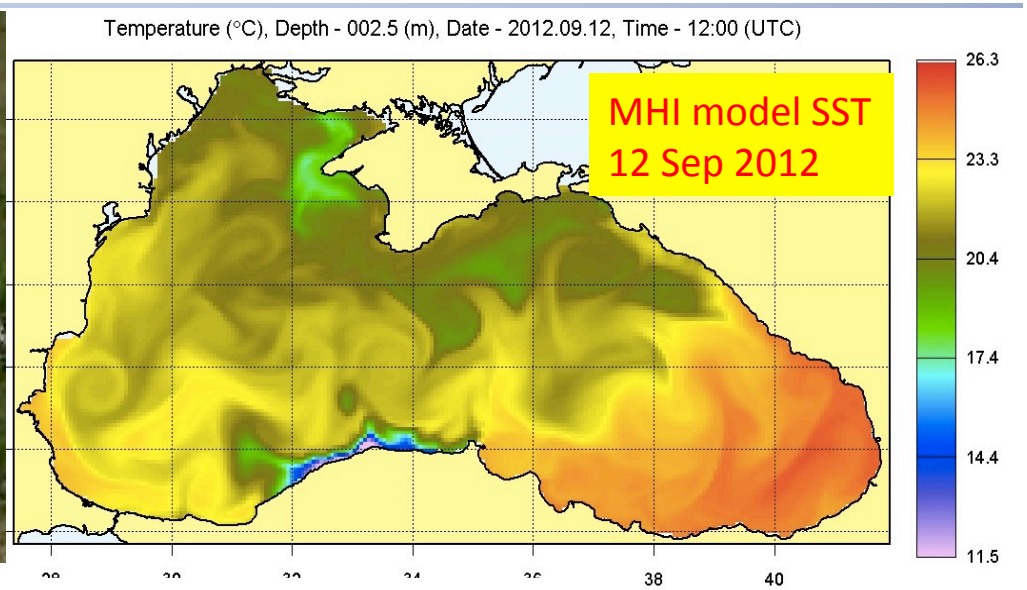

NEMOBlack
hindcast SST
on 12 Sep 2012

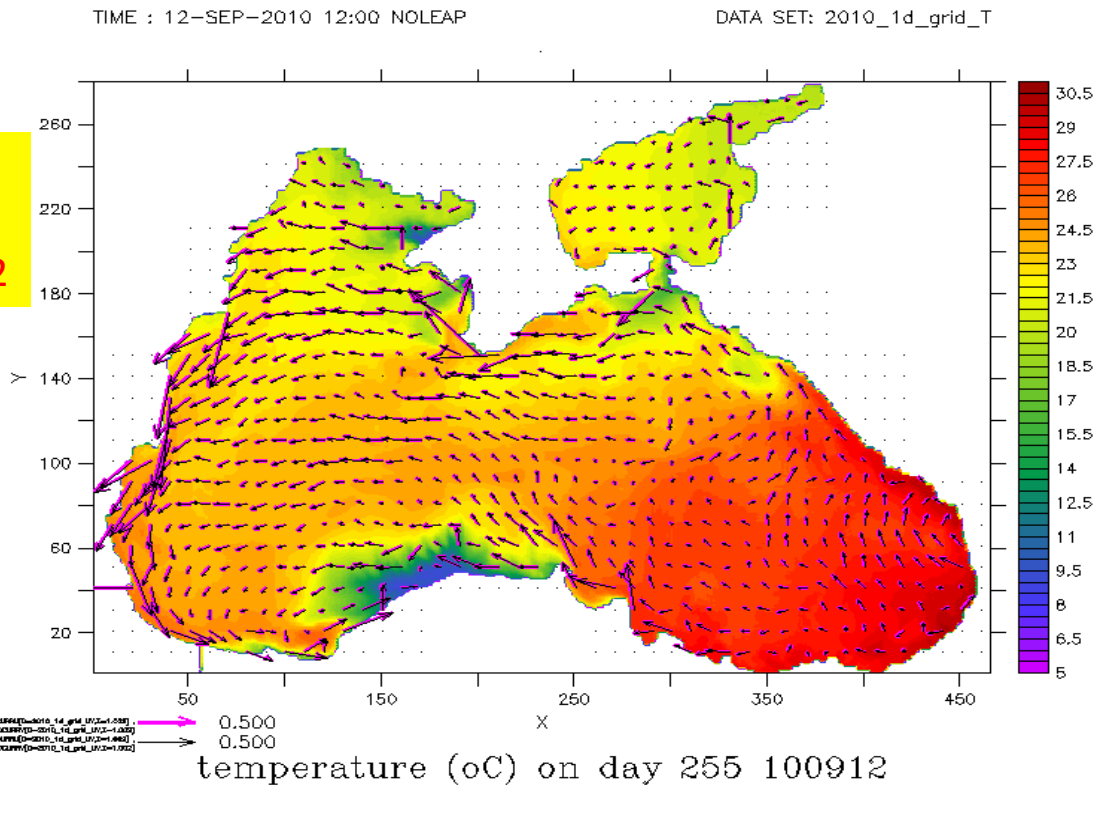

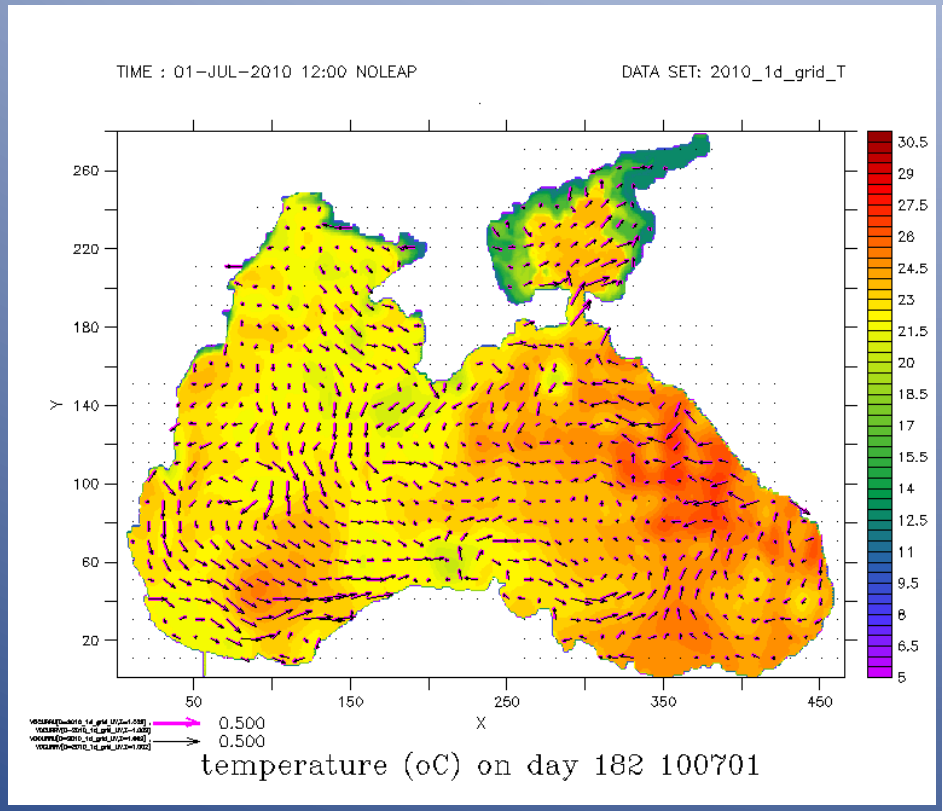

temperature (oC) on day 182 100701

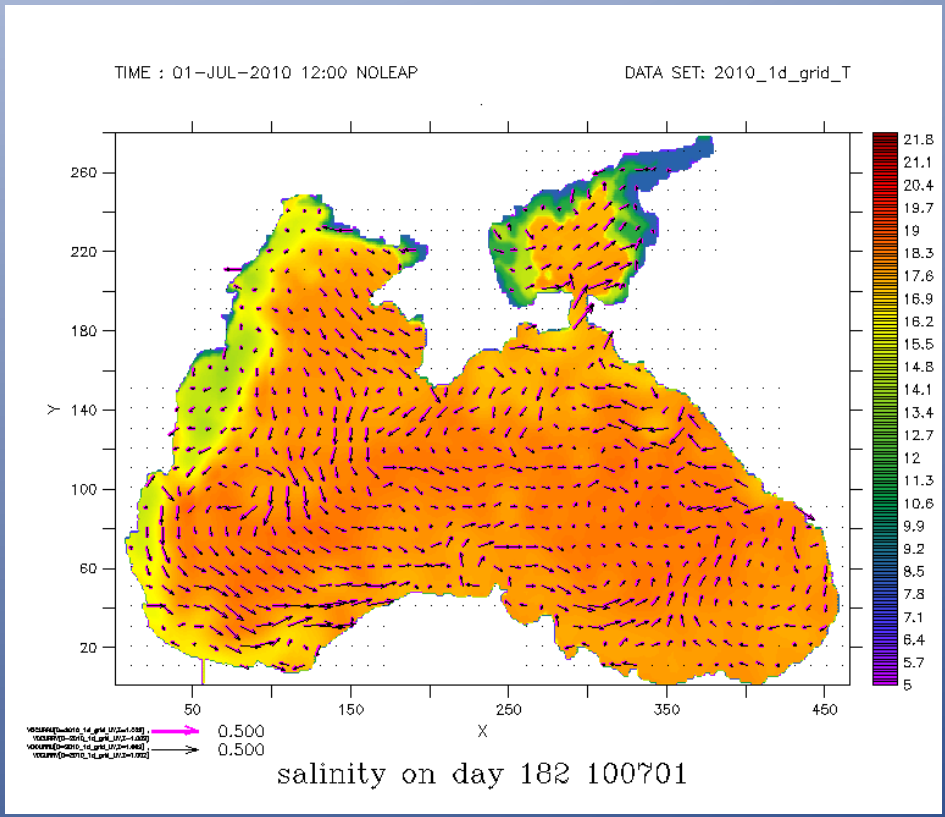

salinity on day 182 100701

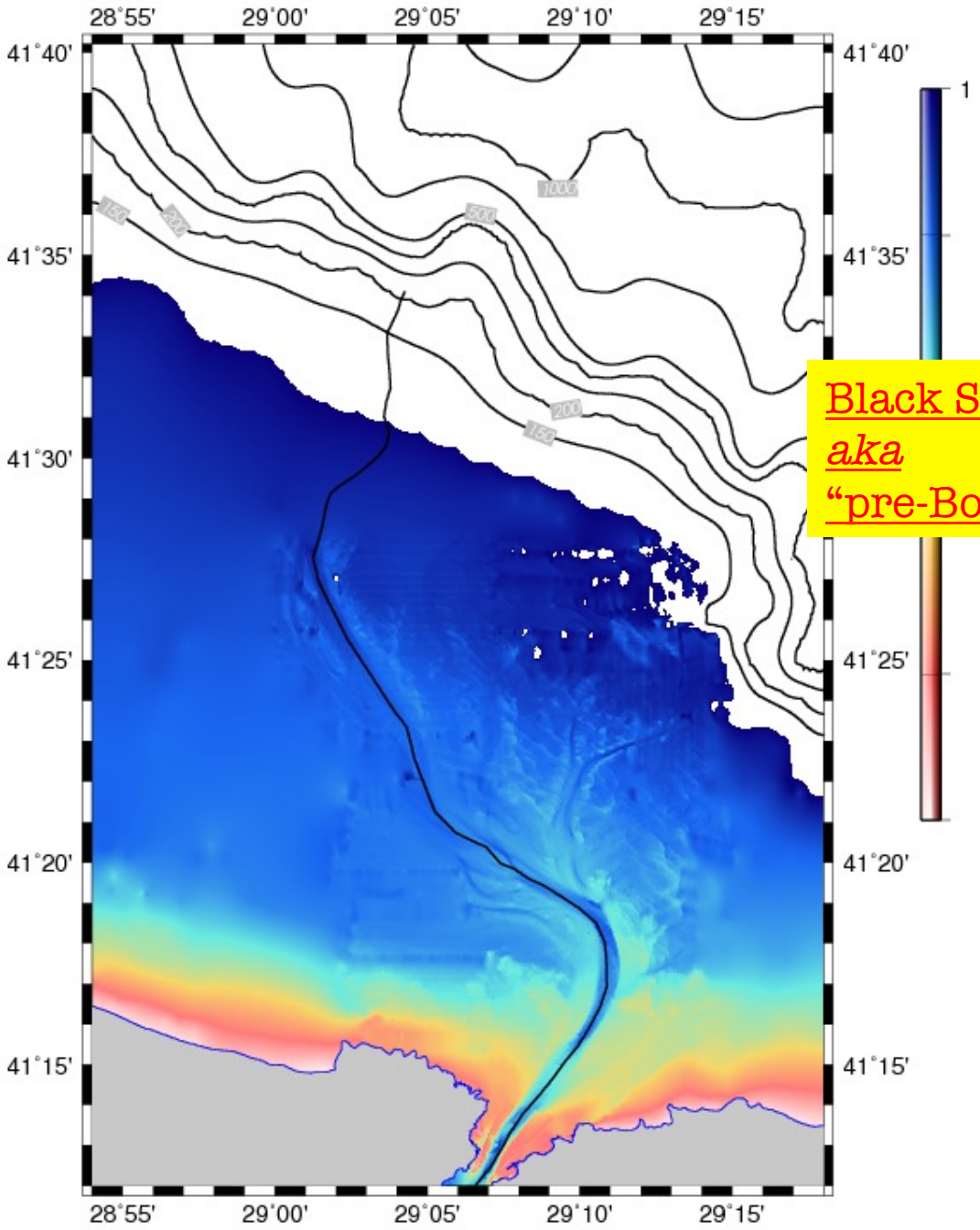

Black Sea exit region
aka
"pre-Bosphorus channel"

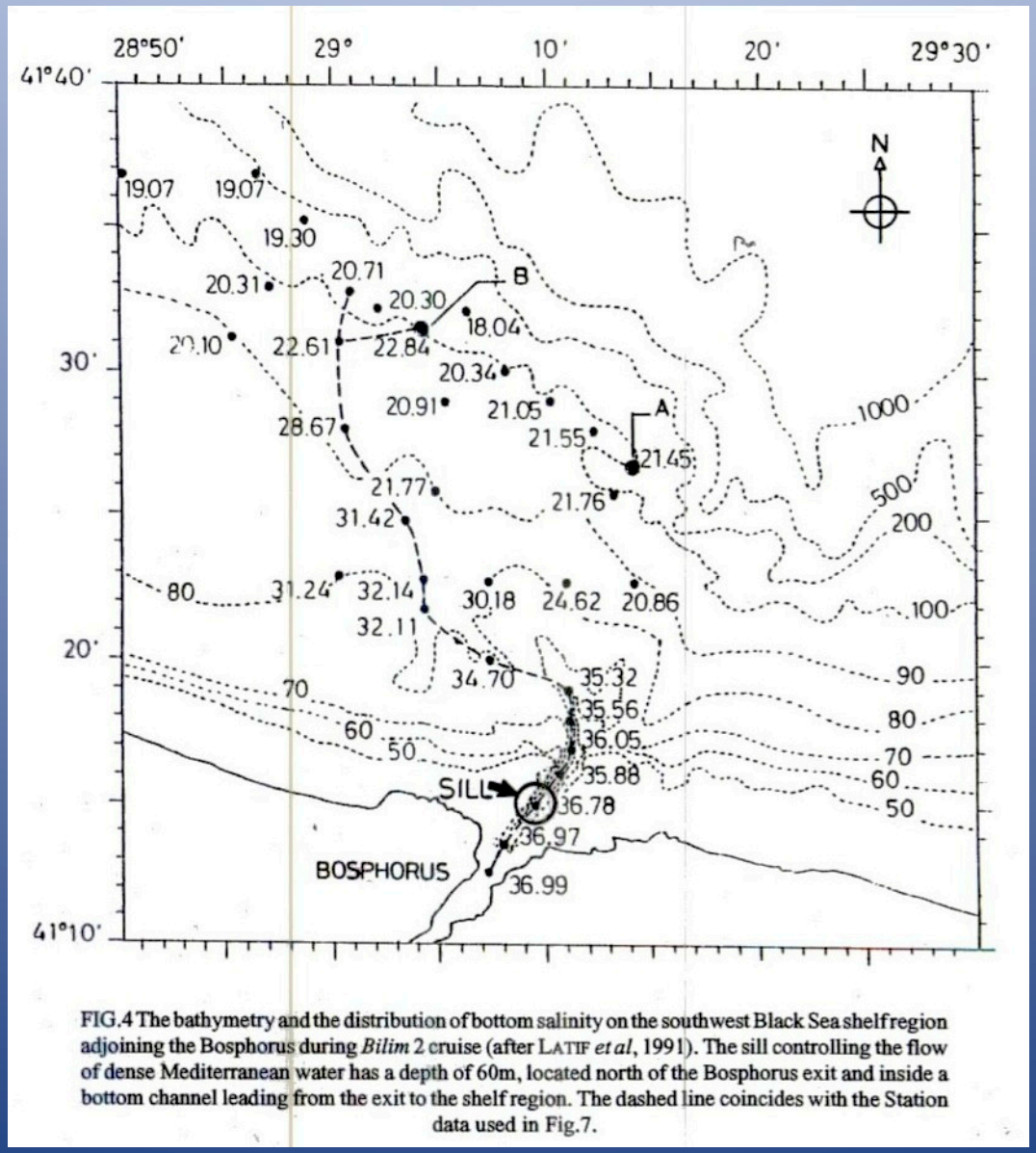

FIG.4 The bathymetry and the distribution of bottom salinity on the southwest Black Sea shelf region adjoining the Bosphorus during *Bilim* 2 cruise (after LATIF *et al*, 1991). The sill controlling the flow of dense Mediterranean water has a depth of 60m, located north of the Bosphorus exit and inside a bottom channel leading from the exit to the shelf region. The dashed line coincides with the Station data used in Fig.7.

Özsoy et al., 2001

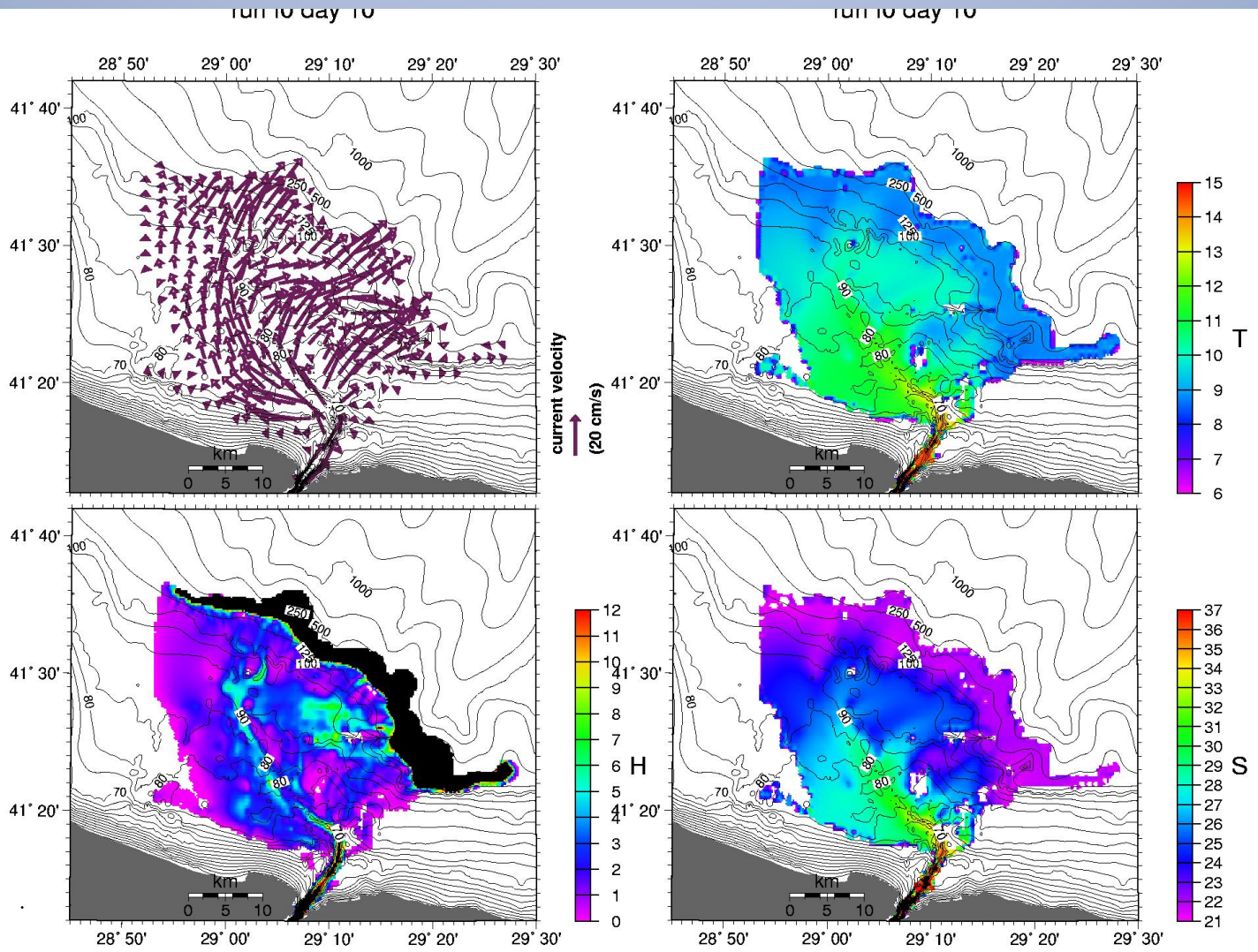

Figure 1: (a) flow velocity, (b) layer thickness, (c) temperature and (d) salinity 10 days after the initialization of the model with continuous outflow from the Bosphorus. Run parameters are: $A_h = 150m^2/s$, $r = 0.003$ for the horizontal eddy coefficient and bottom friction respectively, and $u_o = 0.7$ (direction 45^o) m/s, $S_o = 37$, $T_o = 14.5°C$, $H_o = 40m$ for the initial conditions specified at the Black Sea exit of the Bosphorus. The velocity vectors are plotted at every 10 points in the grid, to simplify the graphics. The thickness in the dark area along the continental slope is outside the scale range.

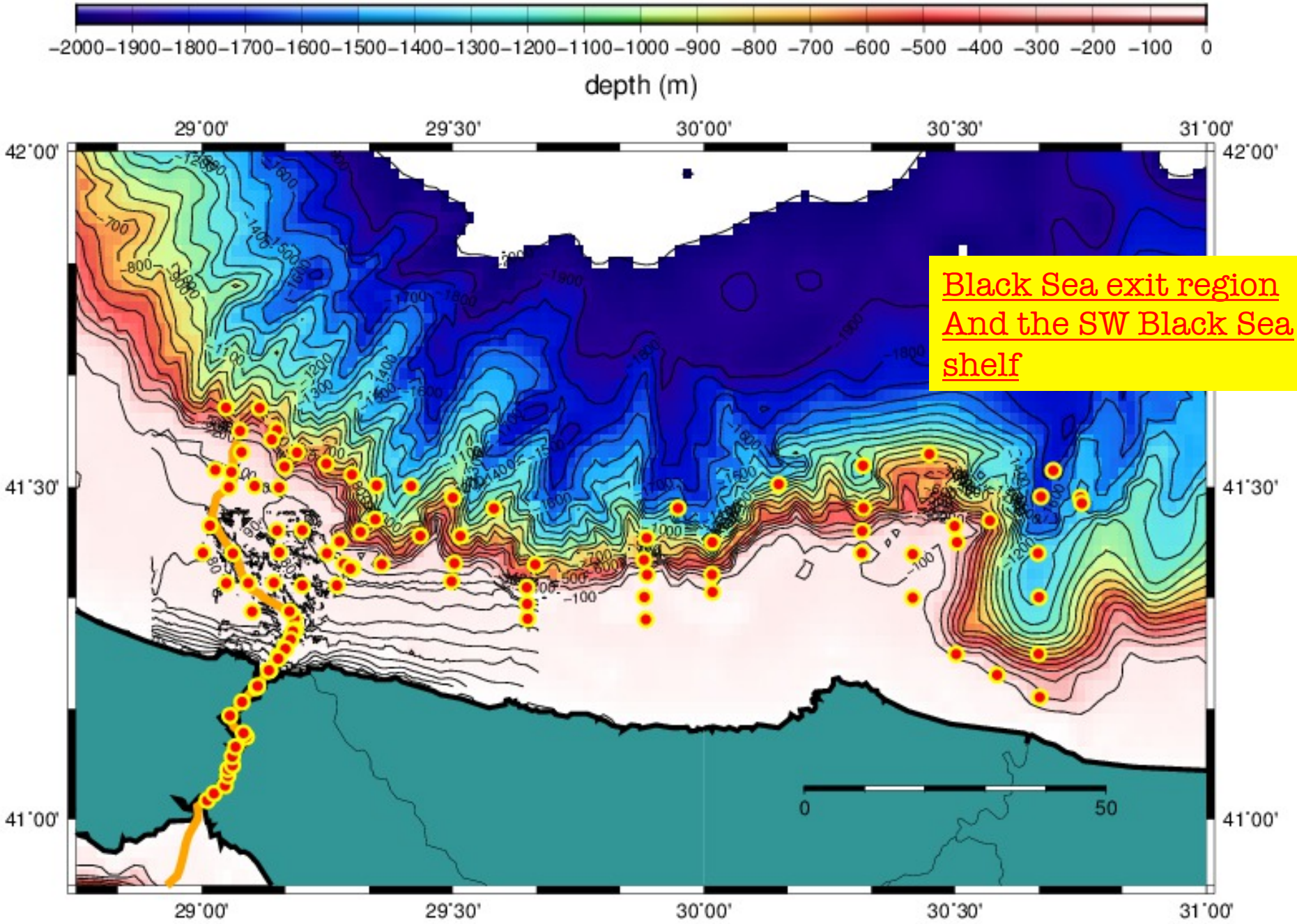
−2000 −1900 −1800 −1700 −1600 −1500 −1400 −1300 −1200 −1100 −1000 −900 −800 −700 −600 −500 −400 −300 −200 −100 0
depth (m)
29°00'
29°30'
30°00'
30°30'
31°00'
42°00'
41°30'
41°00'
0
50
Black Sea exit region
And the SW Black Sea
shelf

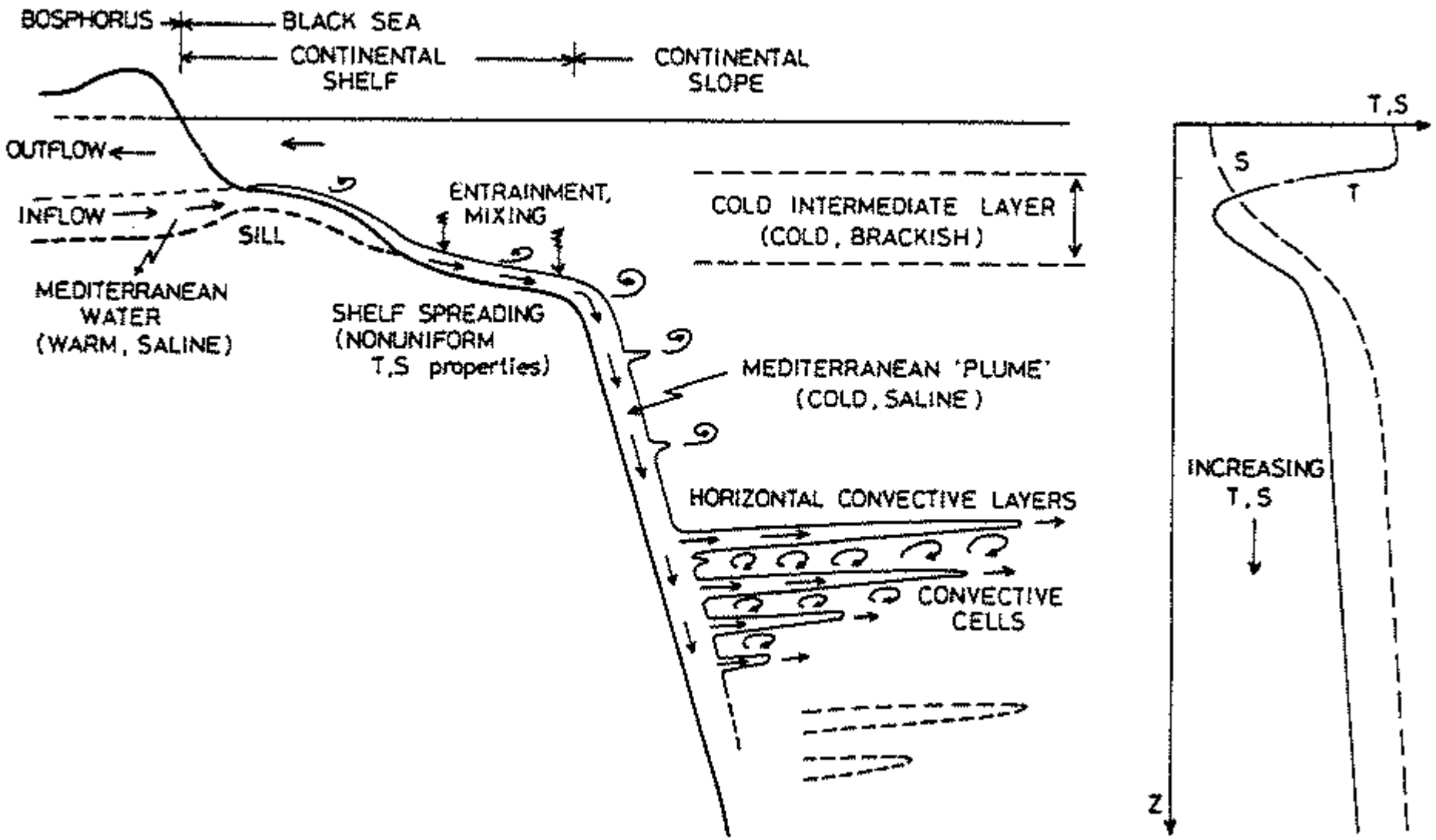
BOSPHORUS
BLACK SEA
CONTINENTAL SHELF
CONTINENTAL SLOPE
OUTFLOW
INFLOW
SILL
ENTRAINMENT, MIXING
COLD INTERMEDIATE LAYER (COLD, BRACKISH)
MEDITERRANEAN WATER (WARM, SALINE)
SHELF SPREADING (NONUNIFORM T,S properties)
MEDITERRANEAN 'PLUME' (COLD, SALINE)
HORIZONTAL CONVECTIVE LAYERS
CONVECTIVE CELLS
T,S
S
T
INCREASING T, S
Z

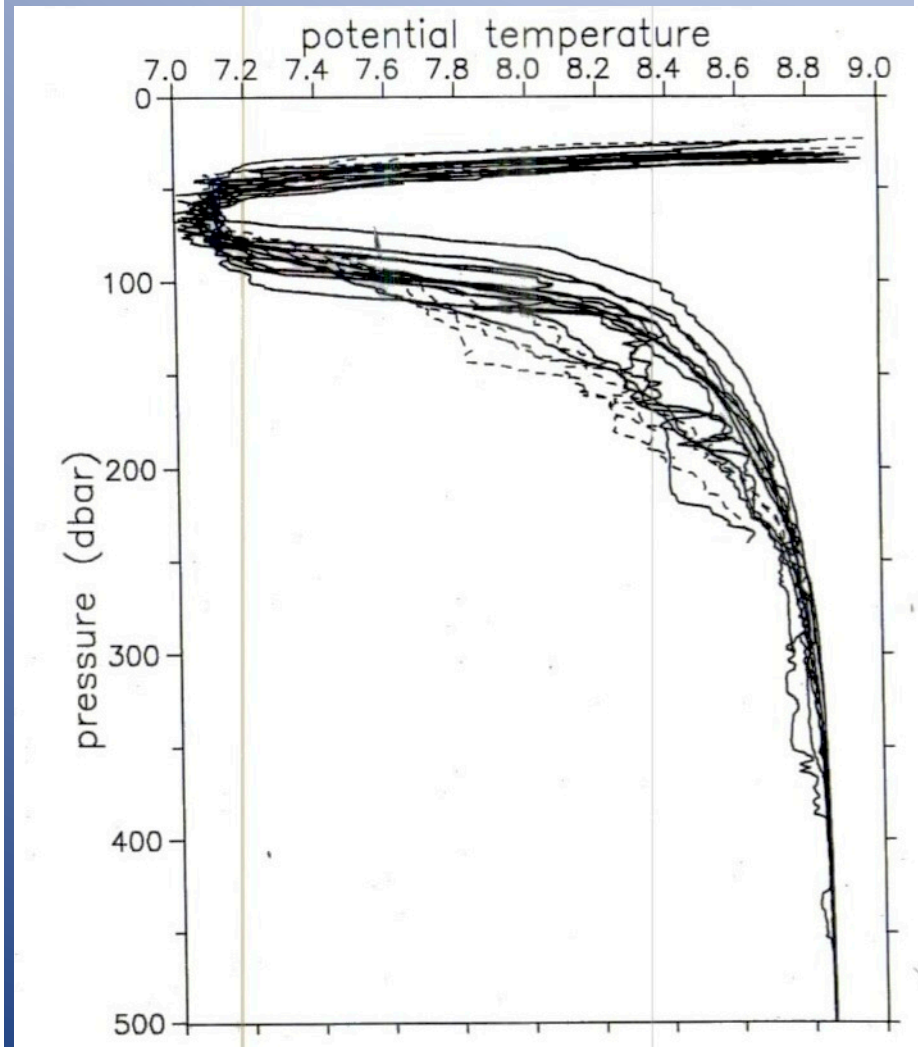

FIG.14. Potential temperature versus depth for *Bilim* 2. Cold temperature anomalies are observed in many of the individual profiles and down to a depth of 500m. Dashed lines represent stations located closest to the continental slope (stations 7, 8, 9 and 10) whose θ-S deviations are shown in Fig.12.

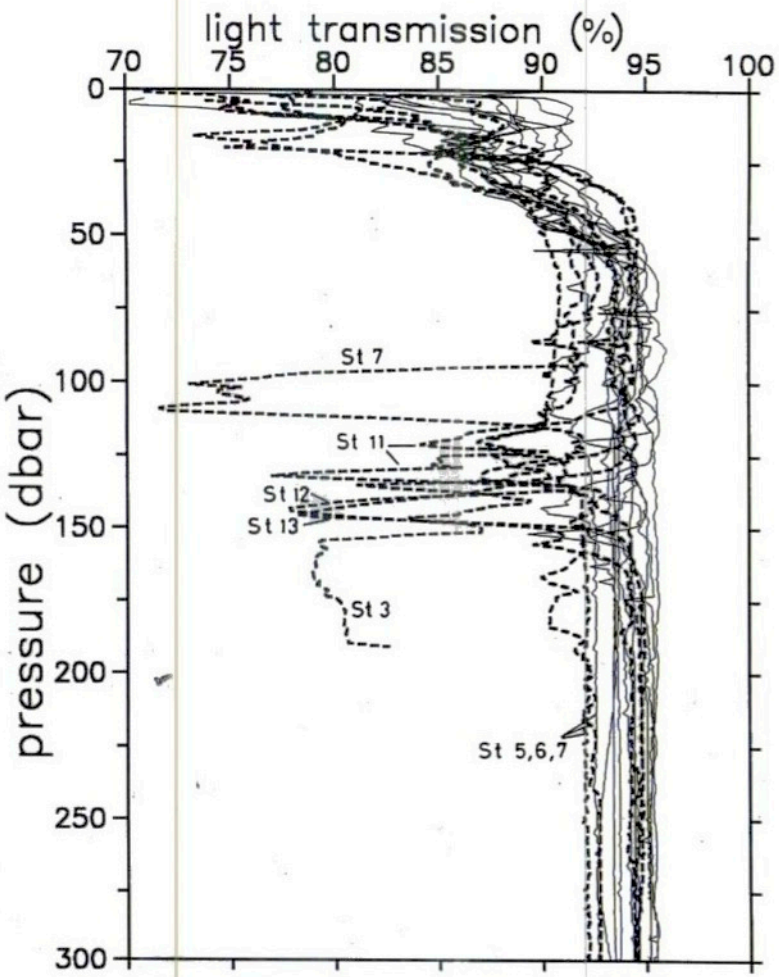

FIG.8. Percent light transmission versus depth profiles observed at *Knorr* Stations 3-27 (Fig.1). Stations with large suspended matter peaks (minima) are shown in dashed lines, and the remaining stations are shown in solid lines. The largest peaks occur at the near-shelf stations in the southwestern part of the Black Sea.

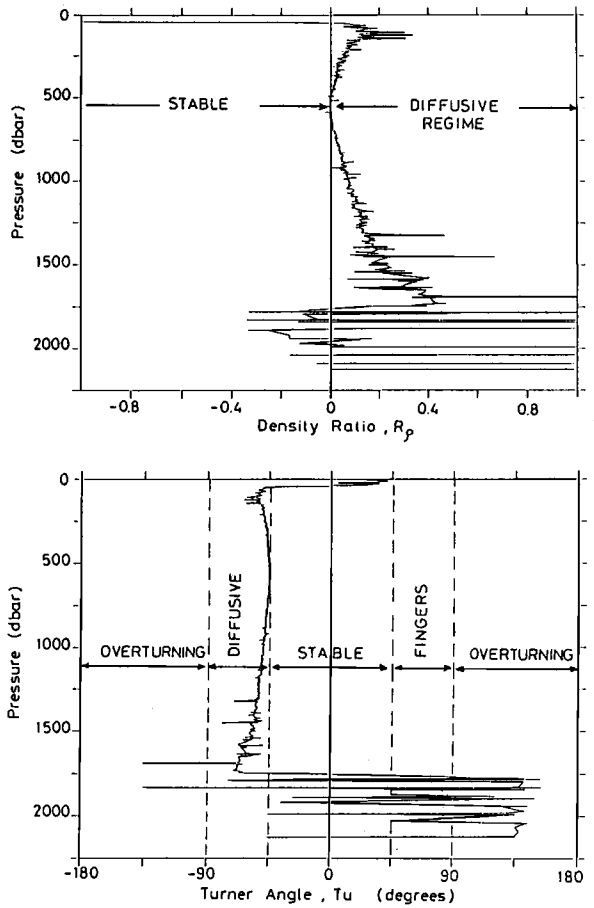

Fig. 5. The average stratification parameters computed from an ensemble of Black Sea deep water profiles: (a) the inverse density ratio $R_\rho^{-1} = \{(\beta dS/dz)/(\alpha dT/dz)\}^{-1}$, and (b) the Turner angle $Tu = tan^{-1}\{(1+R_\rho)/(1-R_\rho)\}$, where α and β are coefficients of expansion for temperature and salinity. The ranges for stable, statically unstable, and double diffusively unstable regimes are indicated. After Özsoy *et al.* (1993).

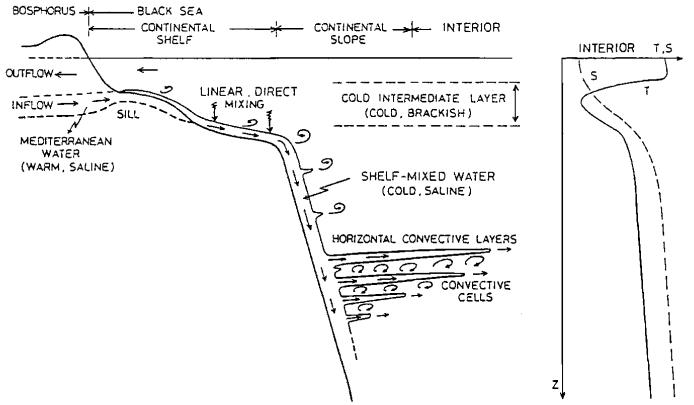

Fig. 3. Schematization of the boundary mixing processes driven by the Mediterranean Water issuing from the Bosphorus. Linear, direct mixing occurs on the shelf region and on part of the slope. At intermediate depths, double diffusive instabilities are generated due to the temperature and salinity contrasts of the intrusions and the potential instability of the interior. After Özsoy *et al.* (1993).

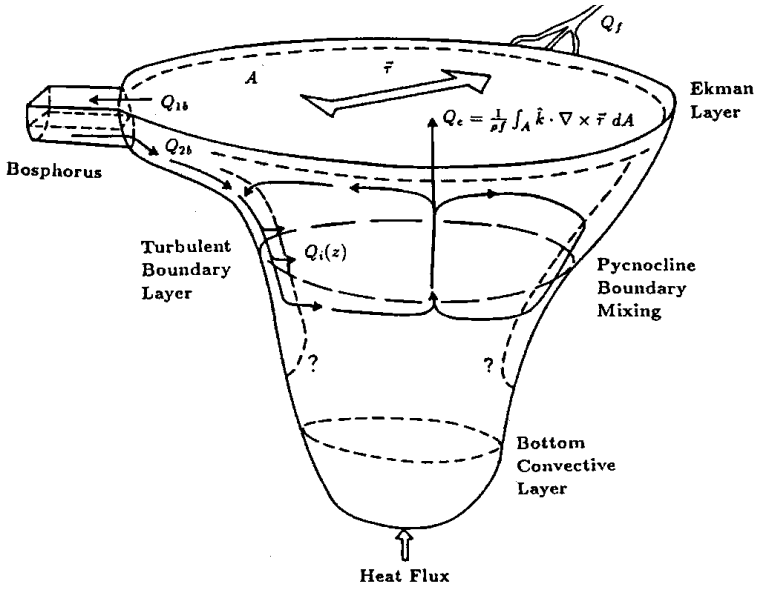

Fig. 13. Schematization of the recirculation driven by boundary mixing processes in the Black Sea. Mechanisms capable of driving a recirculation between boundary layers and the interior are emphasized. After Özsoy *et al.* (1993).

Thank you !
Teşekkürler